In presenting the dissertation as a partial fulfillment of the requirements for an advanced degree from the Georgia Institute of Technology, I agree that the Library of the Institution shall make it available for inspection and circulation in accordance with its regulations governing materials of this type. I agree that permission to copy from, or to publish from, this dissertation may be granted by the professor under whose direction it was written, or, in his absence, by the Dean of the Graduate Division when such copying or publication is solely for scholarly purposes and does not involve potential financial gain. It is understood that any copying from, or publication of, this dissertation which involves potential financial gain will not be allowed without written permission.

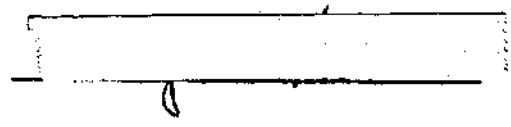

LAMINAR FORCED CONVECTION UNDER THE INFLUENCE OF A RESONANT ACOUSTIC FIELD

A THESIS

Presented to

The Faculty of the Graduate Division

by

Henry Grady Keith

In Partial Fulfillment

of the Requirements for the Degree

Doctor of Philosophy in the

School of Mechanical Engineering

Georgia Institute of Technology

April, 1965

LAMINAR FORCED CONVECTION UNDER THE INFLUENCE OF A RESONANT ACOUSTIC FIELD

Approved:

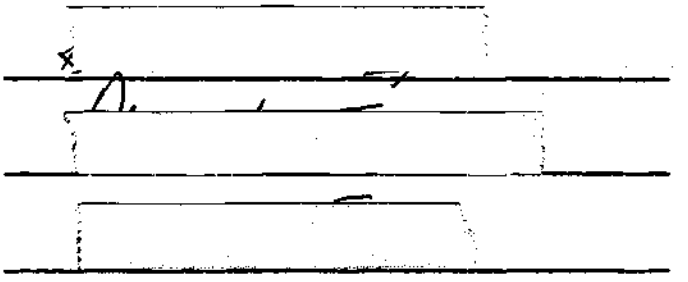

Date Approved by Chairman:

3-30-65

ACKNOWLEDGMENTS

The author is indebted to many individuals who have contributed to the completion of this work. The encouragement, friendship and suggestions of Dr. Kenneth R. Purdy, who was Thesis Advisor, are sincerely appreciated. The cooperation and advice of Dr. T. W. Jackson and Dr. Henderson C. Ward, who served as members of the thesis committee, are gratefully acknowledged. The assistance of Mr. Dwight E. Alford and Mr. J. G. Doyal in setting up the experimental apparatus is greatly appreciated.

The encouragement and spiritual counsel given to the author by his mother and family through the years provided the inspiration for this work. Further, the patience and understanding provided by the wife of the author made the completion of this work possible. The gratitude due these people cannot be adequately expressed.

The author is also indebted to Dr. Jackson for providing a graduate research assistantship during the Summer of 1963, and to the Robert and Company and to the Ford Foundation for the fellowship awards which materially aided the work toward the doctorate. In addition, the author would also like to express appreciation to the Lockheed-Georgia Company for the use of the IBM 7094 computer which was used to carry out the numerical computations required in this investigation.

Finally, a note of appreciation should be given to Mrs. Louwellen Anderson who typed the rough draft, and to Mr. J. D. Templeton who prepared many of the illustrations.

TABLE OF CONTENTS

LIST OF TABLES

LIST OF ILLUSTRATIONS

Figure Page

Figure | Page

SUMMARY

The effect of a resonant acoustic field on heat transfer by forced convection in laminar internal flow was investigated analytically and experimentally. The analytical study was concerned with compressible flow in a parallel plate channel whereas the experimental study was concerned with the flow in a circular tube. The work of Sanders (31) showed experimentally that the density variation of a gas in a resonant acoustic field agreed very closely with that which is predicted by first order acoustics. Therefore, the influence of sound was introduced into the governing equations by: (i) assuming that the density variation of a gas is the same as that predicted by first order acoustics and (ii) assuming that the compression-rarefaction process is isentropic.

The governing equations were obtained by: (i) assuming that the properties of the fluid may be expressed as the sum of a time-mean component and a time-dependent component; (ii) assuming the orders of magnitude for the characteristic values of the properties; (iii) utilizing the solution of the continuity and momentum equations as given by Purdy (27) for the velocity, density, and pressure components; and (iv) performing an order of magnitude analysis of the dimensionless form of the energy equation. This technique reduced the energy equation to a set of linear, partial differential equations; one governing the time-mean temperature field and an infinite number of equations governing the time-dependent temperature field. It was found, however, that by making

a judicious choice of the characteristic values used to form dimensionless variables, the number of equations governing the time-dependent temperature could be reduced to one simple algebraic equation which would give an adequate representation of the time-dependent temperature.

The analytical investigation indicated that the heat transfer coefficient is dependent upon the parameters M/M_o^2, and $(M_o a')^2 Pr_o$ with the first parameter as the dominant one. An interesting correlation of the data shows that the maximum deviation of the local Nusselt number from the corresponding no-sound value can be correlated by the equation

$$(\Delta Nu_{max}/Nu_{no\text{-}sound})Re^{-1/3} = 0.0335(M_o^2/M) \ .$$

The experimental studies showed that a similar equation could also be obtained to correlate the experimentally-obtained results. The equation was

$$(\Delta Nu_{max}/Nu_{no\text{-}sound})Re^{1.526} = 2.58 \times 10^6(M_o^2/M).$$

In each case the acoustical vibrations produced a local Nusselt number which was a slightly-damped periodic function which oscillated above and below the corresponding values of the no-sound Nusselt number. The amplitude of this periodic function is dependent upon the intensity, or amplitude, of the acoustical vibration.

Both the analytical and experimental investigations show that the maxima of the heat transfer coefficient (Nusselt number) occur at, or

near, the velocity antinodes and the minima occur at, or near, the velocity nodes. Actually, there is a phase lag and the maxima and minima occur slightly downstream of the positions at which they would be expected to occur. This phase lag, in some instances, was as high as 20 per cent of the wavelength of the acoustic field. The phase lag seems to vary sporadically with the flow rate and the intensity of the acoustic vibration.

NOMENCLATURE

Symbol		Units
a	Half width of the channel	ft
c	Isentropic speed of sound	ft/sec
c_p	Constant pressure specific heat	ft^2/sec^2-°R
db	Decibels	
i	$\sqrt{-1}$	
k	Thermal conductivity of a fluid	lb/sec-°R
M	Mach number based on U	
M_o	Mach number based on U_o	
p	Pressure of a fluid	lb/ft^2
p_1	Time-dependent pressure	lb/ft^2
$\bar{p}$	Time-mean pressure	lb/ft^2
Q	Volumetric flow rate	ft^3/sec
R	Gas Constant	ft^2/sec^2-°R
SPL	Sound-Pressure level (re 0.0002 μ-bar)	db
t	Time	sec
T	Absolute temperature of a fluid	°R
T_1	Time-dependent temperature	°R
$\bar{T}$	Time-mean temperature	°R
u	X-component of velocity	ft/sec
u_1	Time-dependent component of u	ft/sec
$\bar{u}$	Time-mean component of u	ft/sec
U	Average through-flow velocity based on the mass flow rate	ft/sec

Symbol		Units
U_o	Maximum amplitude of $\|u_1\|$	ft/sec
$\bar{U}$	Characteristic velocity for $\bar{u}$	ft/sec
v	Y-component of velocity	ft/sec
v_1	Time-dependent component of v	ft/sec
$\bar{v}$	Time-mean component of v	ft/sec
V_o	Characteristic velocity for v_1	ft/sec
$\bar{V}$	Characteristic velocity for $\bar{v}$	ft/sec
w	Mass flow rate	lb-sec/ft
x	Space coordinate	ft
X	X-component of the body force	lb/ft^3
y	Space coordinate	ft
Y	Y-component of the body force	lb/ft^3
z	Space coordinate	ft

Greek Symbols

β	Constant	
γ	Ratio of the specific heats - c_p/c_v	
γ_m	Vortex size	
δ	$2\delta_{ac}/\lambda$ or a number much less than unity	
δ_{ac}	A.C. boundary layer thickness	ft
λ	Wavelength	ft
Φ	Viscous dissipation function; also used as a dimensionless parameter defined by equation 4.26	
μ	Dynamic viscosity of a fluid	$lb\text{-}sec/ft^2$
ν	Kinematic viscosity of a fluid	ft^2/sec
π	Constant = 3.14159	

Symbol		Units
ρ	Density of a fluid	$lb\text{-}sec^2/ft^4$
ρ_1	Time-dependent component of ρ	$lb\text{-}sec^2/ft^4$
$\bar{\rho}$	Time-mean component of ρ	$lb\text{-}sec^2/ft^4$
ω	Circular frequency	ft/ft-sec

Subscripts

o	Time mean of the property at $x = 0$, $y = a$

CHAPTER I

INTRODUCTION

Within the past decade there has been a considerable increase in interest in the general subject of the influence of vibrations and fluctuations upon the rate of convective heat transfer from heated surfaces to fluid media. As used here the term "vibration" indicates a relative periodic motion between a surface and a fluid medium in which the relative velocity vector undergoes a periodic change of both magnitude and sign, whereas the term "fluctuation" refers to the same situation except that the relative velocity vector undergoes a periodic change in magnitude only. A term which is often used to describe either type flow is "pulsating flow."

There are several practical situations in which heat is being transferred to flows that involve pulsating motions. For example, an oscillatory motion might take place due to flow instabilities, or when fluid is pumped through a duct by a reciprocating device. A process common to many heat exchange devices is that of forced convection heat transfer to or from a fluid flowing inside a duct. The circulation of blood is a typical case of pulsating flow inside a duct, and the heat interchange between the blood and tissues may, in turn, be influenced by the oscillations. The "screech" phenomenon (concentrated acoustic effects) in jet tail pipes and rocket engines is an example of oscillatory flow which in many cases has led to a structural failure. It is believed

that these failures were caused by the large increases in the heat transfer coefficient from the hot combustion gases to the relatively thin walls of the structure brought about by the acoustically-induced oscillations in the flow. A similar effect has caused the premature failure of rocket nozzles.

Several experimental investigations have been conducted in recent years to study the effects of pulsating flows upon the rate of convective heat transfer from heated surfaces to fluid media. Many of these investigations have been primarily concerned with flow fields around cylindrical bodies rather than through these bodies. Typical of these efforts are the studies of Kubanskii (1, 2) on free convection heat transfer from a horizontal heated cylinder in an acoustic field. Several papers, such as the one by Haveman and Rao (3) have dealt with heat transfer to both laminar and turbulent flows in ducts. The above-mentioned experiments generally indicate an increase in the rate of convective heat transfer in the presence of strong vibrations although some decreases have been reported depending upon the frequency and amplitude of the vibrations and the Reynolds number of the flow. Even though the validity of the data is sometimes doubtful, one important conclusion can be drawn; namely, that the rate of convective heat transfer is appreciably influenced by vibrations only when the vibration is of sufficient intensity to alter the character of the boundary-layer flow in the proximity of the heat transfer surface; otherwise the effect on the rate of heat transfer is negligible.

The effect of vibrations upon convective heat transfer has thus gained a special interest not only because of control and accident con-

siderations, as in the case of rockets and jet engines, but also because of the possibility of increased performance during normal operation with some type of pulsating flow. As far as can be ascertained, all attempts to obtain a general mathematical solution to the problem of convective heat transfer coupled with vibrations have thus far been unsuccessful. This is due to the complexity of the general continuity, momentum, and energy equations for viscous, compressible fluid flow.

The present problem considers laminar forced convection due to the unsteady flow of a viscous, compressible fluid between horizontal parallel plates as illustrated in Figure 1. An isothermal entrance region is assumed to be of sufficient length that at the start of the heat transfer region (thermal entrance) the velocity profile is fully developed and the temperature profile is isothermal at T_o. In the present context, the term "fully developed" is used in the sense that the flow, i.e., the velocity profile, is repeated in half wavelength sections. Heat generation and conduction within the duct walls are neglected so that a known boundary condition may be specified at the inside of the duct wall. That selected is a constant wall temperature; thus heat transfer results from the step increase in wall temperature from T_o to T_w at $x = 0$.

A constant wall temperature boundary condition is of practical engineering interest for condensers and evaporators with thin-walled ducts. Furthermore, the constant wall temperature solution may be used to obtain the solution of the energy equation when an arbitrary wall temperature is specified, or when a heat flux boundary condition is specified, as indicated by Sellars, Tribus and Klein (4).

Previous investigations of convective heat transfer processes resulting from unsteady duct flow either have been approximate or considered special situations in which there was no dependence of the solution on the coordinate parallel to the direction of flow. The present investigation assumes the flow to be viscous, compressible, unsteady, and two-dimensional. These assumptions are the major differences between this investigation and previous investigations.

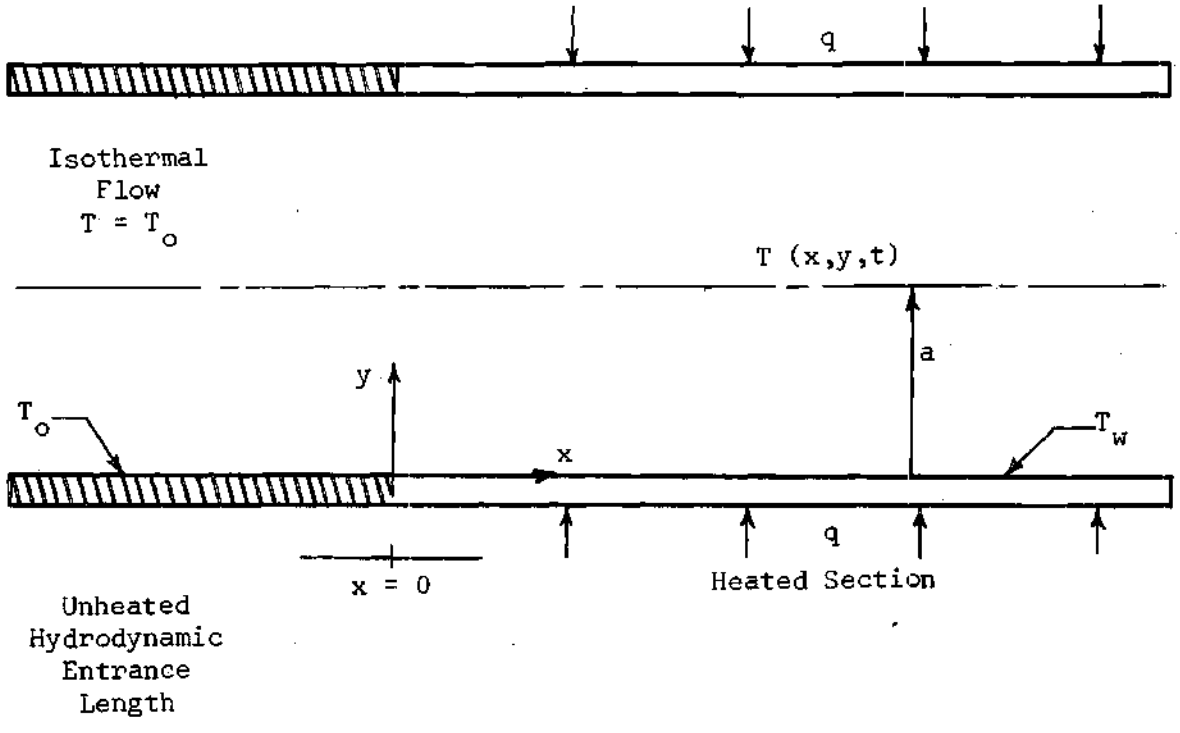

Figure 1. Flow Between Parallel Plates with an Isothermal Entrance Region and a Heat Transfer Region with Constant Wall Temperature.

CHAPTER II

SURVEY OF THE LITERATURE

As stated in Chapter I the subject of heat transfer in unsteady flow has gained a considerable amount of interest in the past several years as evidenced by the recent upsurge in the number of papers appearing in the literature. Many of the most pertinent papers are of an experimental nature and are concerned either with free convection or combined free and forced convection. The main objective has been to determine whether the performance of a heat-exchange device could be improved by unsteadiness in the flow. However, due to the inherent difficulty of making precise measurements in this field, experimental information about the process is meager and sometimes conflicting. In general, however, these experimental investigations report a significant increase in the rate of convective heat transfer in the presence of strong vibrations.

One of the few reports of a decrease in heat transfer rates is given by Darling (5) who studied the heat transfer to liquids in intermittent flow. He found that water and a 50 per cent glycerol solution in intermittent flow in a heated tube gave poorer heat transfer results than in steady flow when the flow was controlled from downstream of the heater. However, when the flow was controlled from upstream the heat transfer was improved by up to 70 per cent over the steady flow values; the increase was caused by the formation of bubbles in the

liquid. In contrast, West and Taylor (6) have been able to increase the coefficient of heat transfer to water in turbulent flow in pipes by as much as 70 per cent by producing pulsations in the flow with the use of a reciprocating pump.

Holman, Gartrell, and Soehngen (7) conducted an investigation of artificially induced oscillations in a free convection boundary layer on a vertical, isothermal, flat plate. They observed that the time-averaged heat transfer coefficient for the oscillating boundary layer was the same as the theoretical steady-state value, within the range of experimental error.

The effect of vibrations on heat transfer from wires to air in forced parallel flow has been investigated by Anantanarayanan and Ramachandran (8). Increases in the heat transfer coefficient as high as 130 per cent were obtained using air velocities ranging from 34 to 63 feet per second and vibrational frequencies ranging from 75 to 120 cycles per second. A correlation of the experimental data revealed that the increase in heat transfer was a function of the ratio of the mean vibrational velocity to the air-stream velocity. Lemlich (9) made a similar study of the effects of transverse vibrations on free convection heat transfer from horizontal, electrically-heated wires to air. Using vibrations in the range of 39 to 122 cycles per second he obtained increases in the film coefficient as high as 400 per cent. No effect was observed for a change in the direction of vibration, but an increase in amplitude or vibrational velocity resulted in an increase in heat transfer.

Many investigators have studied the effects of sound on the heat

transfer from horizontal cylinders. Among these are Sprott, Holman, and Durand (10); Holman and Mott-Smith (11); Fand and Kaye (12); and Fand, Roos, Cheng, and Kaye (13). Increases in heat transfer as high as 300 per cent are reported in these papers. Martinelli and Boelter (14), using a sinusoidally vibrating cylinder in water, found that the rate of heat transfer increased with an increased velocity of vibration. They also report that velocities of vibration yielding magnitudes of Reynolds number less than a "critical value" (about 1000) produced no effect on the rate of heat transfer from the cylinder.

The works cited thus far have, for the most part, considered the effects of vibration on the heat transfer from cylindrical bodies where the flow field is around these bodies rather than through them. Much of this work is very interesting and very valuable in that it provides some knowledge and understanding of how the acoustic forces affect the thermal and hydrodynamic boundary layers.

In the field of combined free and forced convection in vertical tubes, two papers are mentioned. Jackson, et al. (15, 16) used a steam-heated tube with air as the heat transfer medium to study the effect of resonant acoustic vibrations on heat transfer. Their results indicate that for sound pressure levels below 118 decibels free convection forces were dominant and there was little effect on the heat transfer coefficient. Above 118 decibels the free convection forces were apparently negligible and the effect of sound appeared to be considerable. They found that acoustic vibrations increased overall log-mean heat transfer coefficients as much as 54 per cent over corresponding values without vibrations.

The experimental investigations which are more pertinent to the present study will now be discussed. Spurlock, et al. (17) used a horizontal isothermal tube with air flowing inside as the heat transfer medium and found that a threshold sound pressure level exists below which little or no effect is produced. Above this threshold level increases in the local Nusselt numbers up to 75 per cent were produced. For the flow rate used in this study the threshold level was approximately 141 decibels.

Jackson, Purdy, and Oliver (18), using a horizontal, isothermal tube in which there was a simultaneous development of the hydrodynamic and thermal boundary layers, found that under resonant conditions a periodic effect on the local heat transfer coefficient was produced by sound waves superimposed on the flow field. The maxima of the local heat transfer coefficient were at the velocity antinodes, or pressure nodes, of the field; the minima occurred at the pressure antinodes of the field. Jackson, Purdy, Oliver, and Johnson (19), using a similar system, obtained local heat transfer coefficients up to 3.6 times the no-sound values for air flowing through an isothermal, horizontal tube at Graetz Numbers 33 to 5400.

Eastwood (21), using the same system as Jackson, et al. (19), made a study to determine the threshold sound pressure levels for a wide range of Reynolds numbers and, in doing so, discovered a rather interesting effect. He found that for Reynolds numbers below approximately 20,000 maximum values of the local Nusselt number occurred at the velocity antinodes; above 35,000 the maximum values were shifted to the velocity nodes. This shift appeared to take place gradually be-

tween Reynolds numbers 20,000 and 35,000, and within this range of values there was very little effect of the resonant acoustic vibrations on heat transfer rates. The pertinent results of his study are shown in Figure 2.

Alford (20) has studied turbulent convective heat transfer in an acoustically resonant tube which had a hydrodynamic entrance length. Therefore, his experimental apparatus is the same as that which was used in the current study. Alford, however, was unable to obtain any measurable effect on heat transfer in the turbulent range because of the limitation of the sound generation equipment used in his work. This seems to indicate that the threshold sound pressure levels for fully-developed flow are slightly higher than those given by Eastwood (21) for a simultaneous development of the hydrodynamic and thermal boundary layers.

Analytical investigations related to the current study are relatively few in number. Perlmutter and Siegel (22) have analyzed the problem of transient heat transfer with transient laminar flow between horizontal parallel plates which may be either heated or cooled. The transient processes were caused by simultaneously changing the fluid pumping pressure and either the wall temperature or the wall heat flux. By making the slug-flow simplification they were able to obtain a solution for both the thermal entrance and fully-developed heat transfer regions. Even though the velocity at any instant of time was assumed to be uniform throughout the channel, the fluid temperature distribution depended on both the coordinate parallel to the direction of flow and the position within the channel cross-section.

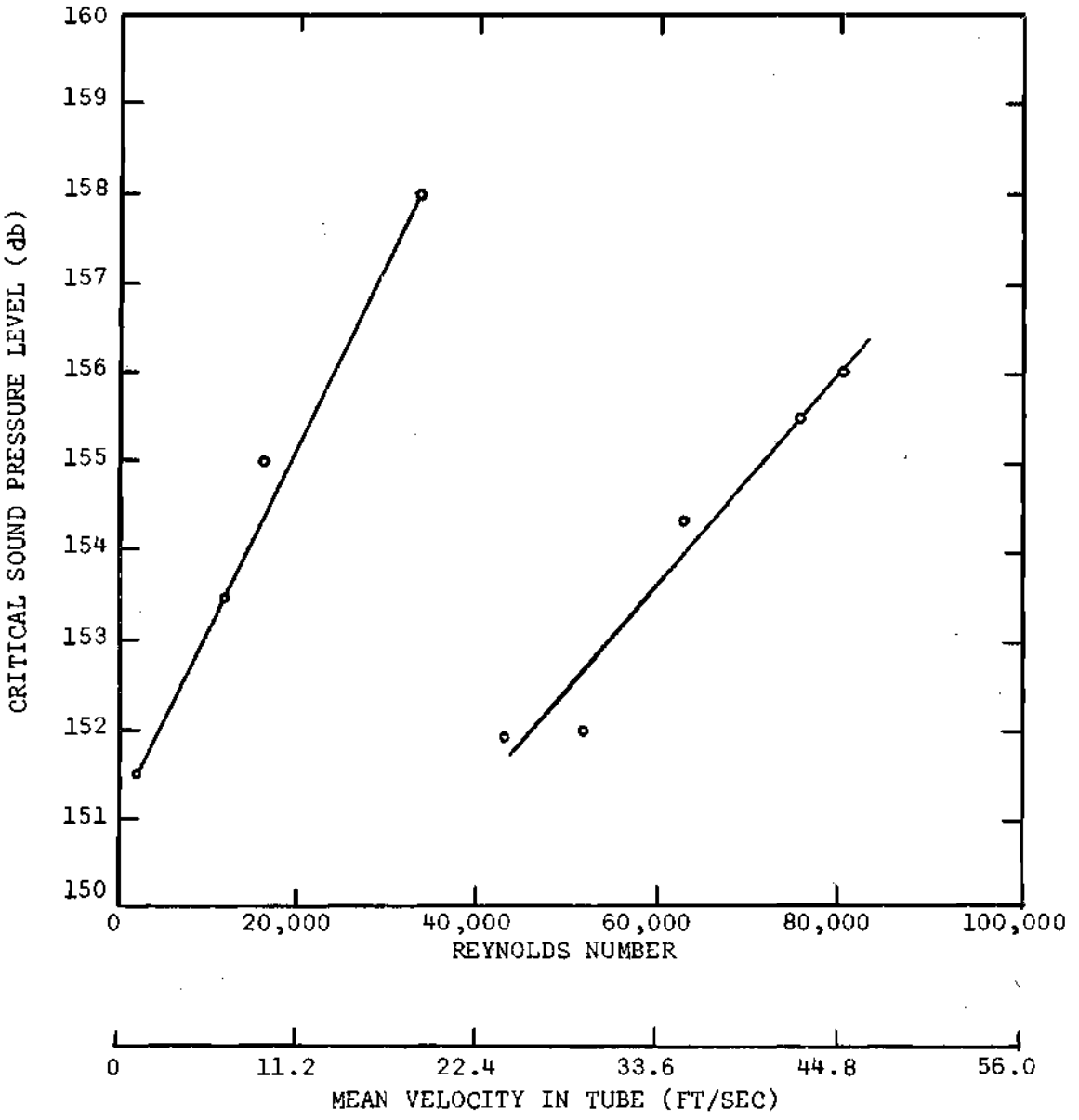

Figure 2. Critical Sound Pressure Level Versus Reynolds Number.

Zeiberg and Mueller (23) have studied transient, laminar, combined free and forced convection in a duct under the assumptions of constant fluid properties and fully developed flow. The transient heating was taken to be the result of wall temperature variations; the wall temperature varied linearly with the coordinate parallel to the direction of flow. They showed that for certain combinations of the Prandtl and Rayleigh numbers an oscillatory approach to the steady state exists which could induce a large reduction of the Nusselt number during the transient period.

Siegel and Perlmutter (24, 25) have obtained solutions for pulsating flow between horizontal parallel plates where the pulsations are produced by superposing an oscillating pressure gradient on the mean pumping pressure. The temperature distributions were two-dimensional, but a slug-flow assumption was used to simplify the velocity distribution for one of their solutions (24), and an integrated form of the energy equation was used to simplify the analysis for the other solution (25). The two solutions exhibited a very similar behavior; there was a difference in numerical values, however.

Ewen (26), in his doctoral dissertation, examined the problem of laminar forced convection due to the nonsteady flow of an incompressible fluid between parallel plates using a constant wall temperature as the boundary condition. He presented an exact solution of the two-dimensional energy equation for small velocity oscillations, and the amplitude and phase of the nonsteady component of the wall heat flux was calculated as a function of position in the direction of flow.

In summary, exact two-dimensional solutions have been obtained for steady flow with arbitrary time variations in wall temperature or wall heat flux, but with the specified wall boundary condition uniform along the duct at any instant of time. In the case of unsteady flows, previous work has been limited either to approximate two-dimensional solutions or very specialized situations in which the coordinate parallel to the direction of flow is not a variable. The present investigation provides an analysis which is valid throughout the entire heat transfer region, rather than being limited to either the thermal entrance region or the fully-developed temperature profile.

Prerequisite to an analysis of the characteristic behavior of forced convection under the influence of an acoustic field is an understanding of the effects of the sound field upon the velocity profile, or flow field. For the geometry considered in the present investigation Purdy (27) has obtained the solution for the velocity components for laminar, two-dimensional flow of a compressible fluid under the influence of a resonant acoustic field. His analysis predicted the presence of standing vortices in the channel both with and without through flow. The vortices were one-quarter wavelength long and the width of the larger vortices is shown to be solely a function of the parameter M/M_o^2, where M is the Mach number based on the average through-flow velocity and M_o is the Mach number based on the maximum amplitude of the x-component of the time-dependent velocity. It is this work by Purdy which forms the basis for the current analysis of the energy equation. Typical velocity profiles and streamline patterns are shown in Figures 3 through 8. Figures 7 and 8 show the streamline pattern and

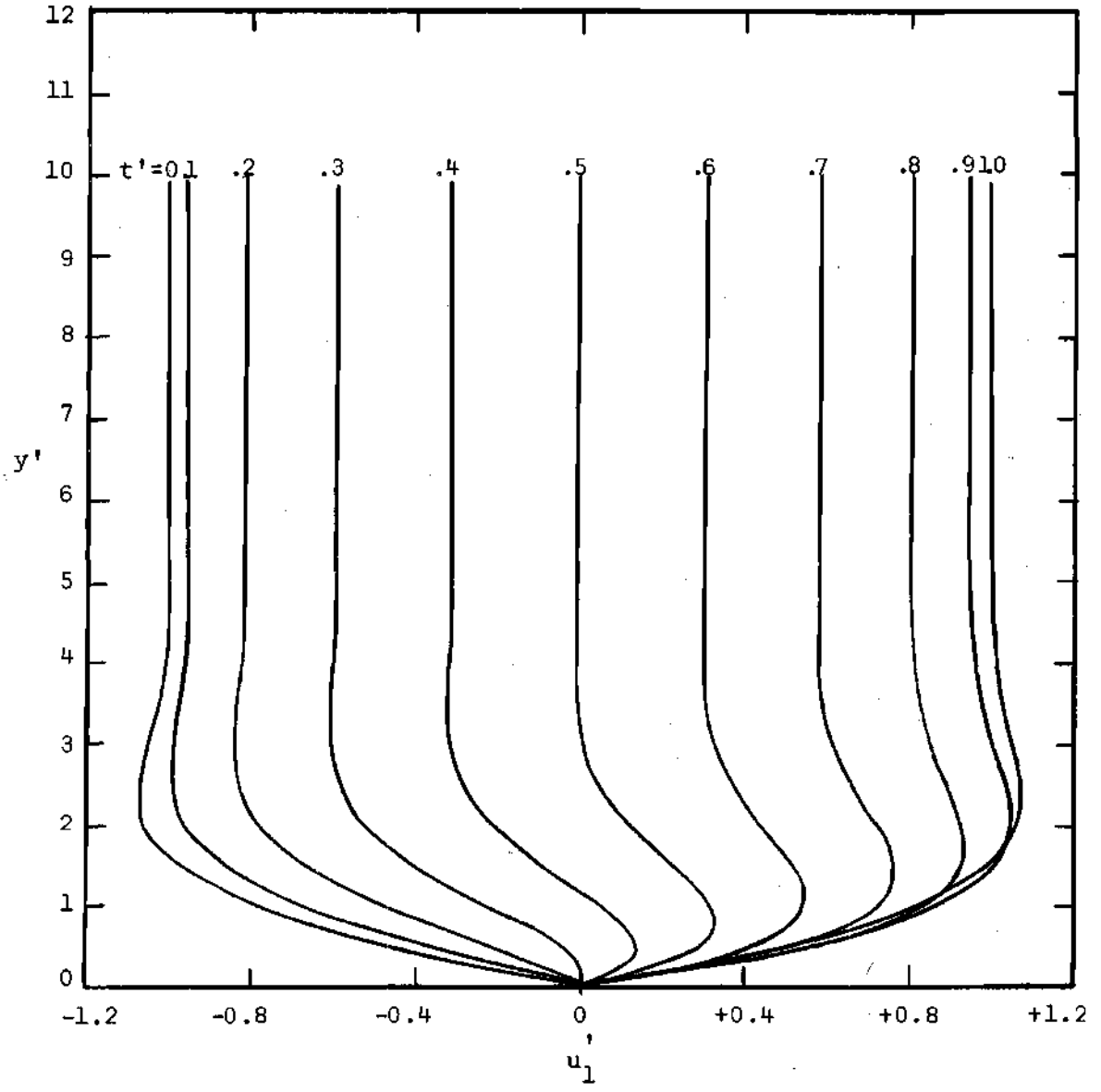

Figure 3. Typical Profiles of the X-Component of the Time Dependent Velocity (x' = 0).

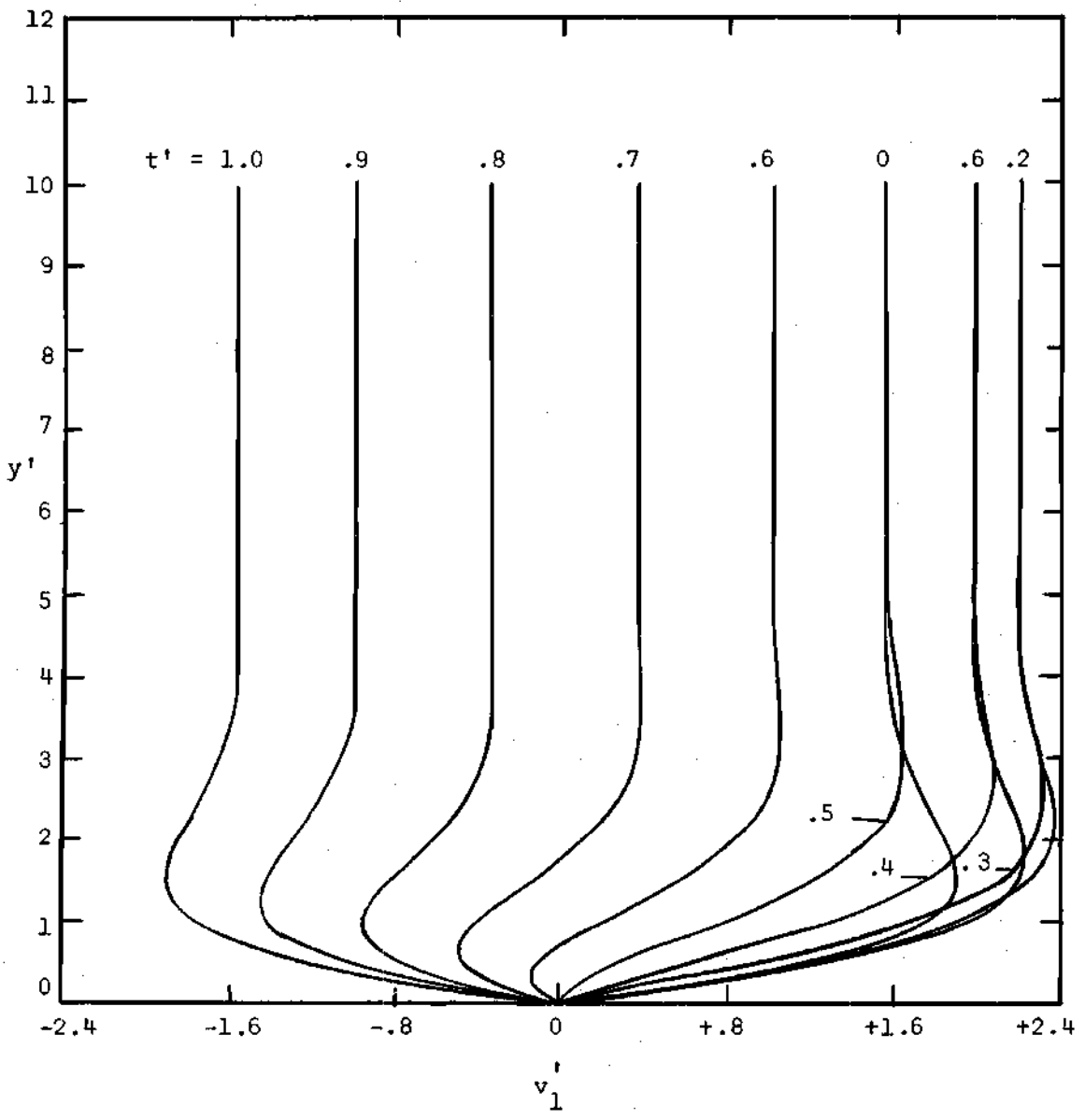

Figure 4. Typical Profiles of the Y-Component of the Time-Dependent Velocity (x' = 1.0)

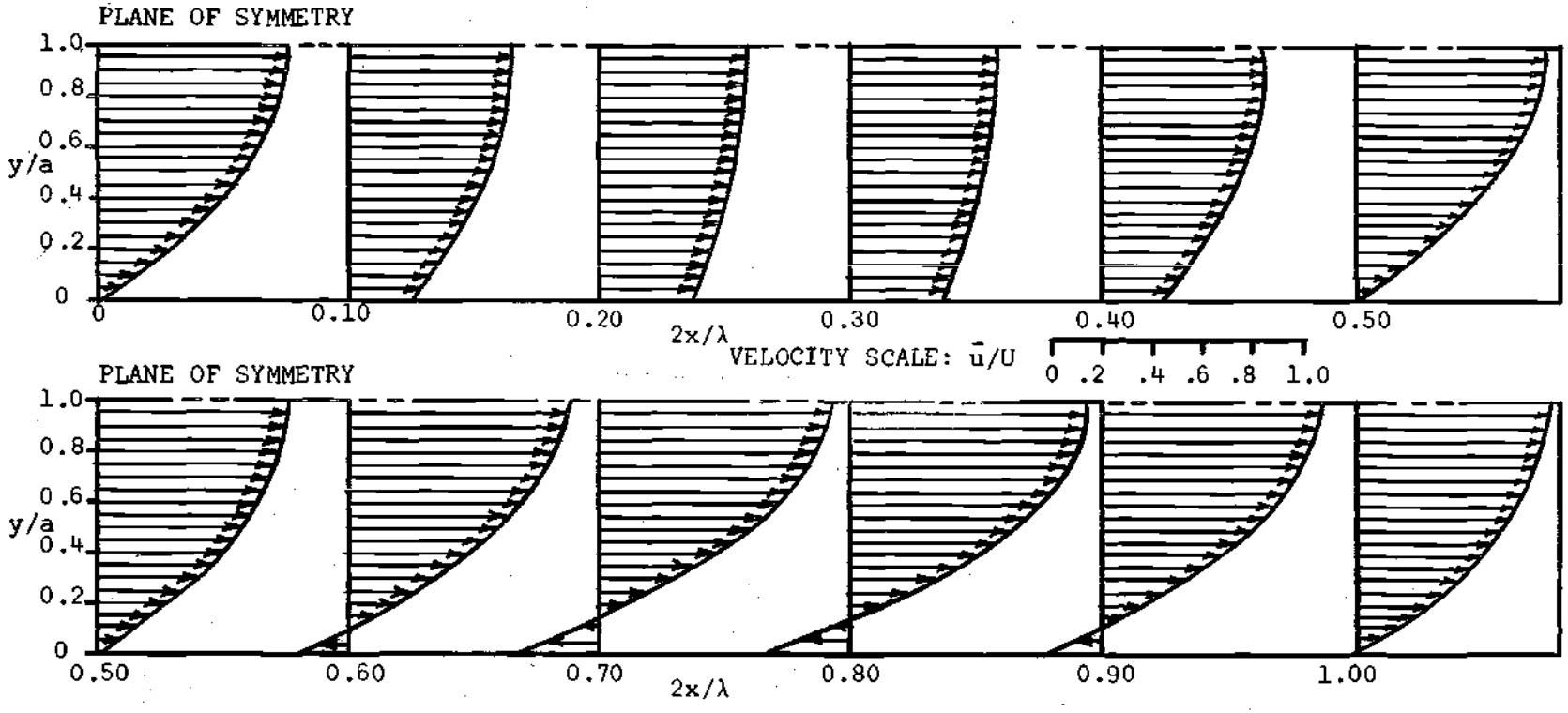

Figure 5. Typical Profiles of the X-Component of the Time-Mean Velocity

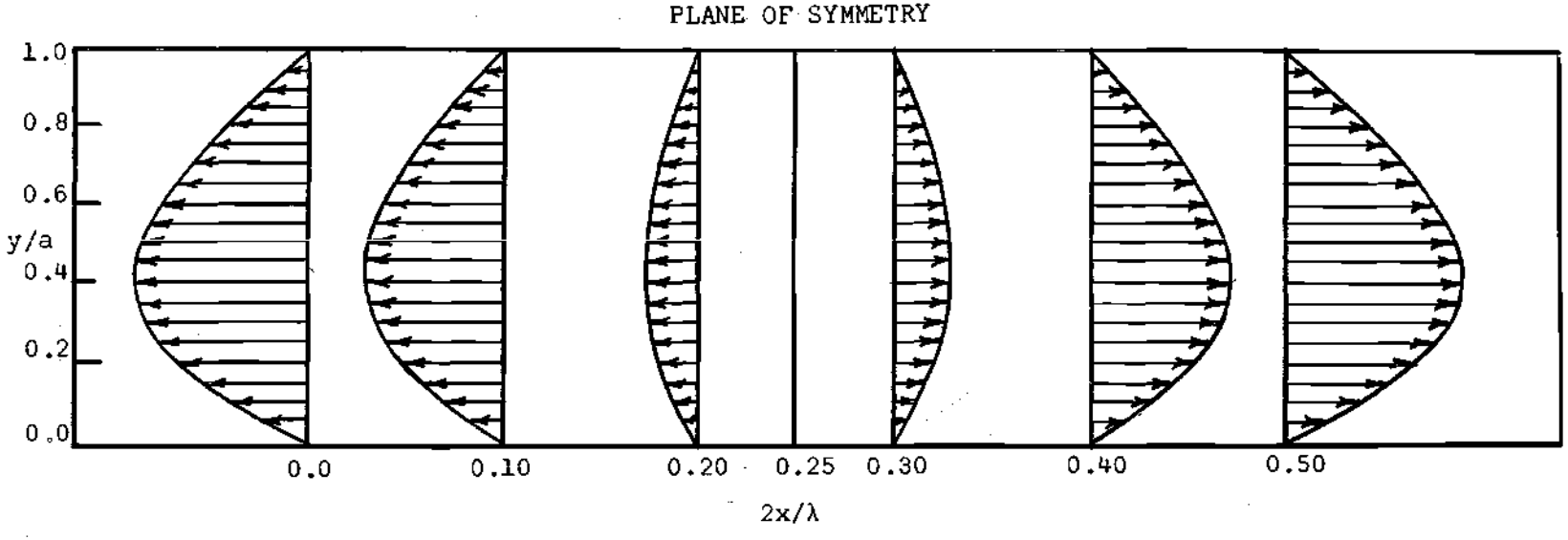

Figure 6. Typical Profiles of the Y-Component of the Time-Mean Velocity.

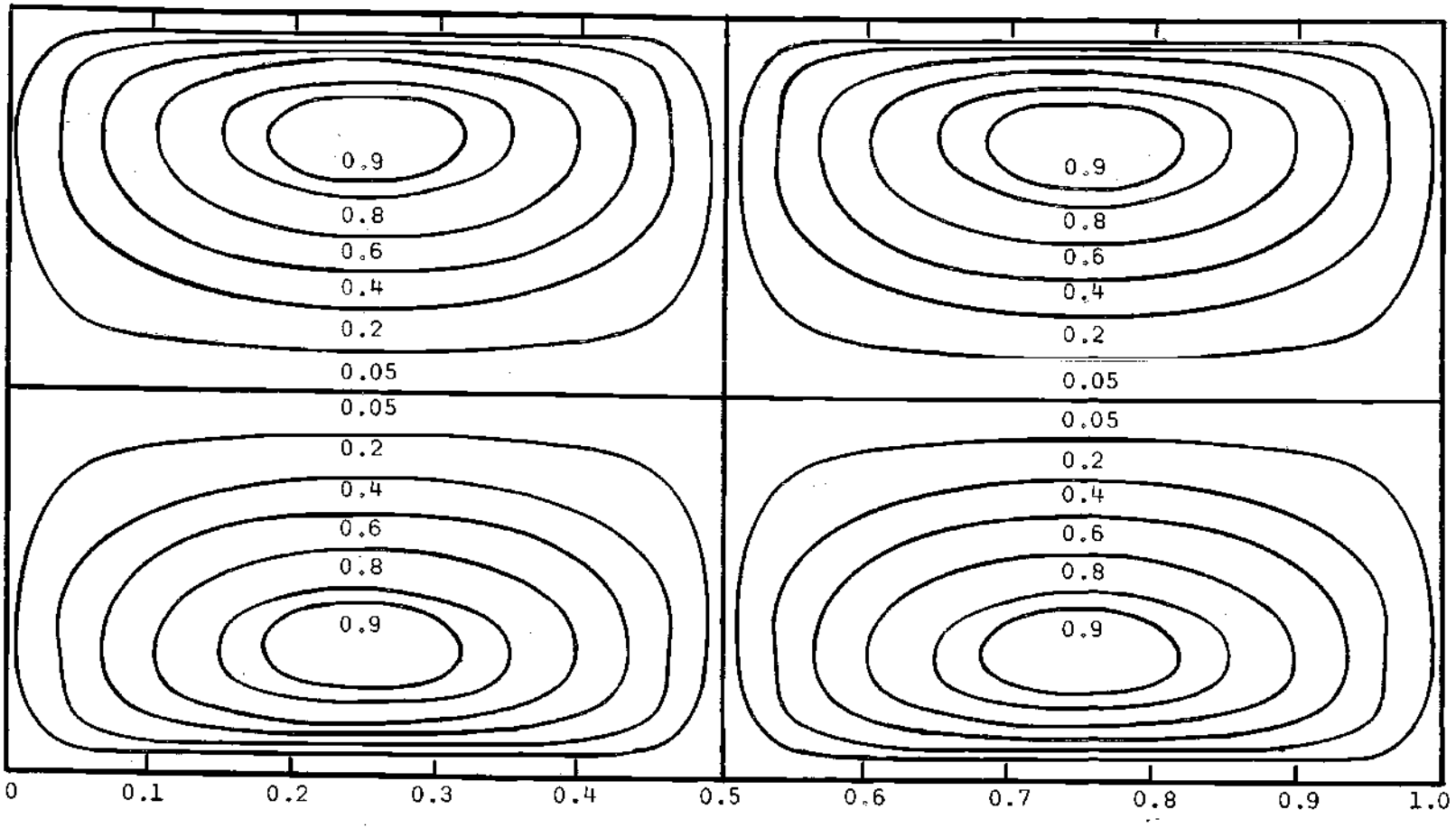

Figure 7. Typical Streamline Pattern and Vortex Formation for $M/M_o^2 = 0$. (No Through-Flow.)

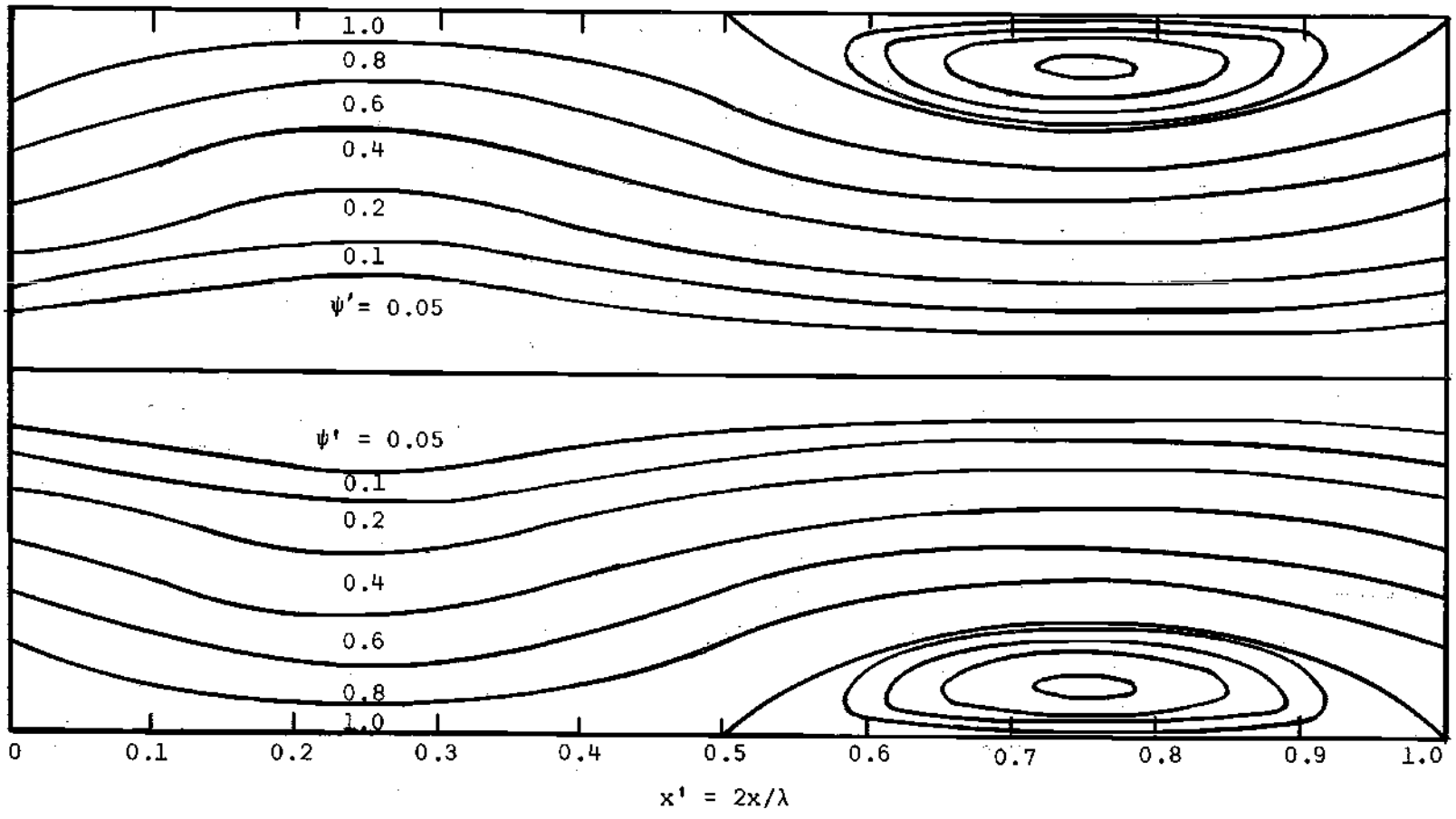

Figure 8. Typical Streamline Pattern and Vortex Formation for $M/M_o^2 = 0.3$.

vortex formations both with and without through-flow. It is the presence of these vortices which gives rise to the periodic effect on the local heat transfer coefficient as observed by Jackson, et al. (18).

CHAPTER III

DEVELOPMENT OF THE MATHEMATICAL MODEL

Statement of the Problem

The mathematical model of the problem as shown in Figure 9 consists of "fully-developed" laminar flow between infinite parallel plates which are separated by a distance 2a. This geometry is usually referred to as a parallel plate channel, or more simply, as a channel. The fluid is assumed to be a viscous, ideal gas. Superimposed upon this flow is a resonant acoustic field having a pressure node (velocity antinode) at $x = 0$.

Assumptions

In order to develop the mathematics to describe the selected model the following assumptions will be made:

(A1) The fluid and the parallel plates are assumed to be at a constant temperature throughout the hydrodynamic entrance length; i.e., for $x < 0$. The walls of the channel in the entrance length are assumed to be maintained at a fixed temperature, say T_o. The channel walls in the heated section are also assumed to be at a constant temperature, T_w, where T_w is greater than T_o.

(A2) The fluid is assumed to be flowing laminarly in the positive x-direction. The flow is assumed to be independent of the z-direction, but due to the secondary flow caused by the impressed acoustic field there will be a y-component of velocity; hence, the flow is

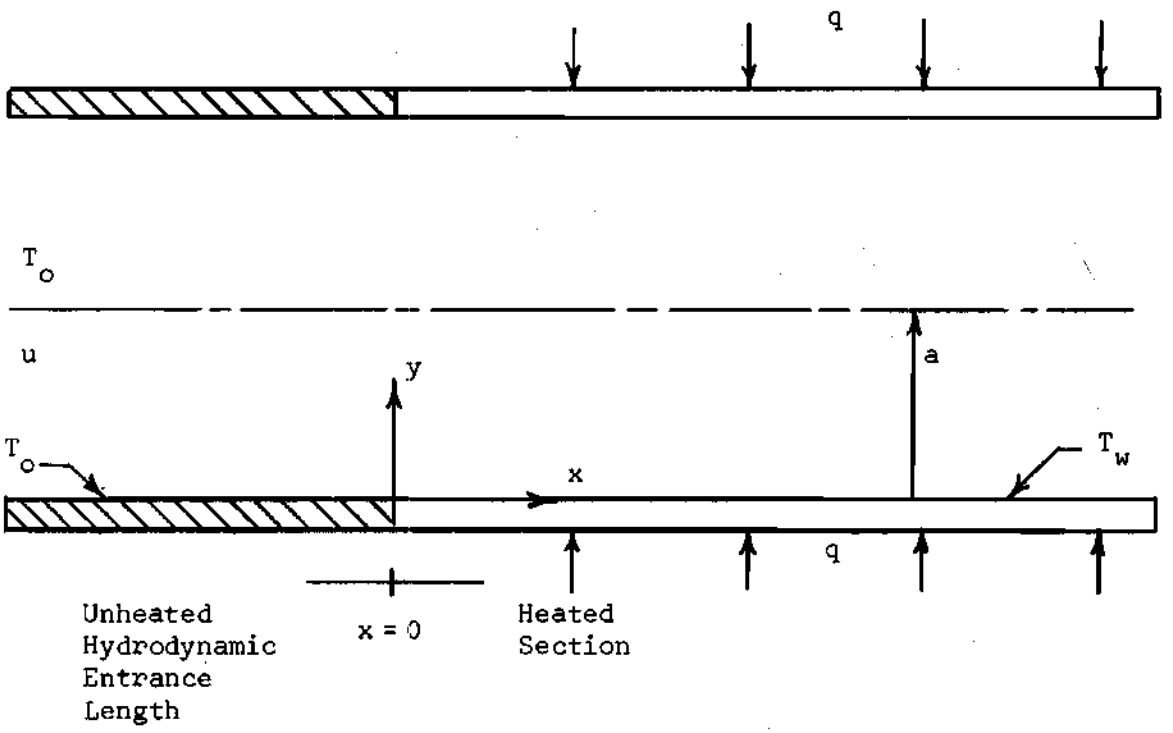

Figure 9. Parallel Plate Channel.

two-dimensional.

(A3) The fluid properties--viscosity, specific heat, and thermal conductivity--will be taken as constant.

(A4) The temperature variations in the gas are assumed to be small enough so that free convection effects may be neglected. This assumption simplifies the mathematics considerably by allowing the continuity and momentum equations to be solved independently of the energy equation.

Governing Equations and Boundary Conditions

The problem is described mathematically by the following basic equations together with their associated boundary conditions:

Continuity

$$\frac{\partial \rho}{\partial t} + \frac{\partial}{\partial x}(\rho u) + \frac{\partial}{\partial y}(\rho v) = 0 \tag{3.1}$$

$$\int_0^a \overline{\rho u} dy = \text{Constant} \tag{3.2}$$

Momentum

$$\frac{\partial u}{\partial t} + u \frac{\partial u}{\partial x} + v \frac{\partial u}{\partial y} = -\frac{1}{\rho}\frac{\partial p}{\partial x} + \tag{3.3a}$$

$$\frac{1}{\rho}\frac{\partial}{\partial x}\{\mu[2\frac{\partial u}{\partial x} - \frac{2}{3}(\frac{\partial u}{\partial x} + \frac{\partial v}{\partial y})]\} + \frac{1}{\rho}\frac{\partial}{\partial y}\{\mu[\frac{\partial u}{\partial y} + \frac{\partial v}{\partial x}]\}$$

$$\frac{\partial v}{\partial t} + u \frac{\partial v}{\partial x} + v \frac{\partial v}{\partial y} = - \frac{1}{\rho} \frac{\partial p}{\partial y} + \tag{3.3b}$$

$$\frac{1}{\rho} \frac{\partial}{\partial y} \{\mu[2 \frac{\partial v}{\partial y} - \frac{2}{3} (\frac{\partial u}{\partial x} + \frac{\partial v}{\partial y})]\} + \frac{1}{\rho} \frac{\partial}{\partial x} [\mu(\frac{\partial u}{\partial y} + \frac{\partial v}{\partial x})]$$

The boundary conditions for the momentum equations are

$$u(x,0,t) = v(x,0,t) \equiv 0 \tag{3.4a}$$

$$\frac{\partial u}{\partial y} = 0 \; ; \; y = a, \text{ all } x \text{ and } t \tag{3.4b}$$

$$v(x,a,t) = 0 \tag{3.4c}$$

Energy

$$\rho c_p \frac{DT}{Dt} = \frac{Dp}{Dt} + k\nabla^2 T + \mu\Phi \tag{3.5}$$

where

$$\Phi = 2[(\frac{\partial u}{\partial x})^2 + (\frac{\partial v}{\partial y})^2] + (\frac{\partial v}{\partial x} + \frac{\partial u}{\partial y})^2 - \frac{2}{3}(\frac{\partial u}{\partial x} + \frac{\partial v}{\partial y})^2 \tag{3.6}$$

The boundary conditions for the energy equation are

$$T(x,0,t) = T_w = \text{constant}, \; x \geq 0 \tag{3.7a}$$

$$\frac{\partial T}{\partial y} = 0;\ y = a,\ \text{all } x \text{ and } t \tag{3.7b}$$

$$T\ (0,y,t) = T_o,\ 0<y<2a \tag{3.7c}$$

Reduction of the Governing Equations

Assumptions

In addition to the assumptions previously made, the following assumptions will be made:

(A5) Since Purdy (27) has solved the continuity and momentum equations corresponding to this problem, his solution for the velocity and pressure fields will be used to determine the coefficients in the energy equation. The validity of this approach is based upon one of the previous assumptions; i.e., that free convection effects are negligible.

(A6) The velocity components, $u(x,y,t)$ and $v(x,y,t)$, and the pressure, $p(x,y,t)$, are known functions of position and time. Purdy (27), in his analysis of the velocity field formed by resonant acoustic vibrations in a parallel plate channel, assumed that the density, pressure, and velocity components could be represented as the sum of a time-dependent component (denoted by a subscript, "1") and a time-mean component (denoted by a barred term). It is plausible, therefore, to assume that the temperature of the fluid may be represented in a similar fashion. Thus, we have

$$\rho(x,y,t) = \bar{\rho}(x,y) + \rho_1(x,y,t) \tag{3.8a}$$

$$p(x,y,t) = \bar{p}(x,y) + p_1(x,y,t) \tag{3.8b}$$

$$u(x,y,t) = \bar{u}(x,y) + u_1(x,y,t) \tag{3.8c}$$

$$v(x,y,t) = \bar{v}(x,y) + v_1(x,y,t) \tag{3.8d}$$

$$T(x,y,t) = \bar{T}(x,y) + T_1(x,y,t) \tag{3.8e}$$

where the time-dependent temperature $T_1(x,y,t)$ is to be expressed as

$$T_1(x,y,t) = \mathrm{Re}\left[\sum_{n=1}^{\infty} T_{1n}(x,y)\exp(-in\omega t)\right].$$

(A7) The energy equation in its present form will not yield readily to a mathematical analysis and, therefore, an order of magnitude analysis will be performed to reduce the energy equation to a more tractable form. In order to perform an order of magnitude analysis it is necessary first to introduce dimensionless forms of each of the properties in the governing equations. In addition, it is necessary to assume an order of magnitude for various quantities.

Dimensionless Variables

Before defining the dimensionless forms of the properties it is first necessary to choose a characteristic value of each property. For this purpose the following characteristic values are assumed:

Property	Characteristic Value
x	$\lambda/2$
y	δ_{ac} and a
t	$\lambda/2c_o$

Property	Characteristic Value
$\bar{u}$	$\bar{U}$
u_1	U_o
$\bar{v}$	$\bar{V}$
v_1	V_o
$\bar{p}$	p_o
p_1	$\rho_o c_o U_o$
$\bar{\rho}$	ρ_o
ρ_1	$\rho_o M_o$
μ	μ_o
c_p	c_{po}
k	k_o
$\bar{T}$	$T_w - T_o$
T_{1n}	θ_n

Utilizing these characteristic values, the following dimensionless variables are formed:

$$x = (\lambda/2)x' \tag{3.9a}$$

$$y = \delta_{ac} y' = a\tilde{y}' \tag{3.9b}$$

$$t = (\lambda/2c_o)t' \tag{3.9c}$$

$$\bar{u} = \bar{U}\bar{u}' \tag{3.9d}$$

$$u_1 = U_o u_1' \tag{3.9e}$$

$$\bar{u} = \bar{V}\bar{v}' \tag{3.9f}$$

$$v_1 = V_o v_1' \tag{3.9g}$$

$$\bar{p} = p_o \bar{p}' \tag{3.9h}$$

$$p_1 = \rho_o c_o U_o p_1' \tag{3.9i}$$

$$\bar{\rho} = \rho_o \bar{\rho}' \tag{3.9j}$$

$$\rho_1 = \rho_o M_o \rho_1' \tag{3.9k}$$

$$\mu = \mu_o \mu' \tag{3.9m}$$

$$c_p = c_{po} c_p' \tag{3.9n}$$

$$k = k_o k' \tag{3.9p}$$

$$\bar{T} = T_w - (T_w - T_o)\bar{T}' \tag{3.9q}$$

$$T_{1n} = T_{1n}' \theta_n \tag{3.9r}$$

where the prime superscript denotes dimensionless variables.

Orders of Magnitude

The characteristic values of length and time were chosen such that derivatives with respect to the dimensionless form of these variables will be of the order of magnitude of one. (This is not necessarily true for the derivatives of the temperature; see Appendix A for the explanation.) The characteristic values of the remaining variables were chosen such that the dimensionless form of each of these variables will be of the order of magnitude of one. In equation form this becomes

$$\theta\left[\frac{\partial}{\partial x'}, \frac{\partial}{\partial y'}, \frac{\partial}{\partial t'}, \bar{u}', u_1', \bar{v}', v_1', \bar{\rho}', \rho_1', \mu', \frac{\partial p_1'}{\partial x'}, \frac{\partial p_1'}{\partial t'}\right] = 1 \qquad (3.10a)$$

In addition to these orders of magnitude, it is assumed that

$$\theta[(T_w - T_o)/T_o, \bar{T}', T_1', c_p', k'] = 1 \qquad (3.10b)$$

$$\theta[M_o, 2\delta_{ac}/\lambda, (a/\lambda)] = \delta \qquad (3.10c)$$

$$\theta\left[\frac{\partial \bar{p}'}{\partial x'}\right] = \delta^2 \qquad (3.10d)$$

$$\theta\left[\frac{\partial \bar{p}'}{\partial y'}\right] = \delta^4 \qquad (3.10e)$$

where

$$\delta_{ac} = \sqrt{2\nu_o/\omega} \qquad (3.11)$$

The assumptions expressed by equations 3.10a, 3.10d, 3.10e and 3.10c are the same orders of magnitude assumed by Purdy (27) in his analysis of the flow field. The assumptions in equation 3.10b are orders of magnitude assumed for the present analysis. An explanation of the basis for these assumptions is given in Appendix A.

Method of Reduction

Under the foregoing assumptions the reduced governing equations can be obtained as follows:

Step 1. The equation for the time-mean temperature is obtained from equation A.30 (the energy equation) by equating the coefficients of the exponential functions, $\exp(-in\omega t)$. For $n = 0$, the terms are independent of time and the governing equation for the time-mean temperature results. This is expressed in dimensional form by equation A.31. By introducing dimensionless variables into equation A.31 and then performing an order of magnitude analysis and retaining only the most dominant terms the following equation for the dimensionless time-mean temperature is obtained.

$$\frac{\partial^2 \bar{T}'}{\partial \bar{y}'^2} - \frac{2}{\pi} Pr_o (M_o a')^2 \bar{u}' \frac{\partial \bar{T}'}{\partial x'} - \frac{1}{\pi} Pr_o (M_o a')^2 \bar{v}' \frac{\partial \bar{T}'}{\partial \bar{y}'} = 0 \qquad (3.12)$$

Step 2. The time-dependent temperature, which is assumed to be of the form,

$$T_1(x,y,t) = \text{Real} \left[\sum_{n=1}^{\infty} T_{1n}(x,y) \exp(-in\omega t) \right] \qquad (3.13)$$

is also obtained from equation A.30 by equating coefficients of the terms $\exp(-in\omega t)$ for n = 1,2,3, ---. The results of this operation are expressed by equations A.32, A.33 and A.34. By introducing dimensionless variables into these equations and then performing an order of magnitude analysis on each of them, the following equations are obtained for the components $T_{1n}(x,y)$:

$$T_{11}(x,y) = - i(\gamma - 1)M_o T_o \sin(\omega x/c_o) \tag{3.14}$$

$$T_{1n}(x,y) = 0, \text{ for } n > 1. \tag{3.15}$$

Equations 3.1 through 3.4 and 3.12 through 3.15 together provide a complete mathematical model for the analytical system shown in Figure 9, subject to the seven restrictions upon which the development in this chapter is predicated. The work of Purdy provides a solution to equations 3.1 through 3.4 and permits the calculation of the coefficients in equation 3.12. Therefore, the present analysis is reduced to the problem of finding a solution to equation 3.12.

CHAPTER IV

SOLUTION OF THE GOVERNING EQUATIONS

Solution for the Temperature Field

The development presented in the previous chapter resulted in a linear partial differential equation for the dimensionless time-mean temperature and a system of defining equations for the components $T_{1n}(x,y)$ which represent the time-dependent temperature

$$T_1(x,y,t) = \text{Real}\left[\sum_{n=1}^{\infty} T_{1n}(x,y)\exp(-in\omega t)\right]. \tag{4.1}$$

For convenience, the defining equations are repeated here.

$$\frac{\partial^2 \bar{T}'}{\partial \bar{y}'^2} - \frac{2}{\pi} Pr_o (M_o a')^2 \bar{u}' \frac{\partial \bar{T}'}{\partial \bar{x}'} - \frac{1}{\pi} Pr_o (M_o a')^2 \bar{v}' \frac{\partial \bar{T}'}{\partial \bar{y}'} = 0 \tag{4.2}$$

$$T_{11}(x,y) = -i(\gamma - 1)M_o T_o \sin(\omega x/c_o) \tag{4.3}$$

$$T_{1n}(x,y) = 0, \text{ for } n > 1 \tag{4.4}$$

These equations have been derived from the general energy equation, equation 3.5, by assuming that the temperature of the fluid could be expressed as the sum of a time-dependent component of the form given

by equation 4.1, and a component which is completely independent of time; equating coefficients of the terms $\exp(-in\omega t)$; and then performing an order of magnitude analysis to eliminate those terms in each of the equations which were felt to be of negligible importance.

The boundary conditions which must be satisfied by equation 4.2 are

$$\bar{T}'(x',0) = 0 \tag{4.5a}$$

$$\bar{T}'(0,\bar{y}') = 1 \tag{4.5b}$$

$$\left.\frac{\partial \bar{T}'}{\partial \bar{y}'}\right|_{\bar{y}'=1} = 0 \text{ for all } x'. \tag{4.5c}$$

The condition at $\bar{y}' = 0$ is based on the assumption that the fluid immediately adjacent to the walls of the channel will have the same temperature as the wall. The condition expressed by equation (4.5c) corresponds to the assumed symmetry condition at the centerline of the channel. The remaining boundary condition is due to the assumption that the fluid is isothermal until it reaches the thermal entrance at $x' = 0$.

Equation 4.2 is a linear, homogeneous, second-order, partial differential equation with variable coefficients. The complexity of the equation becomes apparent when Purdy's (27) solution for the velocity components, $\bar{u}'(x',\bar{y}')$ and $\bar{v}'(x',\bar{y}')$, are introduced into the coefficients. Written in terms of $\bar{y}'$ instead of y' Purdy's solution becomes

$$\bar{u}'(x',\bar{y}') = \frac{3M}{M_o^2}[\bar{y}' - \frac{1}{2}(\bar{y}')^2] \tag{4.6}$$

$$- \frac{1}{8}\sin(2\pi x')\{[9 - \frac{27}{2a'}][\bar{y}' - \frac{1}{2}(\bar{y}')^2]$$

$$- 3 + \exp(- a'\bar{y}')[2\cos(a'\bar{y}') + 6\sin(a'\bar{y}') + \exp(- a'\bar{y}')]\}$$

$$\bar{v}'(x',\bar{y}') = - \frac{\pi}{4}[\cos(2\pi x')\{[9 - \frac{27}{2a'}][\frac{1}{3}(\bar{y}')^3 - (\bar{y}')^2] \tag{4.7}$$

$$+ 6\bar{y}' - \frac{1}{a'}[10 - \exp(- a'\bar{y}')\{9\cos(a'\bar{y}')$$

$$+ 5\sin(a'\bar{y}') + \exp(- a'\bar{y}')\}]\} + \frac{1}{a'}[\exp(- a'\bar{y}')\{\cos(a'\bar{y}')$$

$$+ \sin(a'\bar{y}')\} - 1]\ ].$$

Thus, the mathematical model as developed in Chapter III has been further reduced and simplified to produce a model which offers some hope for solution. Equations 4.1 through 4.7 are considered to be the minimum components of a mathematical description of the problem under consideration.

Attempted Closed-Form Solutions

Several attempts were made to solve equation 4.2, subject to the boundary conditions 4.5, in closed form. Unfortunately, all the attempts were unsuccessful for various reasons; however, a brief summary of these attempts will be given.

(1) The first method which was attempted was that of separation of variables. A separation proved to be impossible because of the form of the velocity components, $\bar{u}'(x',\bar{y}')$ and $\bar{v}'(x',\bar{y}')$, which may be written in the form

$$\bar{u}'(x',\bar{y}') = f_1(\bar{y}') + f_2(\bar{y}')\sin(2\pi x')$$

$$\bar{v}(x',\bar{y}') = f_3(\bar{y}')\cos(2\pi x') + f_4(\bar{y}') \ .$$

If one assumes a solution of equation 4.2 to be of the form

$$\bar{T}'(x',\bar{y}') = F(x')G(\bar{y}'),$$

then it is easily seen that it is impossible to separate the variables to form an equation of the form

$$f\ (x') = g\ (\bar{y}') = \text{constant}.$$

(2) The second method which was attempted consisted of assuming that the solution could be written in the form of a power series; i.e.,

$$\bar{T}'(x',\bar{y}') = \sum_{m=0}^{\infty} \sum_{n=0}^{\infty} A_{mn}(x')^m(\bar{y}')^n$$

The difficulty with this assumption arose in trying to satisfy the boundary conditions, 4.5a and 4.5b. Equation 4.5a implies that

$$A_{m,o} = 0 \text{ for all } m \geq 0 \qquad (a)$$

and equation 4.5b implies that

$$A_{o,o} = 1 \qquad (b)$$

$$A_{o,n} = 0 \text{ for all } n > 0; \qquad (c)$$

hence, equations (a) and (b) are contradictory and the assumed form of the solution appears to be unsatisfactory.

(3) The third method which was attempted to obtain a closed form solution consisted of assuming several variations of a Fourier-type series. However, all the variations were basically a series which could be written in the form

$$\bar{T}'(x',\bar{y}') = \sum_{m=0}^{\infty} f_m(x')g_m(\bar{y}'). \qquad (d)$$

This form has some merit in that both boundary conditions, 4.5a and 4.5b could be satisfied by imposing the restrictions

$$f_m(0) = 1 \text{ for all } m \geq 0$$

$$\sum_{m=0}^{\infty} g_m(\bar{y}') = 1 \ .$$

This latter condition may be satisfied by noting that the Fourier sine

series expansion of unity is

$$1 = \sum_{m=0}^{\infty} \frac{4}{(2m+1)\pi} \sin \frac{(2m+1)\pi\bar{y}'}{2}$$

Therefore, by defining

$$g_m(\bar{y}') = \frac{4}{(2m+1)\pi} \sin \frac{(2m+1)\pi\bar{y}'}{2}$$

we can satisfy all three boundary conditions. However, substitution of equation (d) into equation 4.2 leads to a multitude of difficulties. Some of the manipulations required in order to separate the variables to obtain an equation (or equations) to define the $f_m(x')$ leads to some embarrassing questions concerning the convergence of infinite series. Since in each case some of the series were divergent the method was abandoned, and in fact, the hope of obtaining a closed form solution was abandoned in favor of a numerical solution.

Numerical Solution

A numerical solution may be obtained for equation 4.2 by approximating the derivatives with finite differences. For this purpose the following approximations are used (see Figure 10):

$$\frac{\partial \bar{T}'}{\partial \bar{y}'} = \frac{\bar{T}'_{i+1,j} - \bar{T}'_{i-1,j}}{2\Delta\bar{y}'} \qquad (4.8a)$$

$$\frac{\partial^2 \bar{T}'}{\partial \bar{y}'^2} = \frac{1}{2(\Delta \bar{y}')^2} [\bar{T}'_{i+1,j+1} - 2\bar{T}'_{i,j+1} + \bar{T}'_{i-1,j+1} \qquad (4.8b)$$

$$+ \bar{T}'_{i+1,j} - 2\bar{T}'_{i,j} + \bar{T}'_{i-1,j}]$$

$$\frac{\partial \bar{T}'}{\partial x'} = \frac{1}{12\Delta x'} [(\bar{T}'_{i-1,j+1} - \bar{T}'_{i-1,j}) + 10(\bar{T}'_{i,j+1} - \bar{T}'_{i,j}) \qquad (4.8c)$$

$$+ (\bar{T}'_{i+1,j+1} - \bar{T}'_{i+1,j})]$$

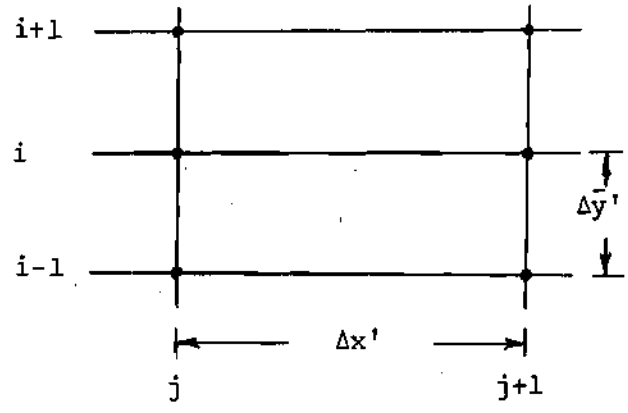

Figure 10. Grid-Point Pattern for Finite Difference Approximations.

Figure 10. Grid-Point Pattern for Finite Difference Approximations.

Substitution of these approximations into equation 4.2 gives the following difference equation

$$A_i \bar{T}'_{i+1,j+1} + B_i \bar{T}'_{i,j+1} + C_i \bar{T}'_{i-1,j+1} = D_i \tag{4.9}$$

where

$$A_i = \frac{6\Delta x'}{(\Delta \bar{y}')^2} + \phi_1(x'_j, \bar{y}'_{i,j}) \tag{4.10a}$$

$$B_i = 10\phi_1(x'_j, \bar{y}'_{i,j}) - \frac{12\Delta x'}{(\Delta \bar{y}')^2} \tag{4.10b}$$

$$C_i = A_i = \frac{6\Delta x'}{(\Delta \bar{y}')^2} + \phi_1(x'_j, \bar{y}'_{i,j}) \tag{4.10c}$$

$$D_i = \phi_1(x'_j, \bar{y}'_{i,j})[\bar{T}'_{i-1,j} + 10\bar{T}'_{i,j} + \bar{T}'_{i+1,j}] \tag{4.10d}$$

$$- \frac{6\Delta x'}{(\Delta \bar{y}')^2} [\bar{T}'_{i+1,j} - 2\bar{T}'_{i,j} + \bar{T}'_{i-1,j}]$$

$$- \frac{6\Delta x'}{\Delta \bar{y}'} \phi_2(x'_j, \bar{y}'_{i,j})[\bar{T}'_{i+1,j} - \bar{T}'_{i-1,j}]$$

$$\phi_1(x'_j, \bar{y}'_{i,j}) = - \frac{2}{\pi} M_o^2 Pr_o (a')^2 \bar{u}'(x'_j, \bar{y}'_{i,j}) \tag{4.10e}$$

$$\phi_2(x'_j, \bar{y}'_{i,j}) = - \frac{1}{\pi} M_o^2 Pr_o (a')^2 \bar{v}'(x'_j, \bar{y}'_{i,j}) \tag{4.10f}$$

Equation 4.9 represents a system of simultaneous linear equations which may be rewritten as

$$A_1\bar{T}'_{2,j+1} + B_1\bar{T}'_{1,j+1} + C_1\bar{T}'_{o,j+1} = D_1 \qquad (4.11a)$$

$$A_i\bar{T}'_{i+1,j+1} + B_i\bar{T}'_{i,j+1} + C_i\bar{T}'_{i-1,j+1} = D_i;\ i=2,3,\ldots,N-1 \qquad (4.11b)$$

$$A_N\bar{T}'_{N+1,j+1} + B_N\bar{T}'_{N,j+1} + C_N\bar{T}'_{N-1,j+1} = D_N \qquad (4.11c)$$

where N represents the number of intervals used to represent the half width of the channel.

Now the boundary condition expressed by equation 4.5a implies that

$$\bar{T}'_{o,j} = 0 \text{ for all } j,$$

and the boundary condition expressed by equation 4.5c implies that

$$\bar{T}'_{N+1,j} = \bar{T}'_{N-1,j} \text{ for all } j.$$

Therefore, equations 4.11 become

$$A_1\bar{T}'_{2,j+1} + B_1\bar{T}'_{1,j+1} = D_1$$

$$A_i\bar{T}'_{i+1,j+1} + B_i\bar{T}'_{i,j+1} + C_i\bar{T}'_{i-1,j+1} = D_i \quad (i=2,3,\ldots,N-1)$$

$$A_N\bar{T}'_{N-1,j+1} + B_N\bar{T}'_{N,j+1} + C_N\bar{T}'_{N-1,j+1} = D_N$$

or, since $A_i = C_i$

$$B_1\bar{T}'_{1,j+1} + A_1\bar{T}'_{2,j+1} = D_1 \qquad (4.12a)$$

$$A_i\bar{T}'_{i-1,j+1} + B_i\bar{T}'_{i,j+1} + A_i\bar{T}'_{i+1,j+1} = D_i \quad (i=2,3,\ldots,N-1) \qquad (4.12b)$$

$$2A_N\bar{T}'_{N-1,j+1} + B_N\bar{T}'_{N,j+1} = D_N \qquad (4.12c)$$

The solution of equations 4.12 gives the dimensionless temperature distribution across the channel cross-section at the $(j + 1)^{th}$ station, assuming that the temperature distribution at the j^{th} station is known. The boundary condition expressed by equation 4.5c provides a known distribution with which the solution may be started and successive solutions of equations 4.12 then give the temperature distribution for as many values of x' as desired. The details of the method of solution used for equations 4.12 are given in Appendix B.

Typical temperature distributions as obtained by the method outlined above are shown in Figures 11 and 12, one case with sound and one case without sound. The value of N which was used in these solutions was N = 100 and the increment of x' was chosen as $\Delta x' = 0.001$. Therefore, the total number of gridpoints was 200,000.

As can be seen from Figures 11 and 12 the effect of sound upon the dimensionless temperature is much less pronounced than in the case of the velocity profile. In fact, without comparing actual values, it is difficult to discern the effects at all on the temperature. However,

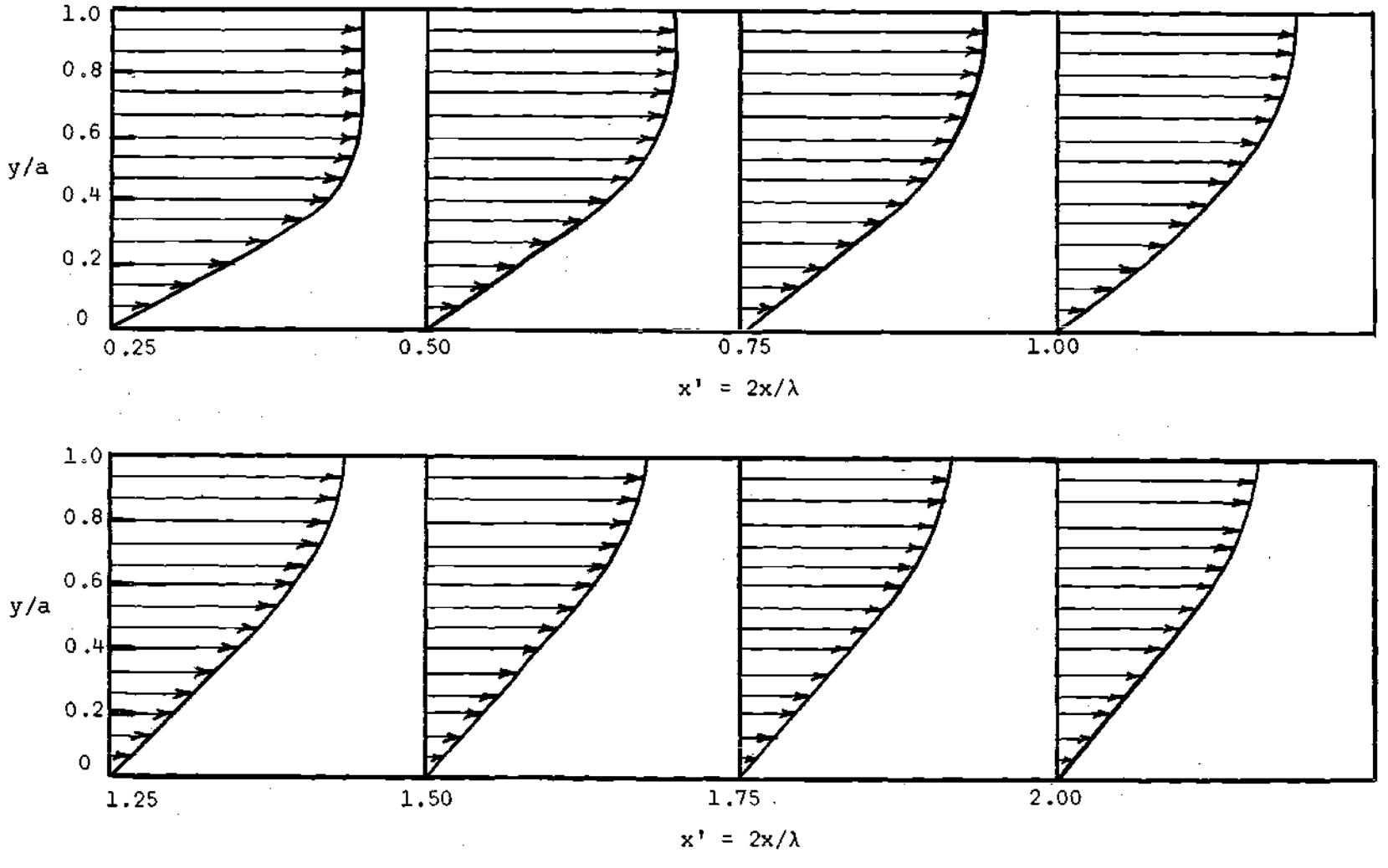

Figure 11. Typical Dimensionless Temperature Profiles for the Case of No-Sound.

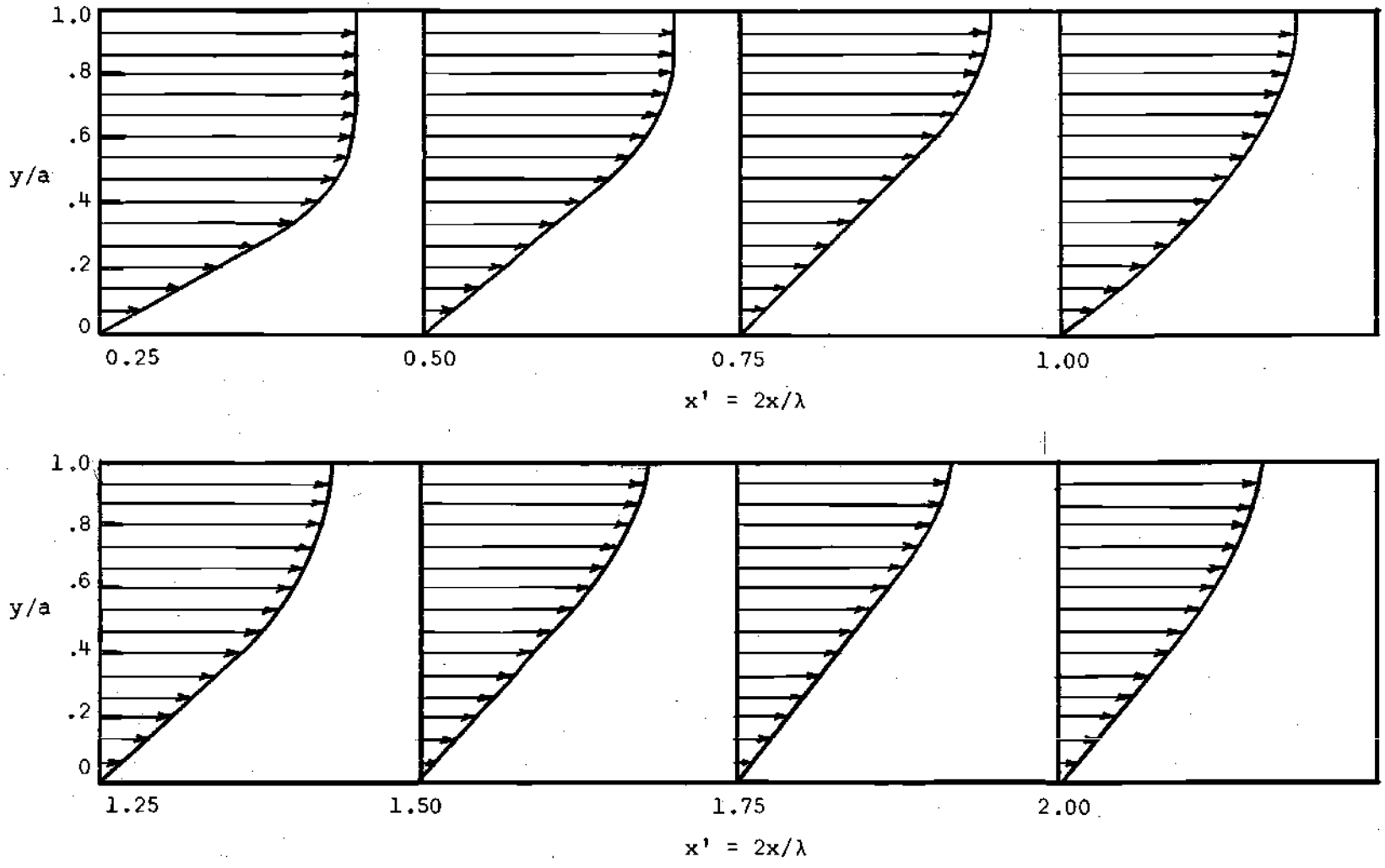

Figure 12. Typical Dimensionless Temperature Profiles with Resonant Acoustic Field Impressed Upon the Flow.

if the two figures are compared quantitatively, it will be found that the profiles with sound do deviate from the profiles without sound.

Heat Transfer Results

Once the temperature distribution has been determined it may be used to calculate the rate of heat transfer through the channel wall into the fluid. The heat transfer calculations are based on the time-mean temperature only since any heat transfer which is due to the fluctuations of the time-dependent temperature will average out to zero over a complete cycle.

The local convective heat transfer coefficient is defined by the energy equation, neglecting changes in kinetic energy; i.e.,

$$hA\Delta T_{am} = \dot{m}c_p\Delta T_B \tag{4.13}$$

where A = Heat transfer area.

ΔT_{am} = Arithmetic mean temperature difference.

$\dot{m}$ = Mass rate of flow.

c_p = Constant pressure specific heat.

ΔT_B = Change in bulk temperature.

h = Local heat transfer coefficient.

In terms of dimensionless quantities, it is shown in Appendix B that the local Nusselt number is given by the equation

$$Nu(x'_{j+1}) = \frac{16(a')^2}{\pi(\Delta x')} Pr_o M \frac{T'_{Bj} - T'_{Bj+1}}{T'_{Bj} + T'_{Bj+1}} \quad . \tag{4.14}$$

It is also shown that the average Nusselt number, based on the logarithmic mean temperature difference, is given by the equation

$$\overline{Nu}(x'_{j+1}) = -\frac{8(a')^2}{\pi x'_{j+1}} Pr_o M \log_e T'_{Bj+1} \qquad (4.15)$$

Correlation of No-Sound Results

In order to test the validity of the numerical technique used to solve equation 4.2 and the usefulness of equations 4.14 and 4.15 several solutions were obtained for various through-flow rates without the presence of an acoustic field. The values of the average Nusselt number as calculated by equation 4.15 were compared with the results of Norris and Streid (41) who have presented theoretically derived values of the heat transfer coefficient for flat ducts with constant surface temperature as a function of the parameter Φ which is defined by (using their notation)

$$\Phi = \frac{c_p GD^2}{kL} \qquad (4.16)$$

where c_p = Specific heat (at constant pressure), BTU/lb-°F.

G = W/S = ρV = weight velocity, lb. per sq. ft. per hr.

D = Equivalent diameter = 4LS/A, ft.

k = Thermal conductivity, BTU per hr. per sq. ft. per °F per ft.

L = Length of duct from entrance of heated portion of duct, ft.

A = Surface area of that part of duct which transfers heat, sq. ft.

S = Cross-sectional area for fluid flow, sq. ft.

It is shown in Appendix B that for a parallel plate channel

$$\Phi = \frac{32}{\pi} (a')^2 Pr_o M/x' . \tag{4.17}$$

The comparison of the results obtained by the methods presented here and those given by Norris and Streid is shown in Figure 13. As can be seen, the results are in excellent agreement.

Sellars, Tribus, and Klein (4) have also solved the problem of heat transfer to laminar flow in a parallel plate channel. Using their results, an equation can be developed (see Appendix B for the derivation) for the average Nusselt number as a function of the parameter Φ defined by equation 4.17. The resulting equation is

$$\overline{Nu}\ (\Phi) = -\frac{1}{4} \Phi \log_e T_B(\Phi) \tag{4.18}$$

where

$$T_B(\Phi) = 1 - 3.0375 \sum_{n=0}^{\infty} \lambda_n^{-7/3} [1 - \exp(-\frac{32}{3} \lambda_n^2/\Phi)] \tag{4.19}$$

$$\lambda_n = 4n + 5/3 \tag{4.20}$$

A comparison of the values calculated with equation 4.18 and those obtained through the numerical solution is shown in Figure 14. Again, the results are seen to be in excellent agreement.

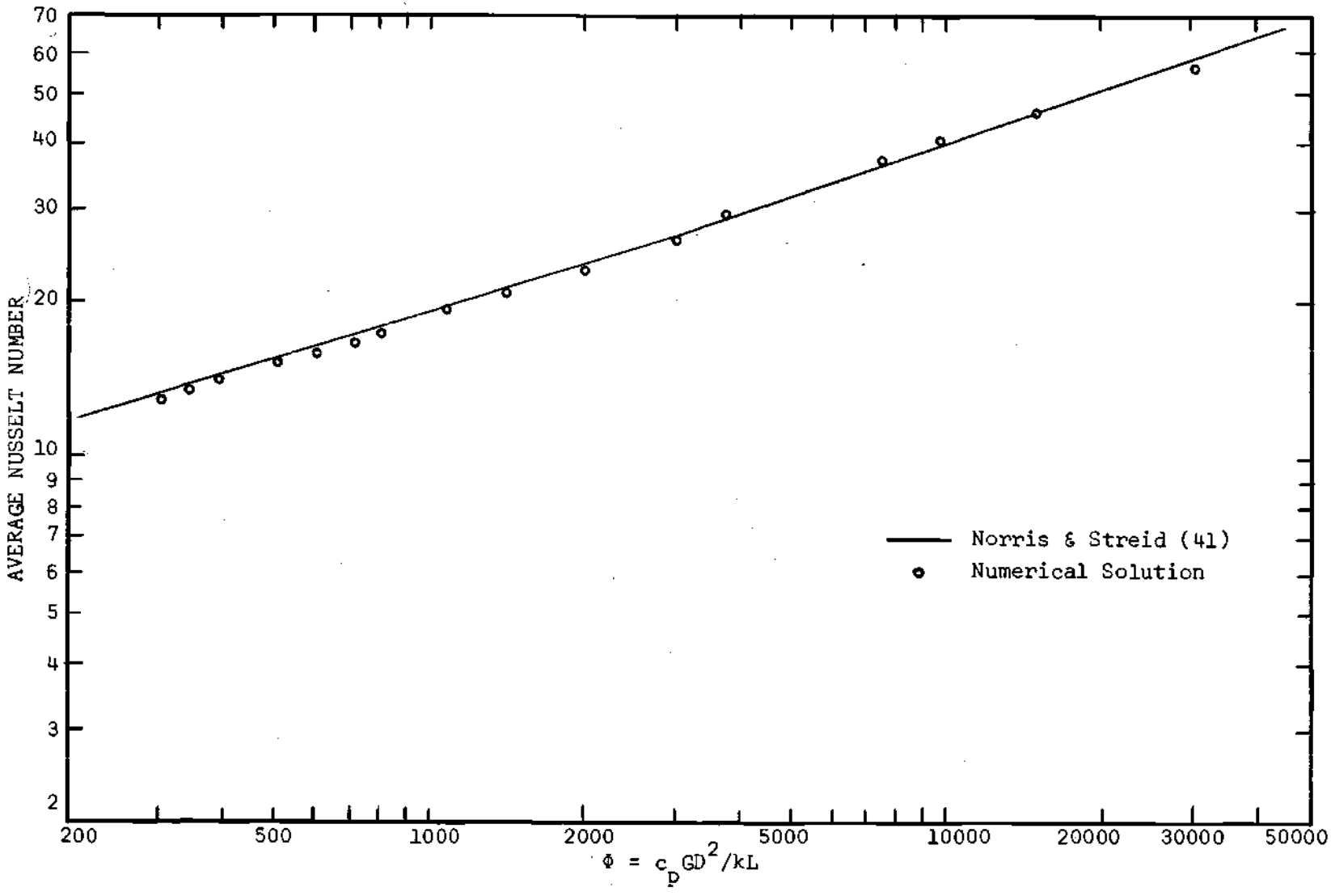

Figure 13. Average Nusselt Numbers Versus Φ. Correlation of No-Sound Data.

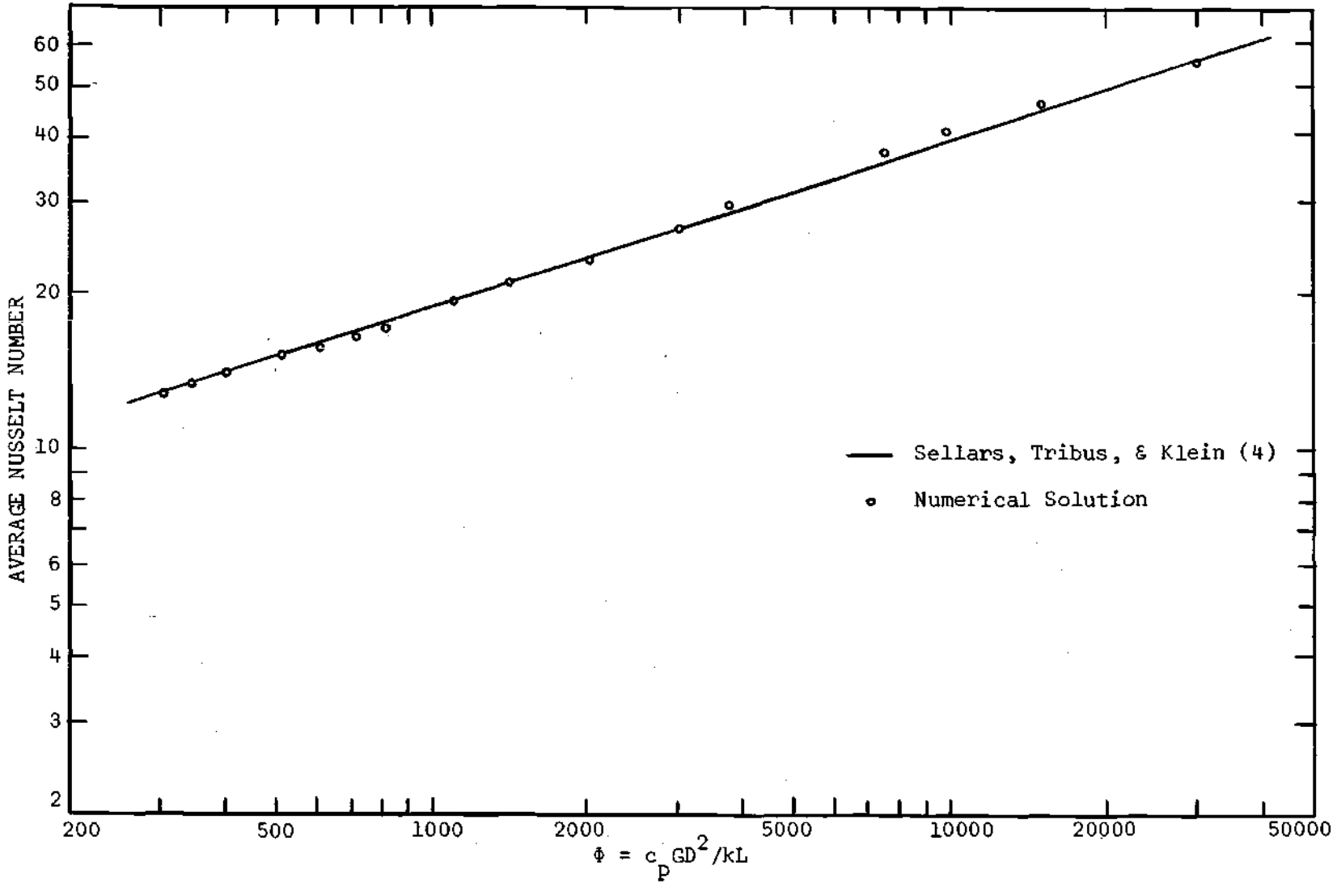

Figure 14. Average Nusselt Number vs. Φ.
Correlation of No-Sound Data.

In addition to the average Nusselt numbers, the results of Sellars, Tribus and Klein can also be used to derive an equation for the local Nusselt numbers, again as a function of the parameter Φ. The equation is

$$Nu(\Phi) = 1.51875 \frac{\Phi^2(1 - \frac{\Delta\Phi}{\Phi})}{\Delta\Phi} \frac{f(\Phi)}{g(\Phi)} \qquad (4.21)$$

where

$$f(\Phi) = \sum_{n=0}^{\infty} \lambda_n^{-7/3} \exp(-\frac{32}{3}\lambda_n^2/\Phi)[1 -$$

$$\exp\{-\frac{32}{3}\lambda_n^2\Delta\Phi/\Phi^2(1 - \frac{\Delta\Phi}{\Phi})\}]$$

$$g(\Phi) = T_B(\Phi) + T_B(\Phi + \Delta\Phi) \qquad (4.22)$$

$$T_B(\Phi) = 1 - 3.0375 \sum_{n=0}^{\infty} \lambda_n^{-7/3}[1 - \exp(-\frac{32}{3}\lambda_n^2/\Phi)] \qquad (4.19)$$

$$T(\Phi + \Delta\Phi) = 1 - 3.0375 \sum_{n=0}^{\infty} \lambda_n^{-7/3} \{1 - \qquad (4.23)$$

$$\exp[-\frac{32}{3}\lambda_n^2(\frac{1}{\Phi} + \frac{\Delta\Phi}{\Phi^2[1 - \Delta\Phi/\Phi]})]\} .$$

A comparison of the values calculated with equation 4.21 and those obtained through the numerical solution is shown in Figure 15.

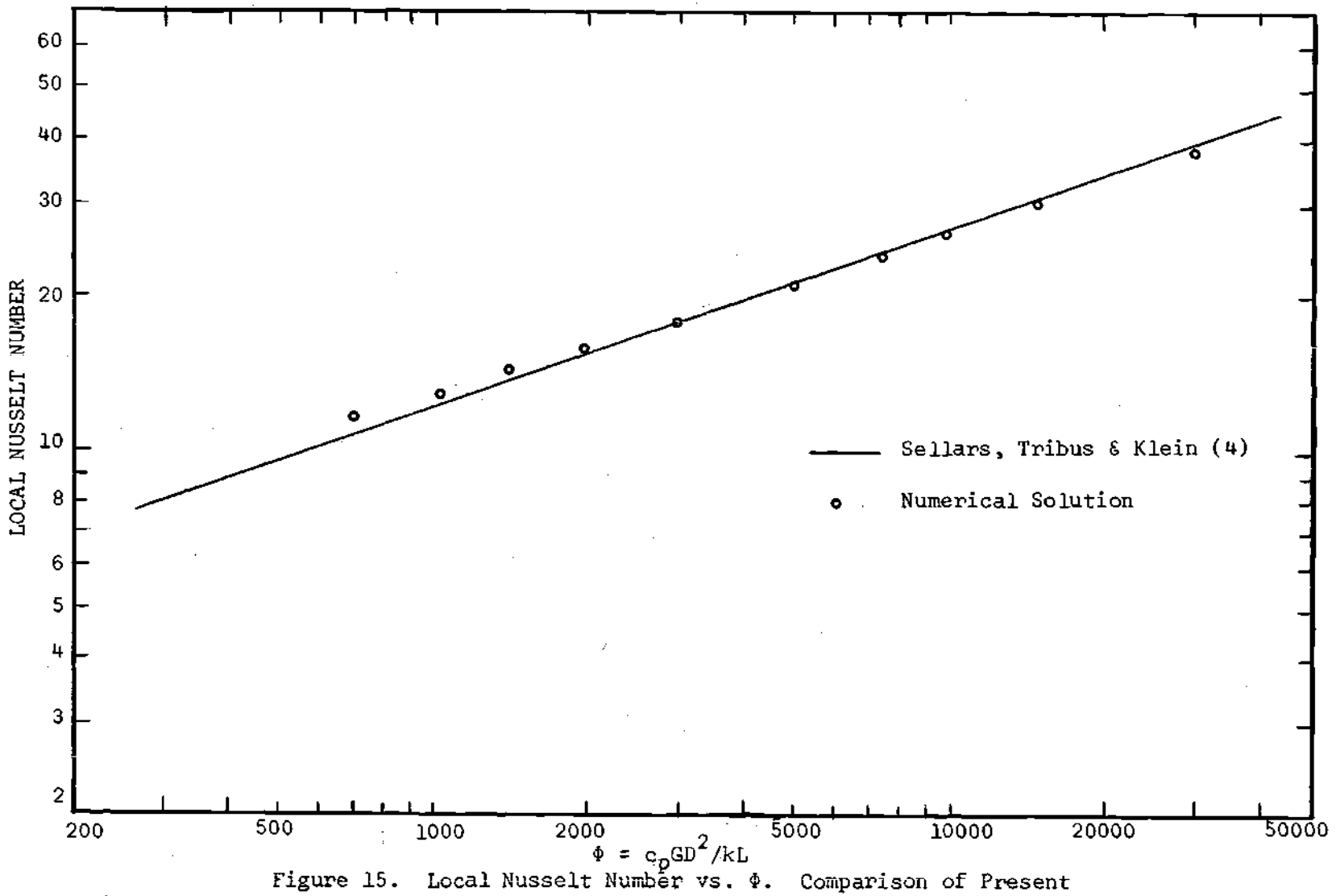

Figure 15. Local Nusselt Number vs. Φ. Comparison of Present Work with that of Sellars, Tribus, & Klein.

The results are in extremely good agreement.

The conclusion to be drawn from the foregoing discussion is that the numerical solution of equation 4.2 and the expressions for the local and average Nusselt numbers give results which are in close agreement with results published in the literature; therefore, the techniques presented here give an accurate prediction of the local and average heat transfer characteristics.

Heat Transfer with Sound

In order to obtain a solution of equation 4.2 for the case of heat transfer with sound, a slight modification in the technique proved to be necessary. It was found that the solution was extremely divergent when the methods of this chapter were used without any modification. The problem of divergence was caused by the velocity $\bar{u}'(x',\bar{y}')$; whenever this function is negative, the coefficient of the diagonal term of the system of finite difference equations is no longer the dominant term in the equation. Unless the diagonal term is the dominant term, then the solution of the system of equations becomes extremely difficult and in this particular problem the results are rapidly divergent. This problem can be avoided by forcing the velocity, $\bar{u}'(x',\bar{y}')$, to be essentially zero in regions where it is actually negative (i.e., in a region containing a vortex). In other words, in the region of vortex flow, the actual velocity, $\bar{u}'(x'_j,\bar{y}'_{i,j})$, was replaced by a velocity $u^*(x'_j,\bar{y}'_{i,j})$ which is defined by

$$u^*(x'_j,\bar{y}'_{i,j}) = \frac{1}{N_1}\sum_{n=1}^{N_1} \bar{u}'(x'_j,\bar{y}'_{n,j}) \quad (i=1,2,\ldots,N_1) \qquad (4.24a)$$

$$u^*(x'_j, \bar{y}'_{i,j}) = \bar{u}'(x'_j, \bar{y}'_{i,j}) \quad (i=N_1+1, N_1+2, \ldots, N) \qquad (4.24b)$$

where N_1 is selected as the minimum number of values of $\bar{u}'(x'_j, \bar{y}'_{i,j})$ required to make $u^*(x'_j, \bar{y}'_{i,j})$ a positive number. By making this simple modification to the numerical technique, the problem of divergence ceases to be critical. In the regions where $\bar{u}'(x'_j, \bar{y}'_{i,j})$ is positive for all $\bar{y}'$, then $N_1 = 1$; i.e., the actual velocity is used.

A logical question which should be asked at this point is, how is the solution affected by this modification of the velocity profile? This can best be answered by referring to Figure 16 which shows a plot of the local Nusselt number as a function of x'. In the shaded intervals of the figure, the velocity profile was modified as described above and in the unshaded intervals the velocity profile was unaltered. As can be seen, the values of heat transfer coefficient which were obtained form a smooth curve with no discernable discontinuities, and since the curve was plotted with only 1/100 of the points actually calculated, it seems reasonable to say that the alteration of the velocity profile does not alter the validity, or usefulness, of the results.

However, in order to obtain an additional check on the numerical procedure, a relaxation technique was employed. After integrating through the region of the vortex, the temperatures thus obtained were used to calculate the residual at each grid point. Due to the limited storage space of the computer, the mesh size used in the relaxation method was approximately ten times as large as the mesh size used for

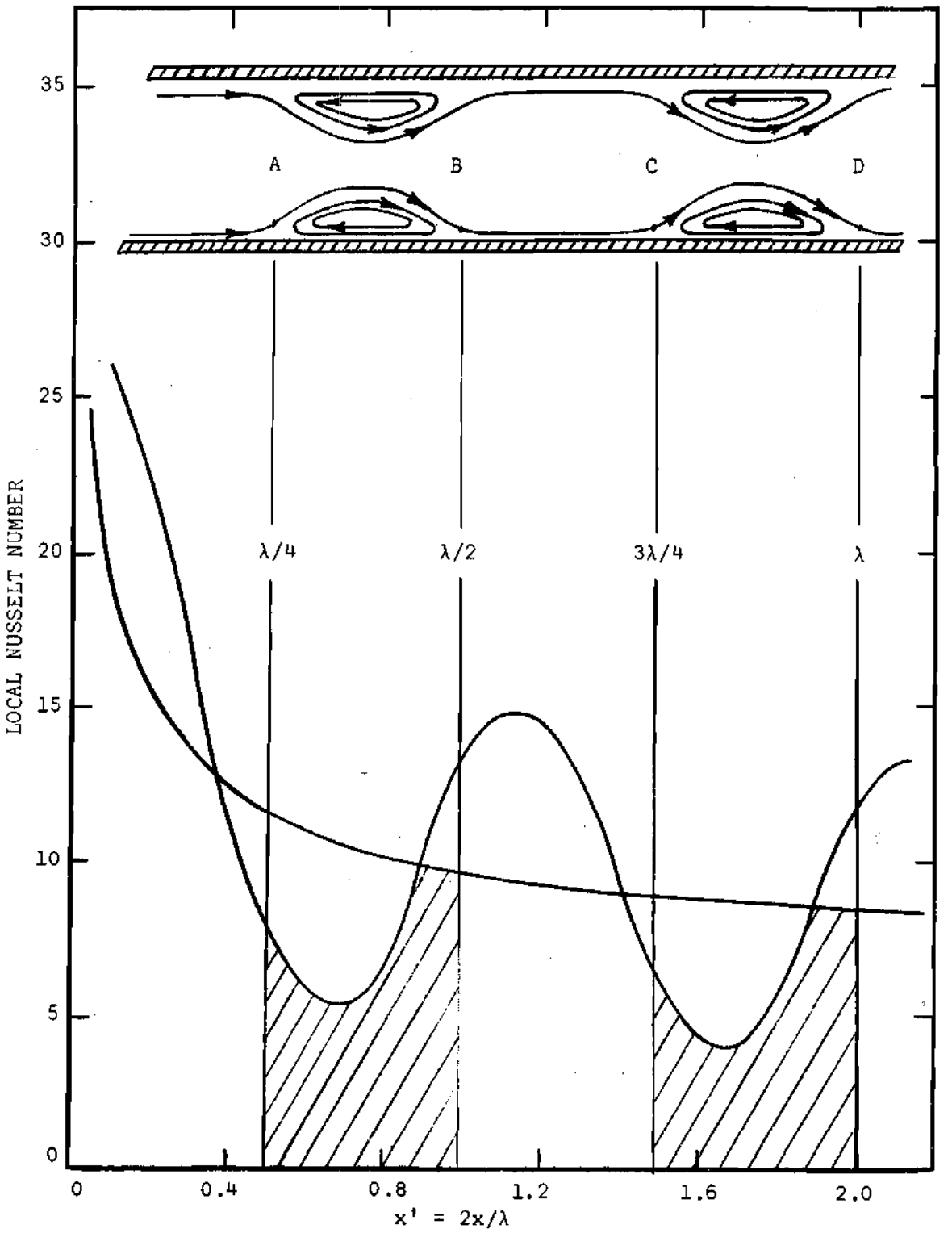

Figure 16. Local Nusselt Number vs. x' Showing Relation of Heat Transfer and Velocity Field and Regions of Approximation.

integration purposes. The residual at each grid point was then relaxed to zero by altering the temperature at the central grid point. After several iterations of the relaxation process, the temperatures had changed by only a negligible amount and the Nusselt numbers were changed also by a negligible amount. Therefore, the relaxation technique was not used except as a check on the results of the numerical integration.

An energy balance was also calculated by noting that the energy which crosses the wall of the channel must show up as a change in the mixed-mean, or bulk, temperature of the fluid. In equation form, this may be stated by

$$\dot{m} c_p \Delta T_B = \int - k\left(\frac{\partial T}{\partial y}\right)_{y=0} dA,$$

where dA represents the elemental area of the channel wall. These two quantities were calculated separately and the results agreed within ± 5 per cent. The ratio, r, defined by

$$r = \frac{\dot{m} c_p \Delta T_B}{\int - k\left(\frac{\partial T}{\partial y}\right)_{y=0} dA}$$

is shown in the tabulated results given in Table 3 of Appendix C.

Using the methods heretofore described, several solutions of equation 4.2 have been obtained using various values of the parameters $M_o^2 Pr_o$, $M_o Pr_o a'$, and M/M_o^2. The results of these solutions are shown graphically in Figures 17 through 28, and in tabular form in Table 3

of Appendix C. Only a representative sample of the solutions actually obtained is shown.

It is to be noted from Figures 17 through 20 that the resonant acoustic field produced a very pronounced effect upon the local Nusselt number. It may be seen that the local Nusselt number varies as a slightly damped periodic function. In other words, an envelope may be drawn such that it is tangent to the maxima (or minima) of the curves representing the effect of sound and the resulting envelope has the shape of an exponentially-decaying function. This envelope, however, will not be parallel to the no-sound curve because it may be noted (by actual measurement) from the curves that the magnitude of the deviation from the no-sound curve is slowly diminishing as x' increases. The period of the function, as determined from the data of Figures 17 through 20, is one-half the wavelength of the acoustic vibration and the amplitude is a function of the intensity or amplitude of the vibration.

It is interesting to note that another important correlation of the data shown in Figures 17 through 20 exists. For a given sound pressure level, the maximum deviation of the local Nusselt number from the corresponding no-sound Nusselt number is used to form the ratio $\Delta Nu_{max}/Nu_{no\text{-}sound}$; then, if this ratio is divided by the cube root of the Reynolds number and plotted as a function of the parameter M_o^2/M the result is a straight line as shown in Figure 29.

Another interesting effect is shown in Figure 16. Purdy (27) predicted the existence of standing vortices which were one-quarter wave-length long. He then theorized that the minimum heat transfer co-

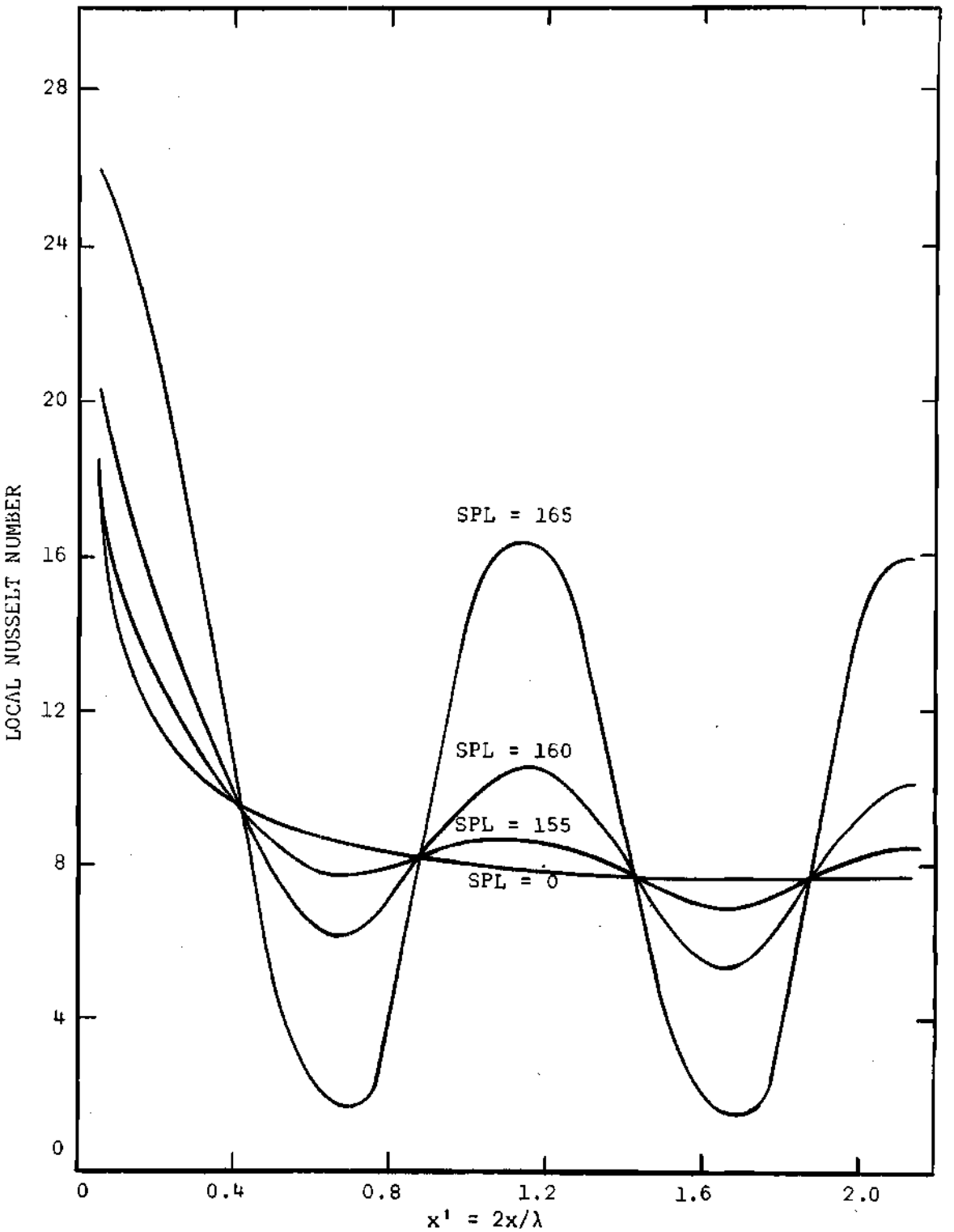

Figure 17. Local Nusselt Number vs. x'.
Channel Reynolds Number = 2000.

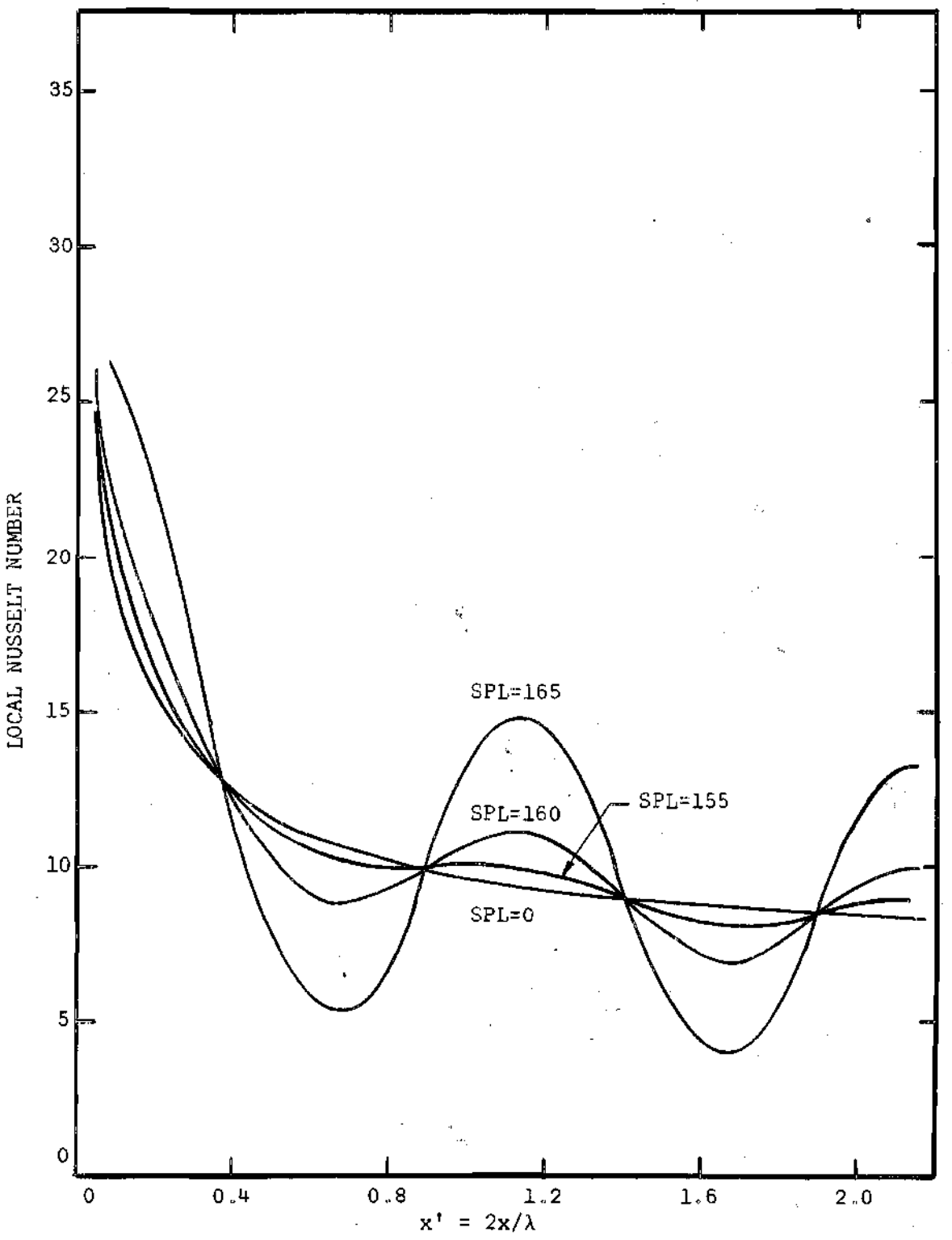

Figure 18. Local Nusselt Number vs. x'.
Channel Reynolds Number = 5000.

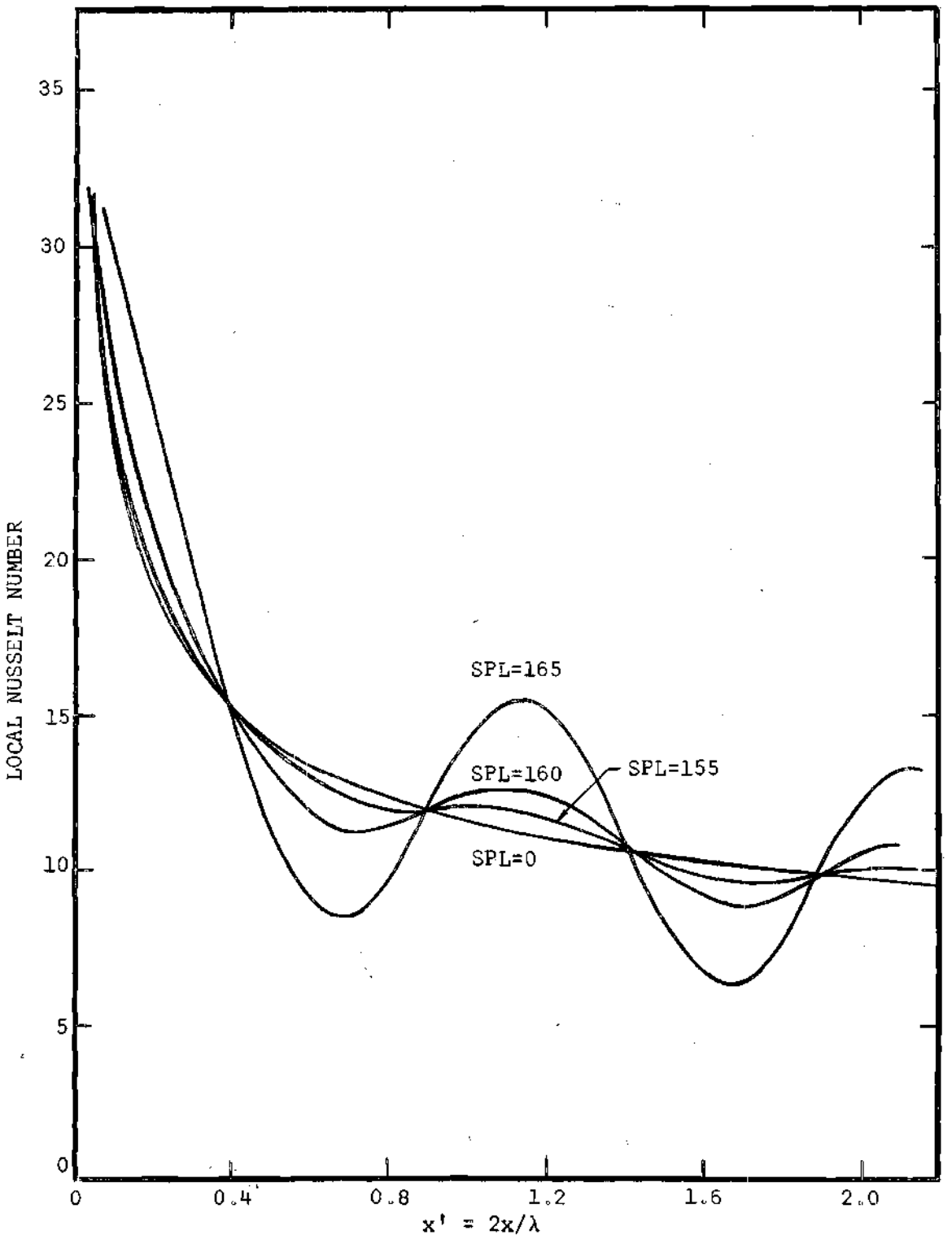

Figure 19. Local Nusselt Number vs. x'.
Channel Reynolds Number = 10000.

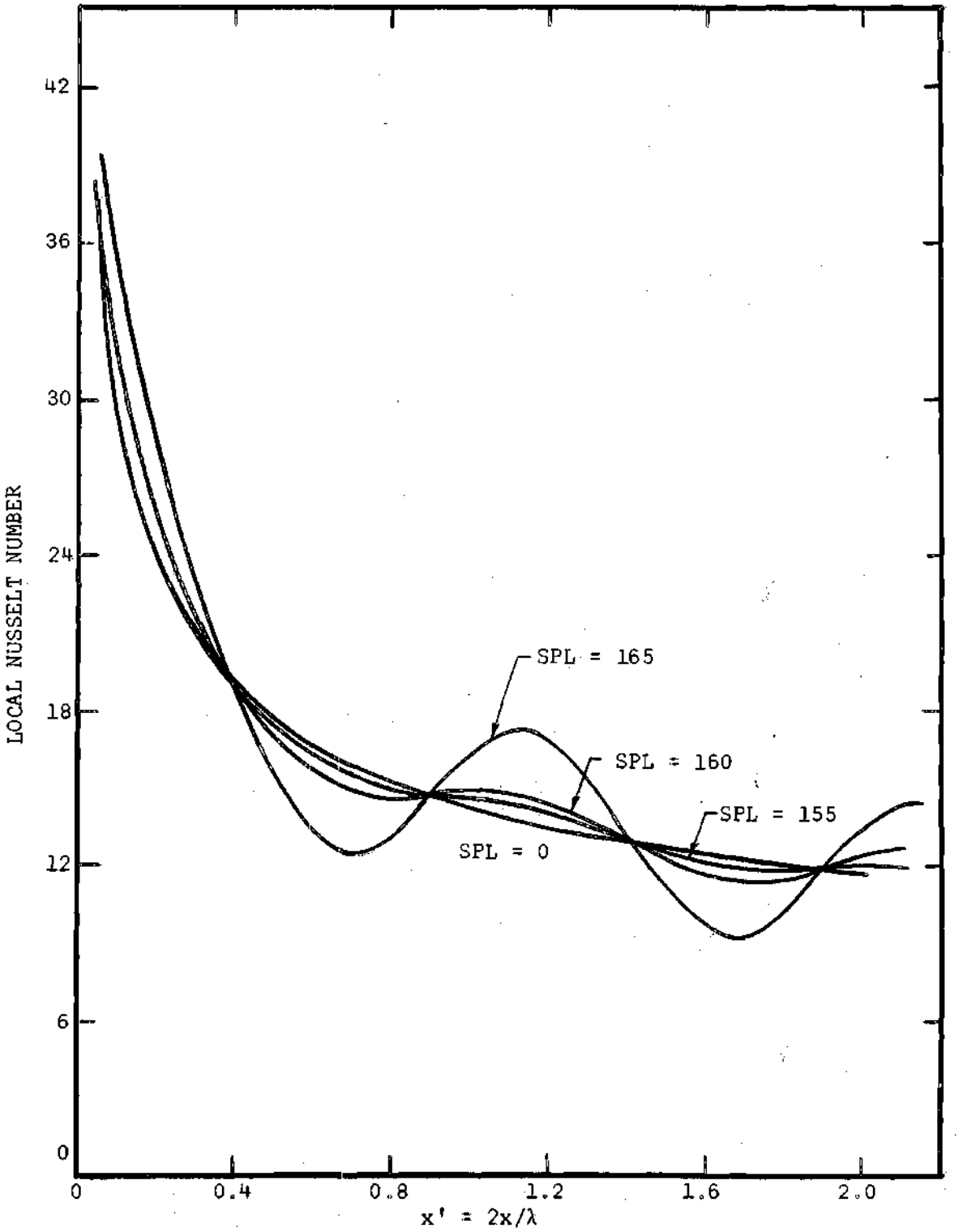

Figure 20. Local Nusselt Number vs. x'.
Channel Reynolds Number = 20000.

efficient should occur at the points labeled A and C in the figure and that the maximum heat transfer coefficient should occur at the points labeled B and D. However, the results of the numerical solution of the energy equation indicate that there will be a phase lag and that the maxima and minima of the heat transfer coefficient actually occur downstream of the positions at which they would be expected to occur from Purdy's explanation. This phase lag has also been observed experimentally.

The effect of frequency and channel width variations is shown in Figures 21 through 28. It may be seen that modest changes in frequency have negligible effect except in the regions of maximum deviation from the corresponding no-sound value of the Nusselt number whereas changes in channel width have a marked effect upon the local values of the Nusselt number. These results are somewhat misleading since a frequency change shifts x' for no change in the no-sound Nusselt number. Again in the case of a change in duct width the heat transfer coefficient may remain constant but the Nusselt number is proportional to the channel width, a. However, for constant Reynolds number (Re) and sound-pressure level (SPL), a variation in channel width (a) forces a corresponding change in the through-flow velocity; i.e., if the channel width is doubled, the through-flow velocity must be halved in order to hold the Reynolds number constant. The change in velocity is also reflected in the parameter M_o^2/M. This result again clearly points out the importance of the parameter M_o^2/M rather than Re and SPL.

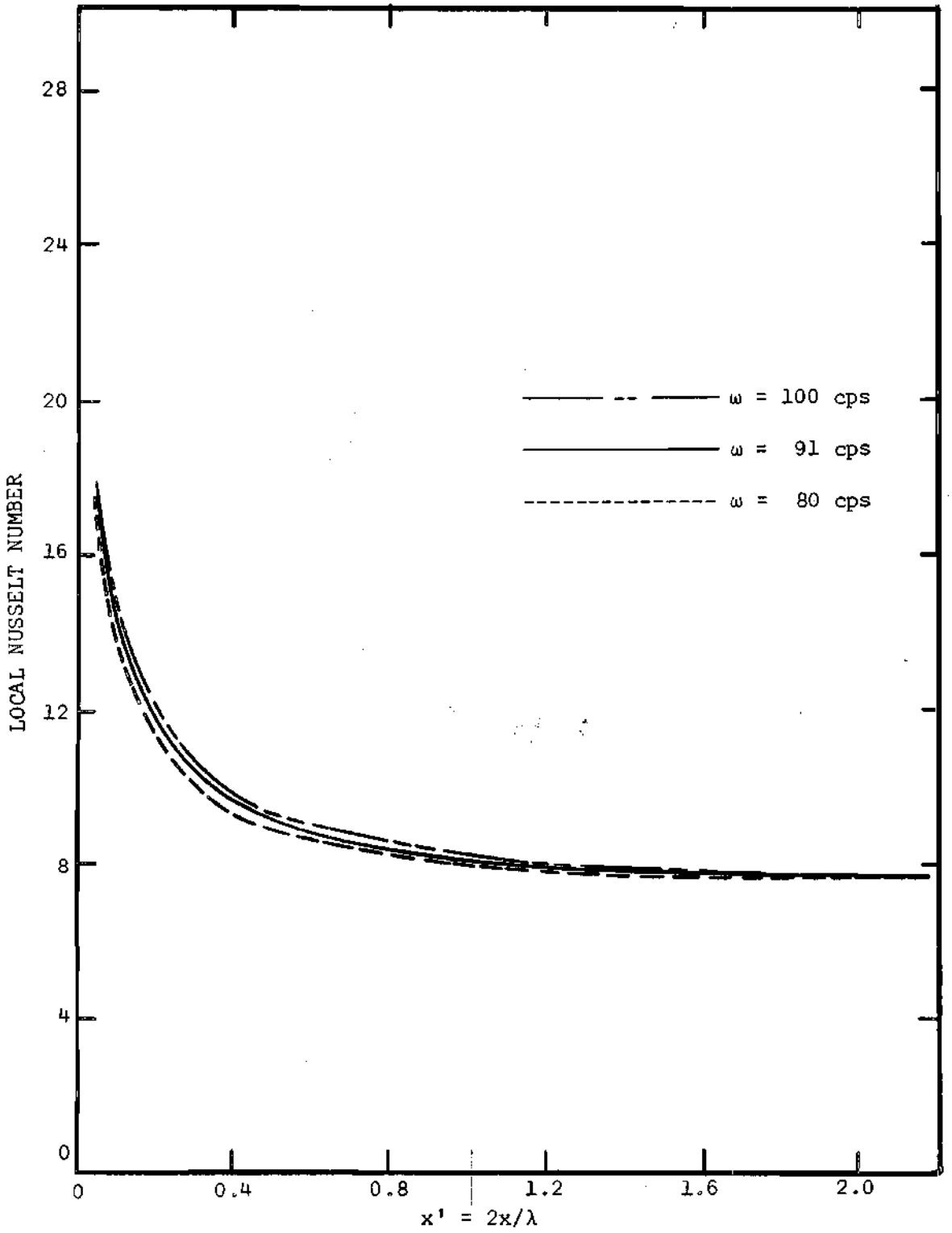

Figure 21. Local Nusselt Number vs. x' with the Frequency, ω, as a Parameter. Channel Reynolds Number = 2000. SPL = 0.

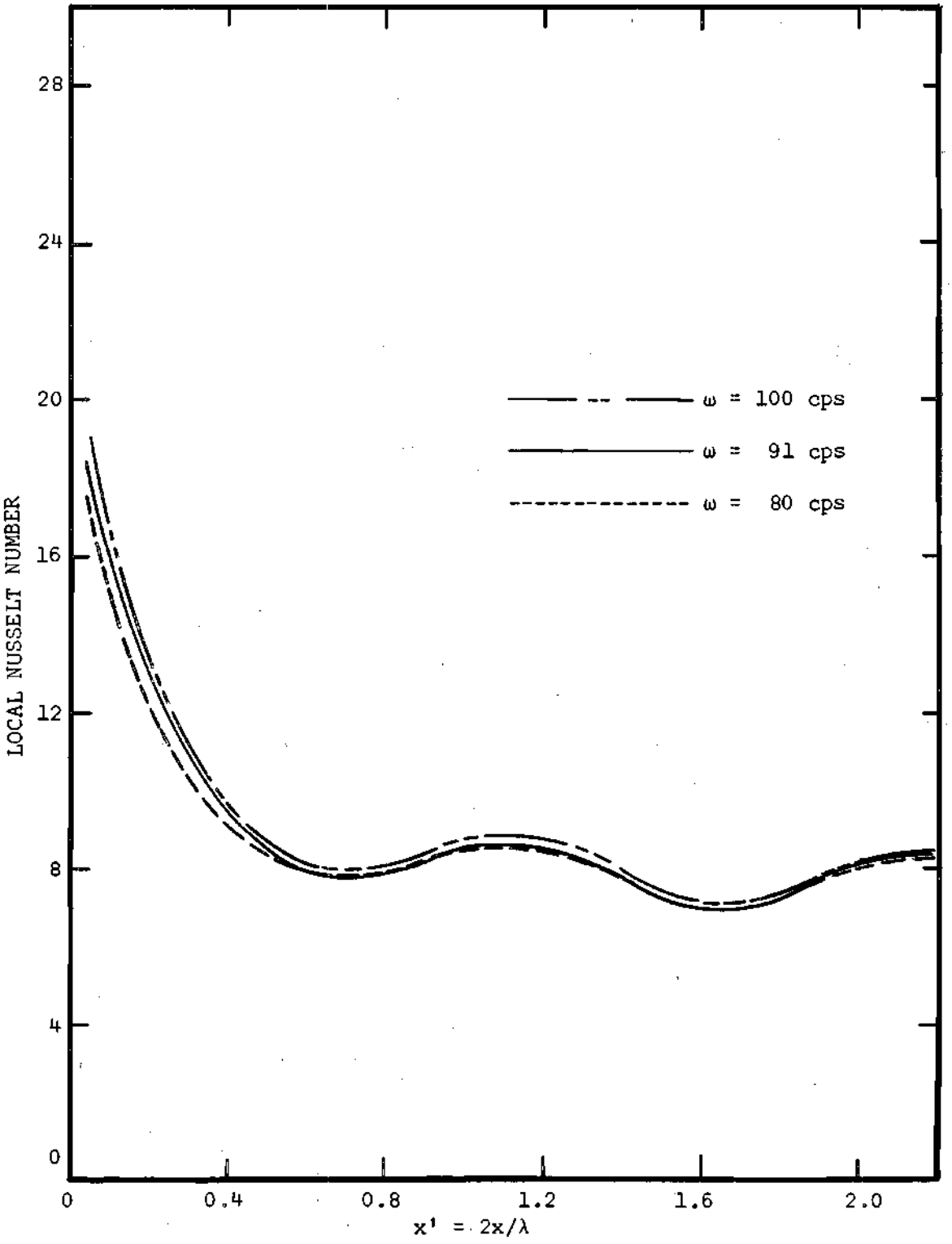

Figure 22. Local Nusselt Number vs. x' with the Frequency, ω, as a Parameter. Channel Reynolds Number = 2000. SPL = 155.

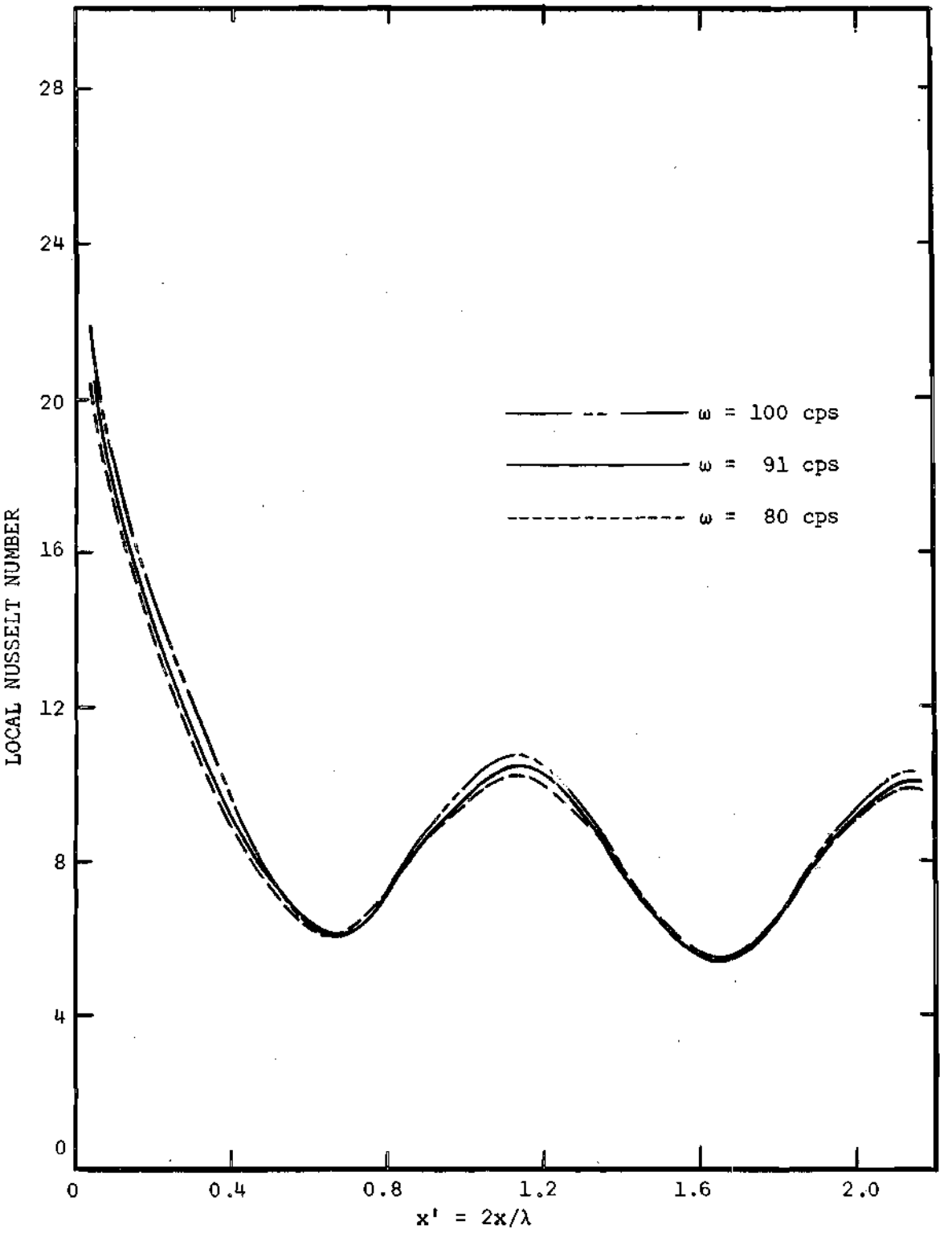

Figure 23. Local Nusselt Number vs. x' with the Frequency, ω, as a Parameter. Channel Reynolds Number = 2000. SPL = 160.

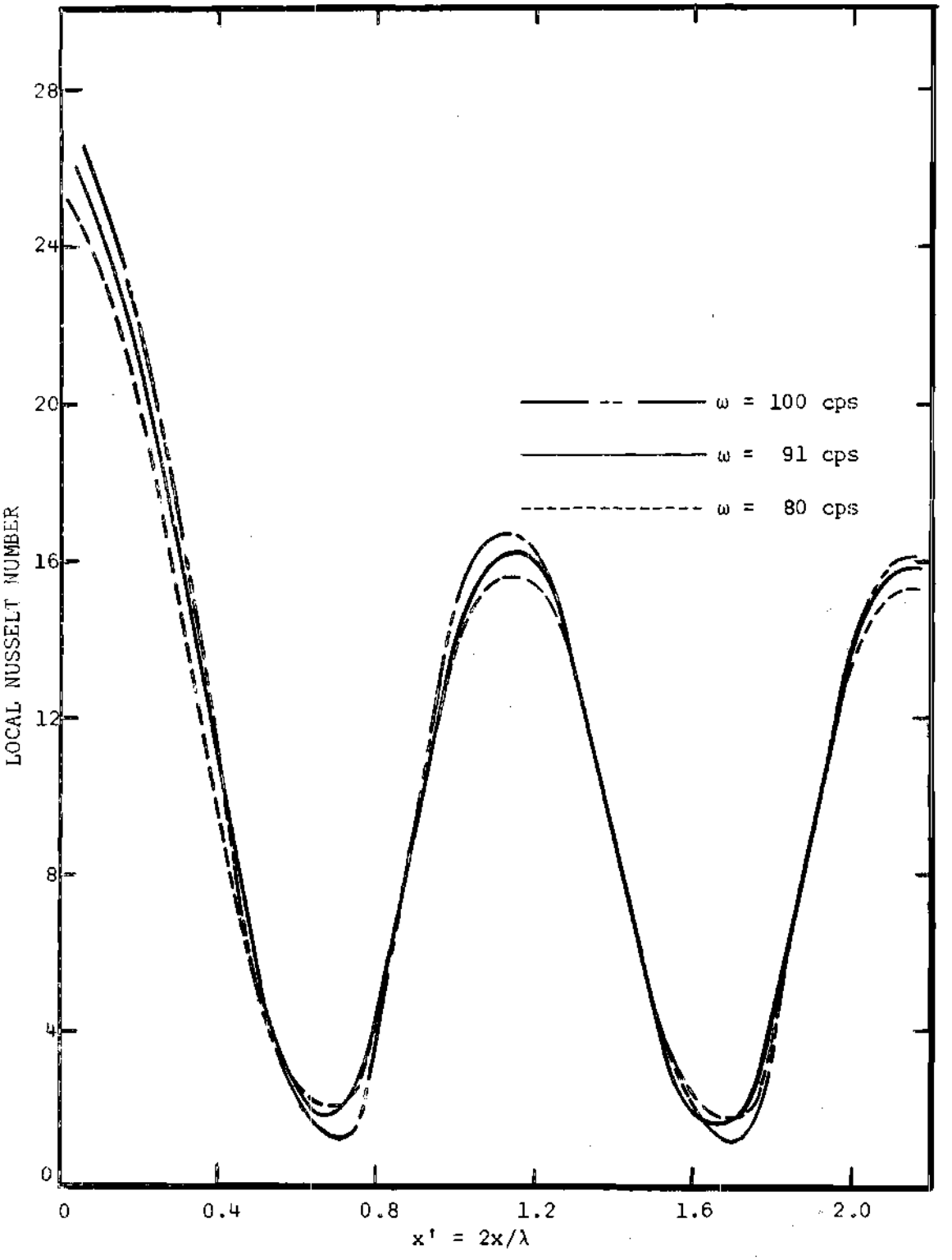

Figure 24. Local Nusselt Number vs. x' with the Frequency, ω, as a Parameter. Channel Reynolds Number = 2000. SPL=165 db.

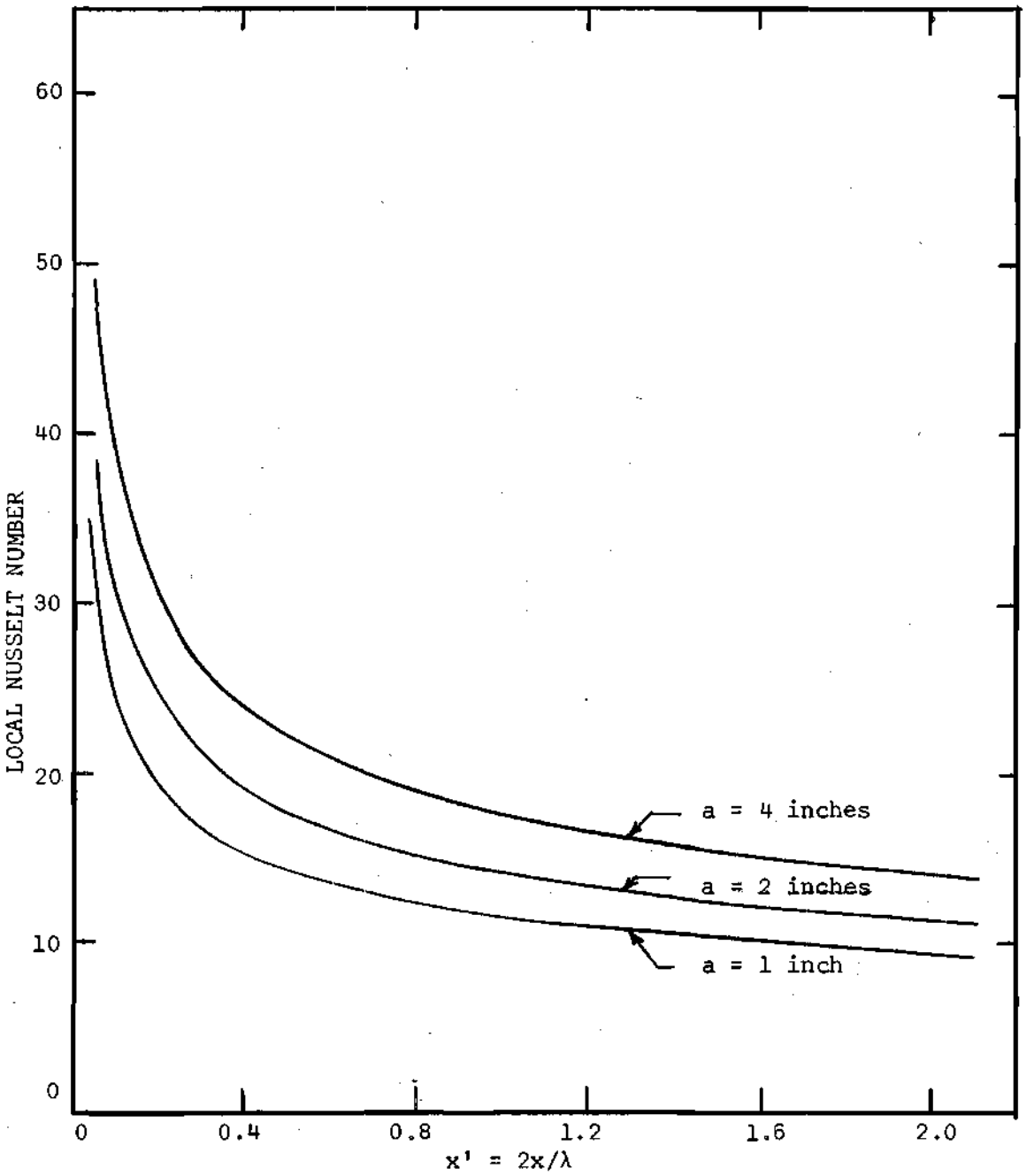

Figure 25. Local Nusselt Number vs. x' with the Channel Width, a, as a Parameter. Channel Reynolds Number = 20000. SPL = 0 db.

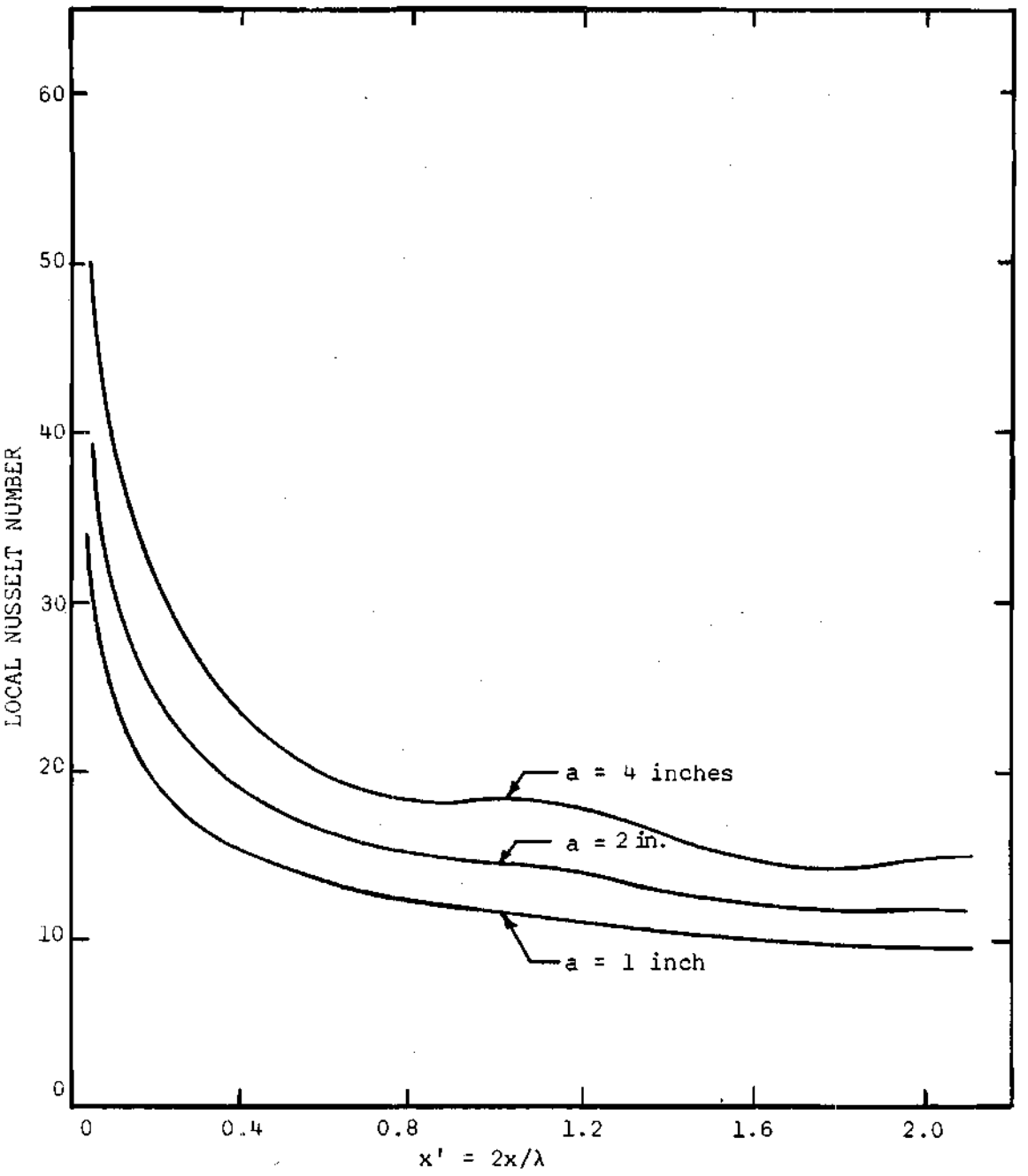

Figure 26. Local Nusselt Number vs. x' with the Channel Width, a, as a Parameter. Channel Reynolds Number = 20000. SPL = 155 db.

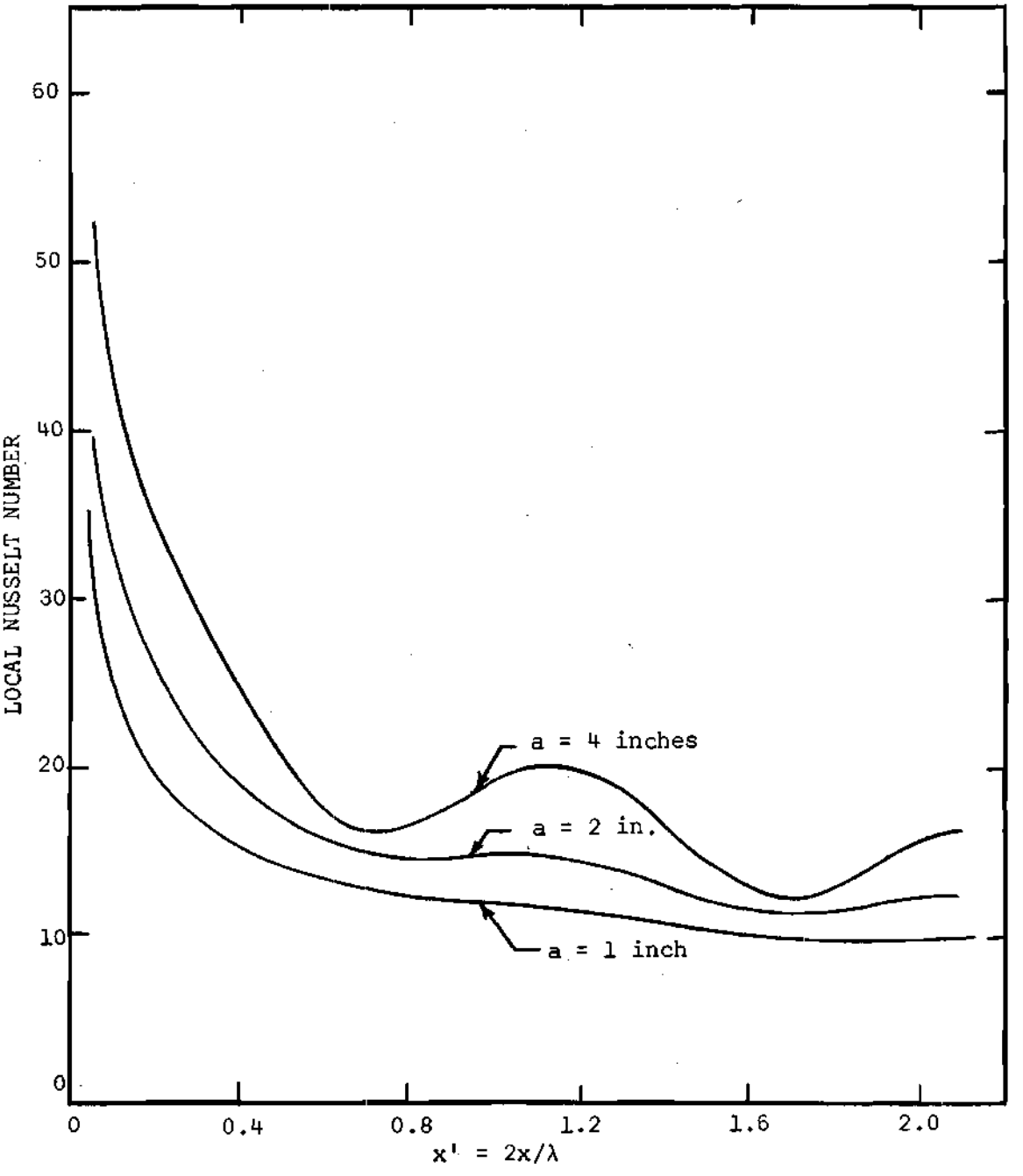

Figure 27. Local Nusselt Number vs. x' with the Channel Width, a, as a Parameter. Channel Reynolds Number = 20000. SPL = 160 db.

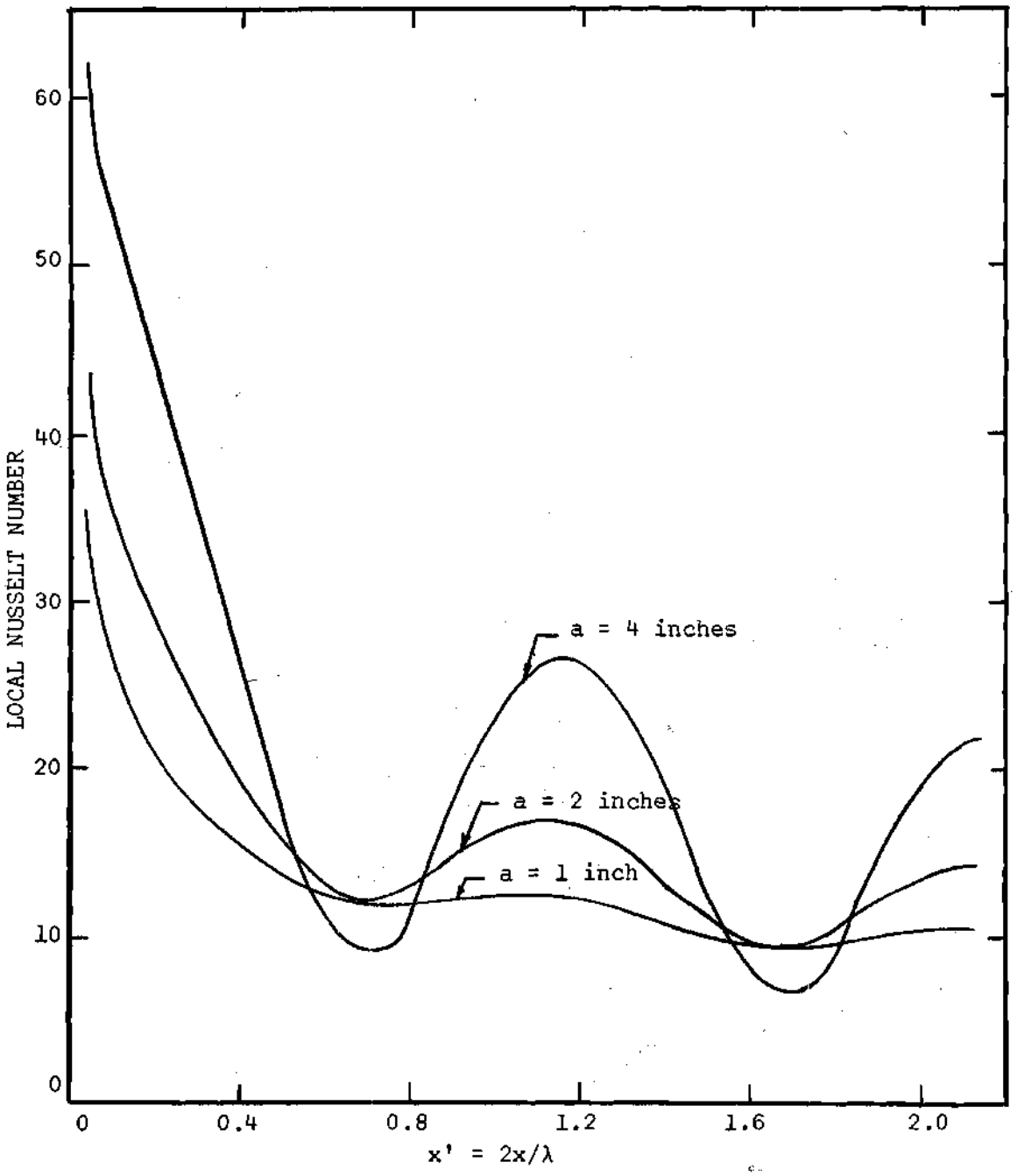

Figure 28. Local Nusselt Number vs. x' with the Channel Width, a, as a Parameter. Channel Reynolds Number = 20000. SPL = 165 db.

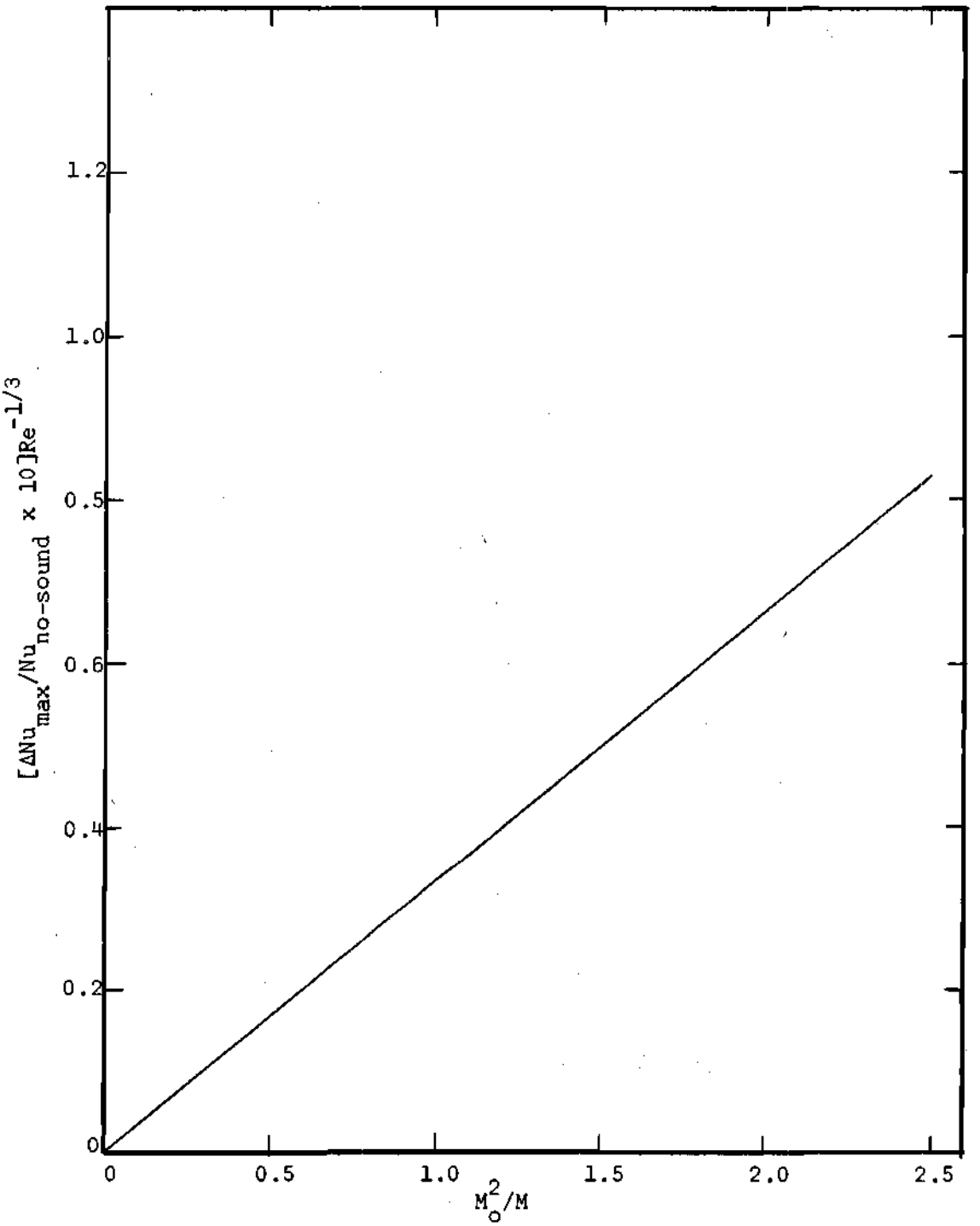

Figure 29. Correlation of Maximum Deviation from No-Sound Nusselt Number.

CHAPTER V

EXPERIMENTAL INVESTIGATIONS

Discussion of Geometry

The geometry which was selected for the experimental investigations was that of a circular tube. Since the analytical investigation presented in Chapters III and IV deals with a parallel plate channel rather than a circular tube, some discussion should be given to explain the choice of these two geometries.

A parallel plate channel geometry was chosen for the analytical investigation because at the time the present work was initiated the solution for the velocity field for the channel was available, whereas the solution for the circular tube was not available. However, from an experimental viewpoint, the parallel plate channel has some distinct disadvantages as pointed out by Purdy (27).

For convenience, some of these disadvantages are summarized below:

(1) Since it is physically impossible to use infinite parallel plates, the channel would have to be approximated by a rectangular duct. In such a duct a side boundary layer is developed, and to minimize its effects, the duct width to height ratio should be quite large.

(2) To obtain the desired acoustic field with a simple driver-horn system, the smallest dimension of the horn outlet should be at least 0.5 inch. This limitation would make the minimum frequency, which can be used without injuring the driver, about 1000 cycles per second

and the corresponding wavelength for normal atmospheric air would be approximately 14 inches.

(3) In order to have plane wave propagation, the largest duct dimension should be small in comparison with the wavelength.

Now, if condition 3 is satisfied, then the largest duct dimension should be no longer than about 0.5 inch, and if condition 1 is satisfied, it then becomes impractical to try to introduce a horn system into the duct to produce the acoustic field. A new method of producing the sound field would have to be devised.

Consideration of the same factors for a circular tube shows that the only outstanding limitation which exists is the difficulty in relating the quantitative results to the analytical solution for a channel. Due to the axial symmetry of the circular tube no extraneous side boundary layer effects are present to dictate the limits of the tube diameter to be used.

As for a correlation of theory and experiment, there may be no basis for a quantitative comparison. However, the velocity field, as predicted by Purdy (27), for a parallel plate channel exhibited the same characteristics as that observed experimentally in a circular tube. That is, Purdy theoretically predicted the presence of standing vortices which were one-quarter wavelength long, and that the ratio of the width of a large vortex to the half-width of the channel is a function of the single parameter M/M_o^2, where M is the Mach number based on the average through-flow velocity and M_o is the Mach number based on the maximum amplitude of the x-component of the time-dependent velocity. Using a circular tube for his experimental studies, Purdy then verified the

existence of standing vortices and within the accuracy of the measurements that were made, he found that the width of the larger vortices was again a function of the same parameter M/M_o^2. On the basis of these results, it was felt that the heat transfer characteristics for a parallel plate channel and a circular tube could also be compared qualitatively. That is, the heat transfer coefficient in each case should be a function of the same parameters.

Instrumentation and Equipment

The equipment used in these experiments consisted primarily of a steam-heated test section and an electronic system for producing and measuring a stationary acoustic field. The various components which comprised the test section, sound system, and the acoustic shield are as follows:

1. Heat Transfer Apparatus
    a. Steam Heated Tube
    b. Condensate Collection System
    c. Air Circulating and Flow Measurement System
    d. Temperature Control and Measurement System
2. Sound Generating Equipment
    a. Signal Generator and Amplifier
    b. Vibrator and Horn
3. Sound Measuring Equipment
    a. Microphone
    b. SPL Meter
4. Thermal and Acoustic Shield

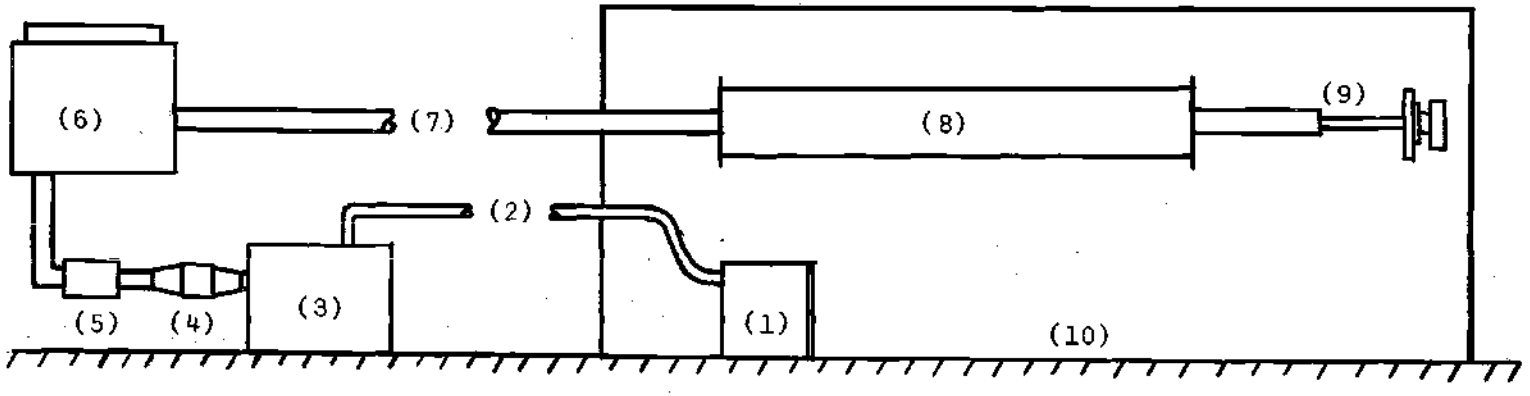

1. Secondary Blower
2. Return Duct
3. Primary Blower
4. Laminar Flow Meter
5. Air Preheater
6. Plenum Chamber
7. Unheated Inlet Section (Supply Duct)
8. Heat Transfer Section
9. Vibrator and Horn
10. Air Conditioned Room

Figure 30. Schematic Diagram of Experimental Apparatus.

A detailed discussion of each of the above components is given below. The system is shown schematically in Figure 30.

Heat Transfer Apparatus

Steam Heated Tube. The circular tube used for this investigation was made from a 3.86 inch I.D. type K copper tube which was approximately 42.75 feet long. The first 28.26 feet of the tube was an unheated hydrodynamic entrance section insulated with 2 inches of Johns Manville "Micro-Lox." This section was approximately 88 diameters long and was used to provide a "fully-developed" velocity profile at the entrance to the test section. The test section itself was approximately 10 feet, 6 inches long and was mounted concentrically within a 16-inch steel pipe. The annular region between the tube and the pipe was filled with saturated steam from the laboratory low-pressure steam line. The gage pressure of the steam was regulated by means of a globe valve. The condensing steam produced an essentially isothermal test section. There was a continuous flow of steam through the steam chest to maintain a constant steam pressure. Downstream from the test section was an additional section of the copper tube which was approximately 4 feet long. The horn for the sound-generating equipment was mounted in this section.

The test section is shown schematically in Figure 31.

Condensate Collection System. The system used to collect the condensate from the steam chest consisted of two chambers 3 inches long and 19 chambers 6 inches long. The first chamber started 0.38 inches from the entrance of the test section. The chambers were formed by soldering diamond-shaped partitions, cut from 48-ounce soft-rolled copper sheet, to the 4.125 inch O.D. copper tube, and then soldering

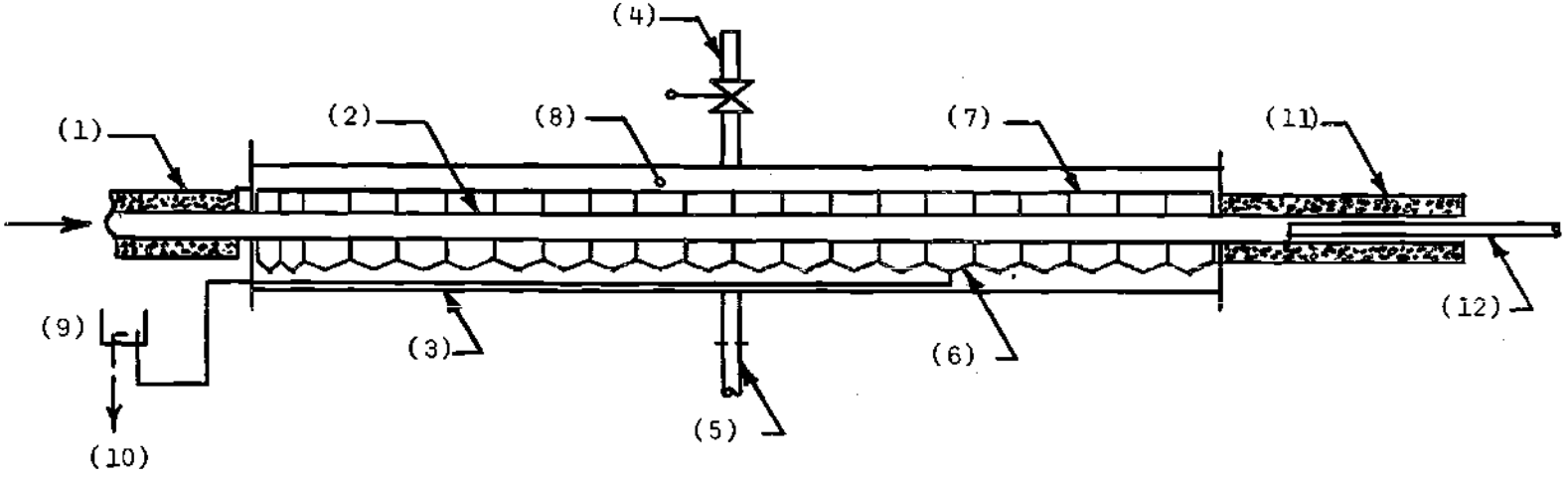

1. Supply Duct
2. Steam Heated Tube
3. Insulated 16-inch Pipe
4. Steam Inlet
5. Steam Outlet
6. Condensate Collector
7. Drip Shield
8. Saturated Steam
9. Condensate Transfer Cup
10. To Burette
11. Insulated Duct
12. Horn

Figure 31. Schematic Diagram of Heat Transfer Section.

a preformed 16-ounce copper collection pan in the shape of an inverted pyramid to the bottom of each chamber. To each chamber was attached a drain line which ran horizontally through the steam chest and through the brass head-plate at the entrance end of the test section. One-quarter-inch O.D. copper tubing was used to run the drain lines from the head-plate to the outside wall of the acoustic shield and one-quarter-inch O.D. Neoprene tubing was used between the copper drain lines and the transfer cups and from the transfer cups to the calibrated burettes where the condensate was measured as a function of time.

Air Circulation and Flow Measurement System. The components of this system are illustrated schematically in Figure 32. Each of the components illustrated in the schematic will be discussed individually.

The air was circulated through the system by means of a Lockwood pressure blower Model PB-10 with a capacity of 360 cfm at a pressure of 7 inches of water. The noise level associated with the blower was insufficient to produce any effects on the heat transfer apparatus. The rate of flow was controlled by means of a throttle (6-inch gate valve) mounted on the blower inlet.

The mixing compartment was a box made from half-inch plywood. The dimensions of the chamber were 22 by 22 by 25 inches. A partition of half-inch plywood separated the chamber housing, the blower, and the mixing chamber. Thus the air was discharged from the blower into the mixing chamber after which it passed through a filter before entering the flow meter.

The laminar flow meter was a Meriam Instrument Company Model 50MC2-4PF flow measuring instrument. The device indicated volumetric

flow rate by producing a differential pressure across a flow element which was composed of a matrix of small-diameter passages. It had a linear response between volumetric flow rate and differential pressure with a flow range of 100 to 1 possible. The accuracy of the instrument was within 1/2 of 1 per cent of the Meriam Instrument Company flow standards.

A micro-manometer, a Meriam Instrument Company Model 34FB2, was used to measure the static pressure and the differential pressure at the laminar flow meter. The instrument had a range of differential pressure of 10 inches of water and an accuracy of ± 0.001 inches of water. The maximum possible operating pressure was 20 psig.

An electrical resistance heater was placed in the air stream immediately downstream from the laminar flow meter. It consisted of 2 600-watt resistance coils mounted concentrically inside a short section of 3.86-inch I.D. copper tube. It was used to control the temperature of the air in the plenum chamber at the desired operating temperature.

The plenum chamber consisted of two plywood boxes, one within the other (see Figure 32). The inner chamber was constructed from 3/4-inch plywood and was insulated on both the inside and the outside surfaces with 1-inch Johns Manville fiberglass. The outer box was constructed from 1/2-inch plywood and was insulated on the inside surface only. The two boxes were assembled in such a manner that there was a 2-inch air gap between them. The purpose of the gap was to allow air to be circulated in the space between the two chambers. This air was circulated by a small fan and heated by a guard heater (a small electrical resistance heater of the same type discussed in the previous

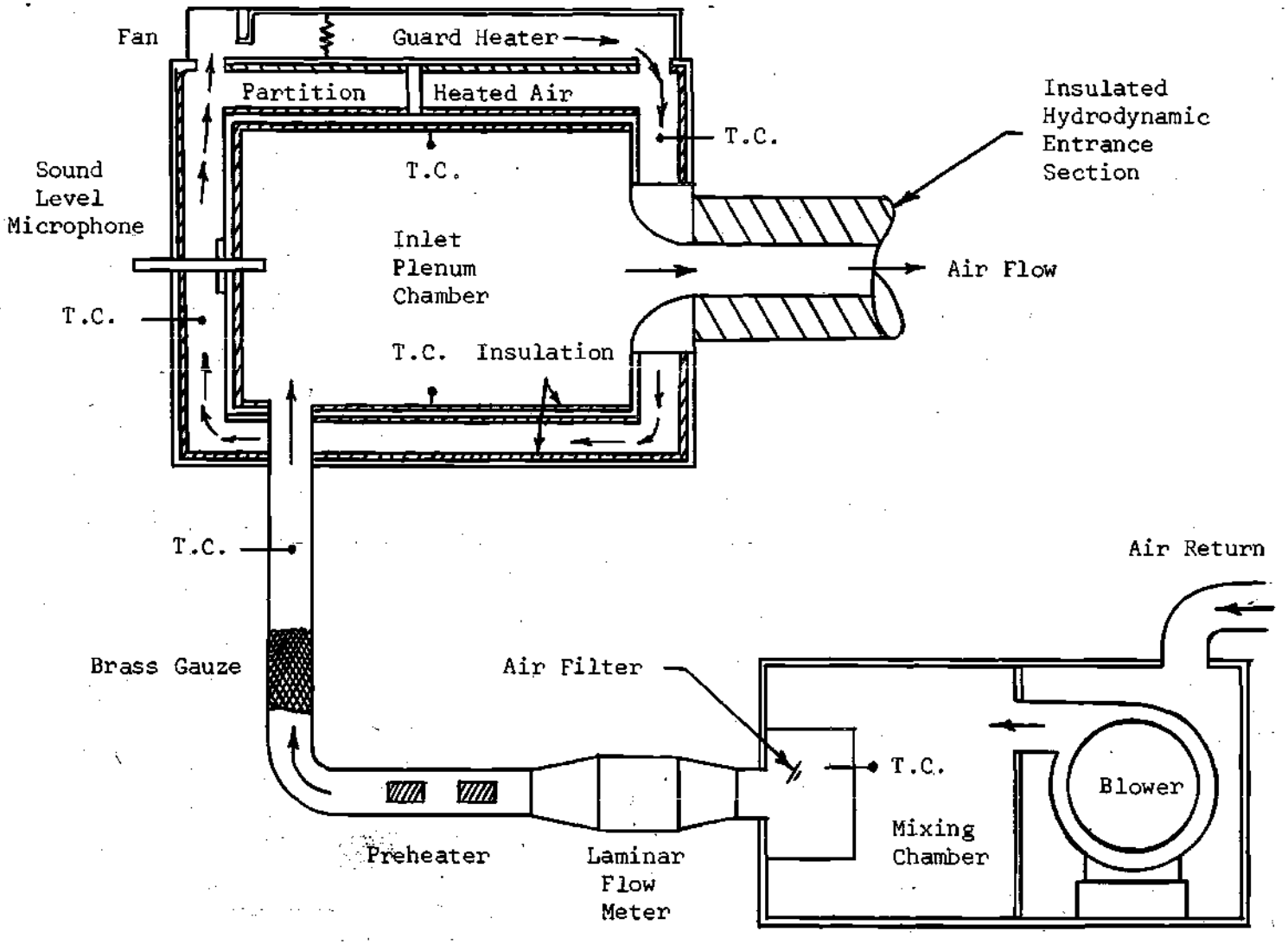

Figure 32. Air Circulation System.

paragraph) to the same temperature as the air in the plenum chamber. This eliminated any significant heat transfer to or from the plenum chamber. The exit from the plenum chamber was a bellmouth-shaped section leading into the 3.86-inch I.D. copper tube; this provided a uniform velocity profile at the entrance to the tube.

After the air had passed through the test section and exited into the acoustic shield enclosing the test section, it was returned to the blower by means of a 4-inch diameter galvanized duct, thereby completing its cycle.

Temperature Control and Measurement System. Several thermocouples were located at various points throughout the system for the purpose of controlling and/or measuring the temperature at desired locations. Two iron-constantan thermocouples were placed in the air gap between the two boxes which comprised the plenum chamber and were connected to a Leeds and Northrup Type H direct reading temperature indicator. These thermocouples were used to monitor the temperature of the air in the gap; the temperature was monitored visually and the guard heater was controlled manually to hold the air at the desired operating temperature.

Four 24-gauge copper-constantan thermocouples connected in parallel were placed in the plenum chamber, one each on the two sides, the top and the bottom of the chamber. These thermocouples were connected to a Leeds and Northrup Type G Speedomax Recorder in conjunction with a Series 60 controller. The recorder monitored the thermocouples and automatically controlled the power input to the air heater to maintain the air temperature at the desired operating temperature to within

an accuracy of ± 0.25°F.

Additional thermocouples in the system were used to determine the temperature of the air (both wet-bulb and dry-bulb) inside the acoustic shield surrounding the test section, inside the mixing chamber just before entering the flow meter, and inside the plenum chamber; the temperature of the steam in the test section, the temperature of the tube wall at the thermal entrance, and the temperature of the insulation (both inside and outside the acoustic shield) on the hydrodynamic entrance section of the tube. All of these thermocouples were made of 24-gauge copper-constantan duplex thermocouple wire and the emf produced by them was measured with a Leeds and Northrup 8686 millivolt potentiometer.

Sound Generating Equipment

The sound generating equipment is shown schematically in Figure 33. A Hewlett-Packard Model 200CD Wide Range Oscillator provided a source of continuously variable audio-frequency voltage at a total distortion level of less than 0.5 per cent. This signal was amplified by an MB Electronics Type PA11-G amplifier. The electrical to mechanical conversion was achieved with an MB Electronics Model C11 Vibration Pickup Calibrator in conjunction with a 2-inch O.D. cylindrical horn several feet long.

In order to properly couple the driver-horn system to the resonant acoustic field in the tube, it was necessary to mount the driver-horn assembly on a sliding platform that could be moved in the axial direction. The axial position of the horn was adjusted to give the maximum sound pressure levels in the tube. When the sound generating system was

properly adjusted, wave analyses of the acoustic field showed that the distortion level was less than 1 per cent at sound pressure levels ranging from 150 to 155 db. At high SPL (165 db) the distortion was as high as 5 to 6 per cent but the microphone has a non-linear response to these sound pressure levels. Sound pressure levels as high as 166 decibels at a frequency of 91 cycles per second could be obtained with this system.

Sound Measuring Equipment

The sound pressure level in the tube was determined as a function of axial position by measuring the sound pressure level with a General Radio Model 1551-P1H high level microphone assembly in conjunction with a General Radio Model 1551-A SPL Meter which was accurate to ± 1 db (Reference 0.0002 μ bar). The microphone was mounted on one end of a 35-foot long, 3/4-inch diameter conduit. With this rod, which passed through a packing gland on the rear panel of the inlet plenum chamber, the sound pressure level in the hydrodynamic entrance section was determined as a function of position.

Thermal and Acoustic Shield

The thermal and acoustic shield, an 8 by 28 foot room, 8 feet high, enclosed the test section and the driver-horn assembly in order to reduce the sound pressure level in the laboratory to a safe and comfortable level. The room had a 2 by 4 wood framework with double layers of 3/8-inch sheetrock inside and outside. The room had a door at one end to allow easy access to the test section. The room temperature was controlled by a Mathes Custom room air-conditioner. With this system the room temperature was held constant within ± 1.0°F.

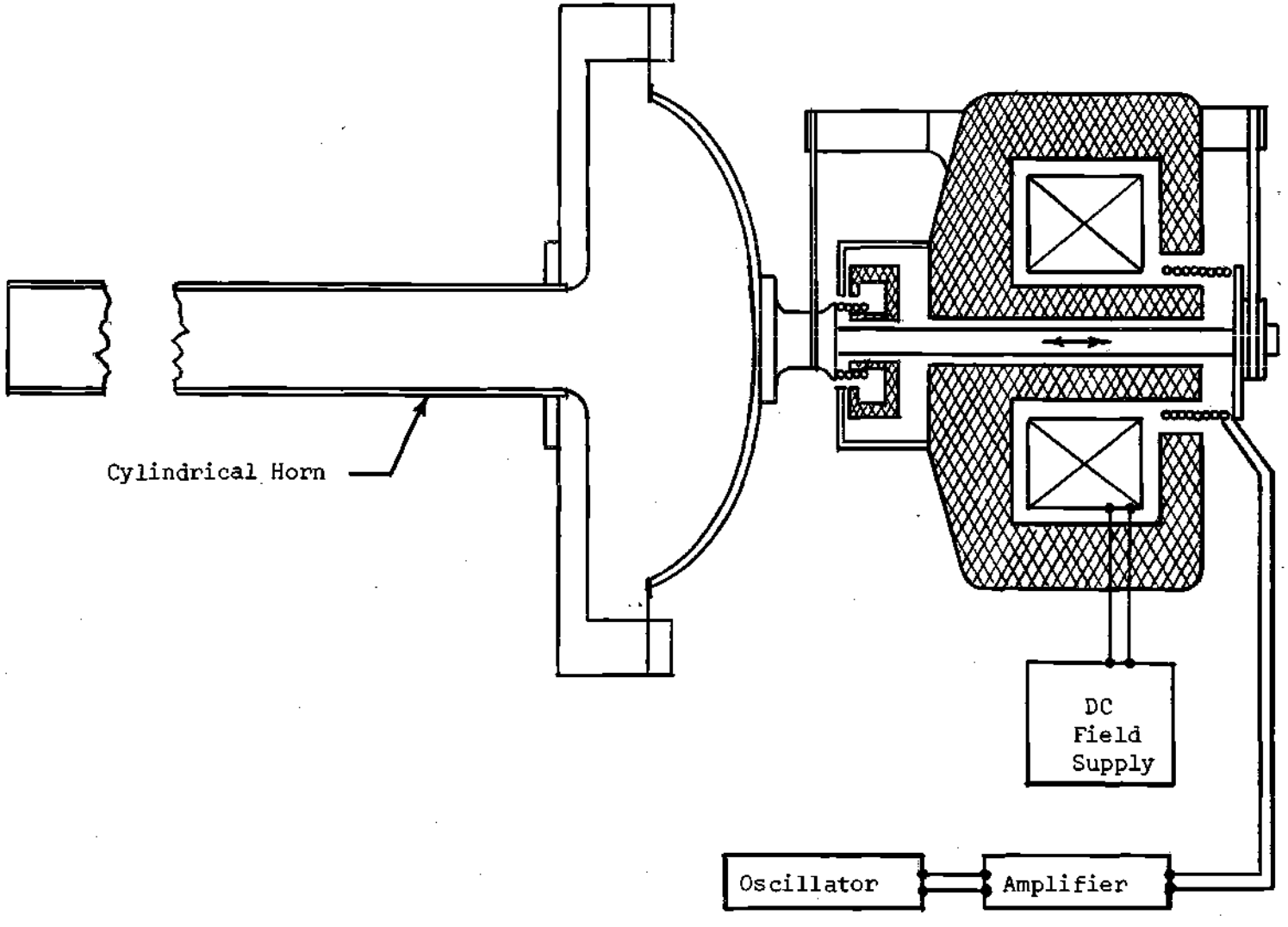

Figure 33. Drawing of Sound Generating Equipment.

Experimental Procedure

Calibration Tests Without Sound

Heat transfer runs without sound were conducted at two values of Reynolds number to determine the reliability of the results obtained with the experimental apparatus. The steam pressure in the steam chest and the flow rate of air through the test section were adjusted until the desired settings were attained. In all tests, the apparatus was allowed to run for 6 to 12 hours to establish thermal equilibrium before any data were recorded.

These tests were conducted as follows: the throttle on the blower was adjusted to give the flow rate that corresponded to the desired Reynolds number (Appendix B gives an approximate formula for the differential pressure required at the flow meter to give the desired Reynolds number) and the system was allowed to reach equilibrium. An individual test run was initiated by first draining all burettes. A stopclock was started and initial readings for each burette were recorded. The following readings were taken at half-hour intervals and averaged over the duration of the run: the wet-and-dry-bulb temperatures within the thermal and acoustic shield, the mixing chamber temperature, the plenum chamber temperature, the steam temperature within the steam chest, the tube wall temperature at the entrance to the test section, the temperature of the insulation both inside and outside the thermal and acoustic shield, ambient laboratory temperature, barometric pressure, steam pressure inside the steam chest, and the static and differential pressure at the laminar flow meter. In addition to these readings, the time required to collect 50 ml. of condensate for each

burette was recorded and from this the condensate flow rate was determined for each collection chamber. The length of a test run ranged from three to six hours, the time required for a minimum of two fills of the burettes.

Preliminary Sound Field Tests

Before the simultaneous heat transfer and acoustic vibration tests were initiated, an investigation was made to determine the resonant frequencies of the tube and to determine the modal positions of the standing wave in the tube. Three criteria were used in the selection of a particular resonant frequency. First, the resonant frequency should be low to produce a wavelength considerably greater than six inches since quasi-local Nusselt numbers were to be obtained and since the steam condensate collectors were six inches long; this was to prevent the possible masking out of the local effects on the heat transfer. Secondly, the highest possible sound pressure levels should be obtainable. Thirdly, the nodal positions should be located so that a pressure node (velocity antinode) would be located at the thermal entrance. However, the third criterion was relaxed considerably since it was sufficient to require only that the beginning of a vortex region lie just inside the thermal entrance as shown in Figure 34.

It was found during these tests that the three criteria could best be satisfied by choosing a resonant frequency of 91 cycles per second in conjunction with an inlet air temperature of 120°F. This frequency resulted in a half-wavelength of 77.5 inches. Figure 35 shows a typical plot of sound pressure level along the axis of the tube.

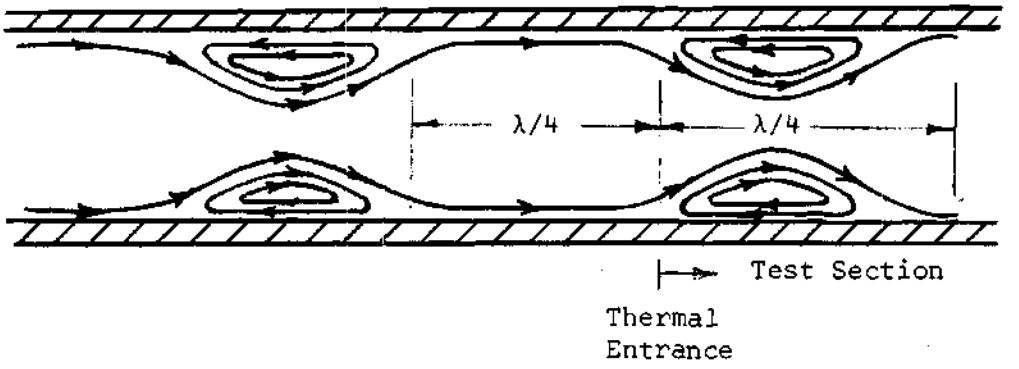

Figure 34. Schematic Diagram of Vortex Patterns

Test Runs With Heat Transfer and Acoustic Vibrations

These tests were conducted exactly the same as the tests without a sound field except that a resonant acoustic field was impressed on the air flow. The controlled variables were the sound pressure level, frequency, inlet air temperature and the air flow rates through the tube. An actual data run was started in the same manner described for the no-sound tests after steady state conditions had been obtained. A period of 6 to 12 hours was allowed for the system to reach equilibrium. The maximum sound pressure level and frequency were recorded at the beginning and end of a run and average values were used in the calculations. Whenever the maximum SPL varied as much as 0.5 db, the run was discarded. The length of a test run ranged from three to six hours.

Discussion of Results

Heat Transfer Without Sound

The Reynolds numbers selected for investigation were of such mag-

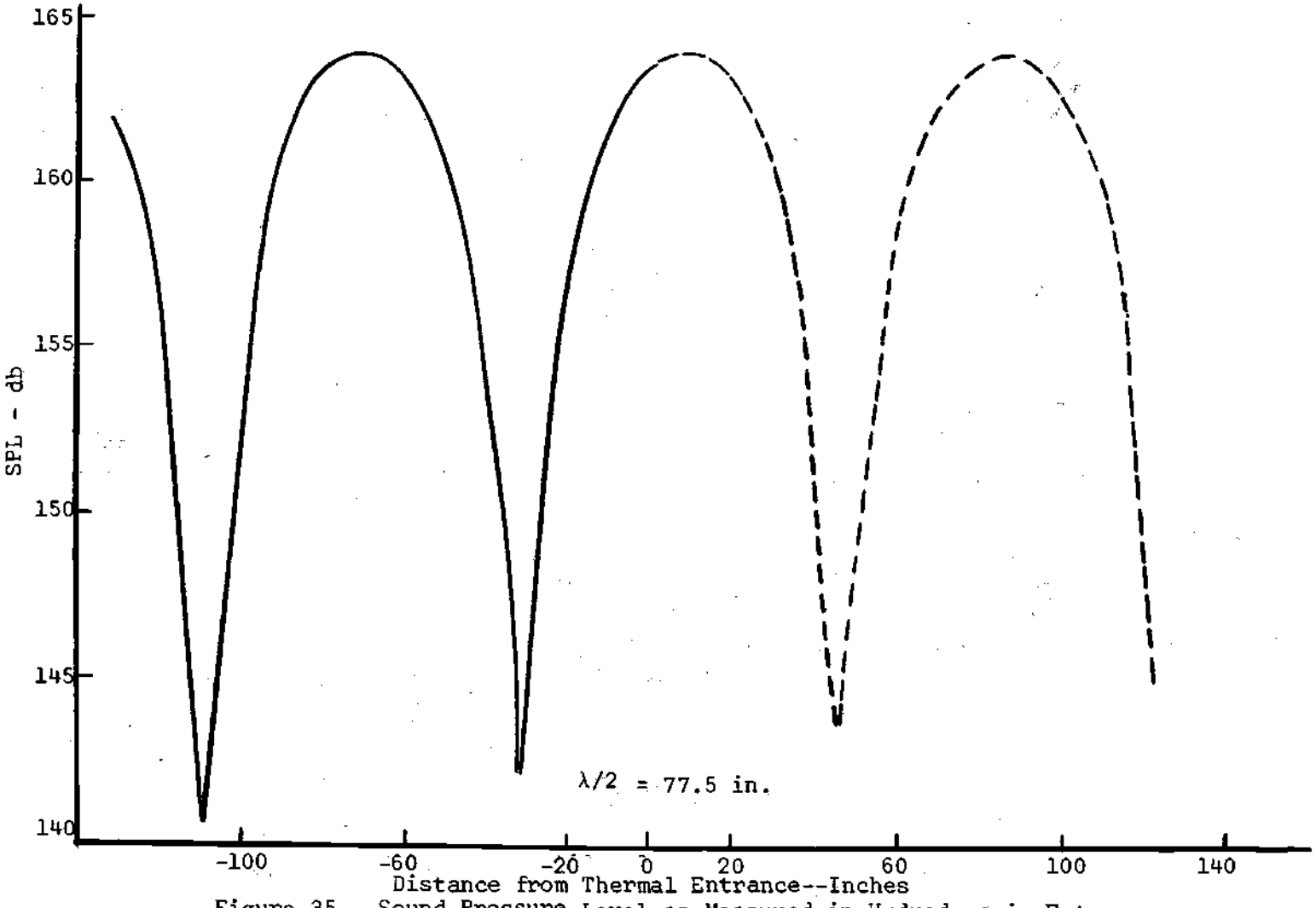

Figure 35. Sound Pressure Level as Measured in Hydrodynamic Entrance Section and Extrapolated into Test Section.

nitude that the flow with no sound was definitely in the turbulent regime. These high Reynolds numbers were used in an effort to minimize the effects of free convection heat transfer. Therefore, the no-sound data must be correlated on the basis of turbulent theory rather than that of laminar theory.

The theoretical determination of the heat transfer to or from a fluid in turbulent flow through a tube is still more difficult than for laminar flow because of the more complicated flow conditions.

However, Latzko (33) devoted a rather thorough theoretical investigation to the subject and derived the following equation for a local heat transfer coefficient, which is based on the local mean temperature (which is computed by assuming a uniform, or constant, velocity distribution) instead of the cup-mixing temperature:

$$h = 0.0346\, v_m \rho c_p \left(\frac{\nu}{v_m D}\right)^{1/4} \phi(x) \tag{5.1}$$

where

$$\phi(x) = \frac{1.078e^{-m_1 x} + 0.134e^{-m_2 x} + 0.980e^{-m_3 x}}{0.970e^{-m_1 x} + 0.024e^{-m_2 x} + 0.006e^{-m_3 x}} \tag{5.2a}$$

$$m_n = \beta_n \frac{1}{D}\left(\frac{\nu}{v_m D}\right)^{1/4} ; \quad n = 1,2,3. \tag{5.2b}$$

D = the tube diameter.

x = the axial position of a point of the fluid from the inlet.

v_m = the mean velocity.

ν = the kinematic viscosity.

$$\beta_1 = 0.1510 \tag{5.2c}$$

$$\beta_2 = 2.844 \tag{5.2d}$$

$$\beta_3 = 29.42 \tag{5.2e}$$

After some rearrangement, equation 5.1 may be written as

$$Nu = 0.0346\ (Re)^{3/4} Pr\phi(x) \tag{5.3}$$

and equation 5.2b becomes

$$m_n = \beta_{nD} \frac{1}{}(Re)^{-1/4} \tag{5.4}$$

The values of the local Nusselt numbers have been calculated using equation 5.3 and the results are shown graphically in Figures 36 and 37 along with the local Nusselt numbers obtained experimentally in the present investigation. These figures show that the Nusselt numbers (or, equivalently, the heat transfer coefficient) given by equation 5.3 are somewhat lower than the experimentally obtained values and

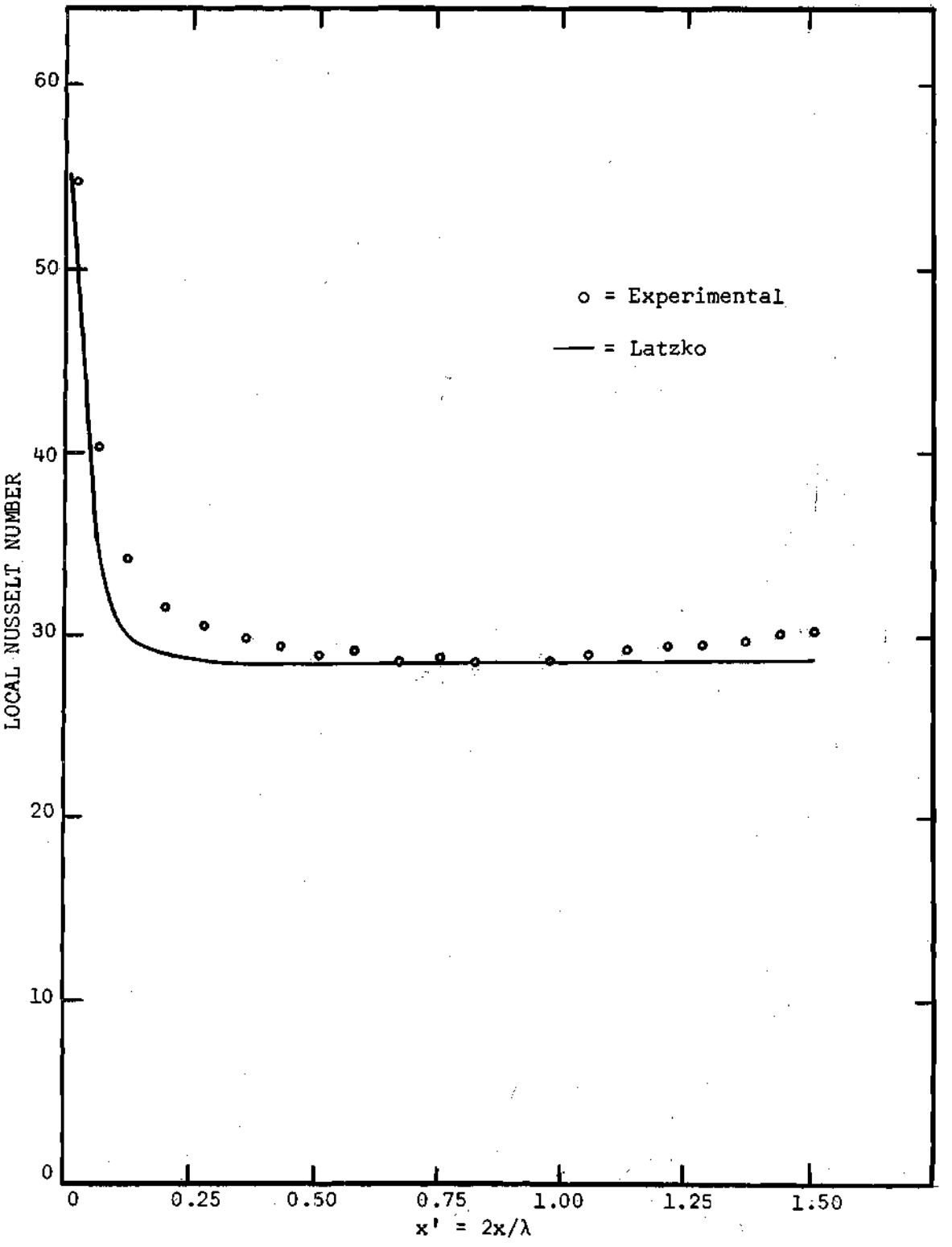

Figure 36. Local Nusselt Number vs. Axial Tube Position. Reynolds Number = 10384.

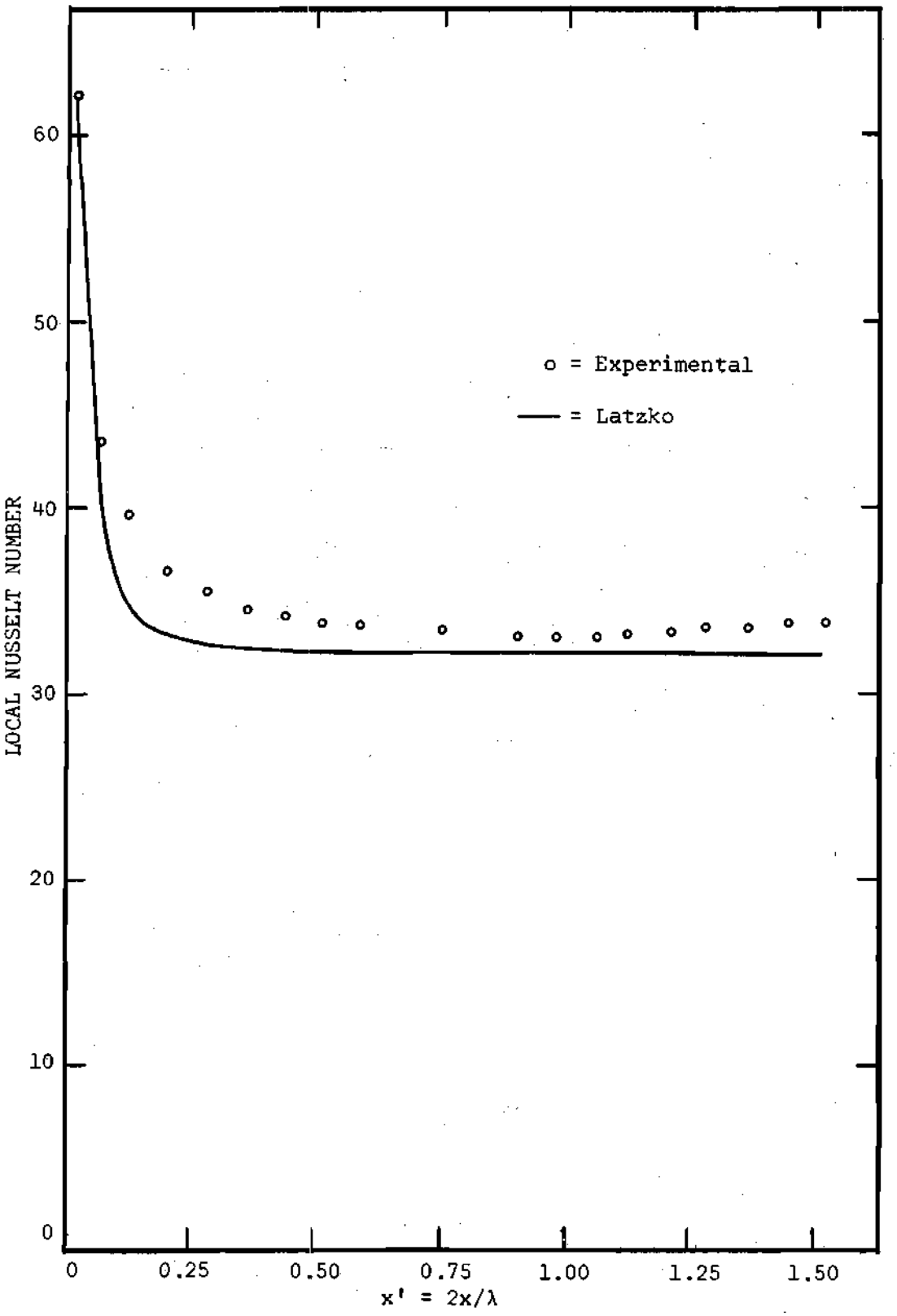

Figure 37. Local Nusselt Number vs. Axial Tube Position. Reynolds Number = 12436.

that the theoretical values decay much more rapidly to the asymptotic value than do the experimental values.

McAdams (34) gives an empirical equation, also attributed to Latzko, for the average heat transfer coefficients for fully developed turbulent flow:

$$\frac{h_m}{h_\infty} = 1 + \frac{1.4D}{L} \quad (\frac{L}{D} > 5) \tag{5.5}$$

where h_∞ represents the local heat transfer coefficient at a position in the flow where the temperature distribution is fully developed. If we take the limit of equation 5.3 as x approaches infinity, the following value is obtained:

$$Nu_\infty = 0.0384\ (Re)^{3/4} Pr \tag{5.6}$$

From equation 5.5 the average Nusselt number becomes

$$Nu_{avg} = 0.0384\ (Re)^{3/4} Pr\ (1 + \frac{1.4D}{L}) \tag{5.7}$$

for values of L/D greater than five. If D is taken to be the tube diameter and if L is interpreted as the distance from the thermal entrance to the midpoint of a condensate collection chamber, then equation 5.7 gives an excellent correlation for the experimentally obtained values of the average heat transfer coefficients for chambers 5 through 20. Figure 38 shows a comparison between the experimental average heat

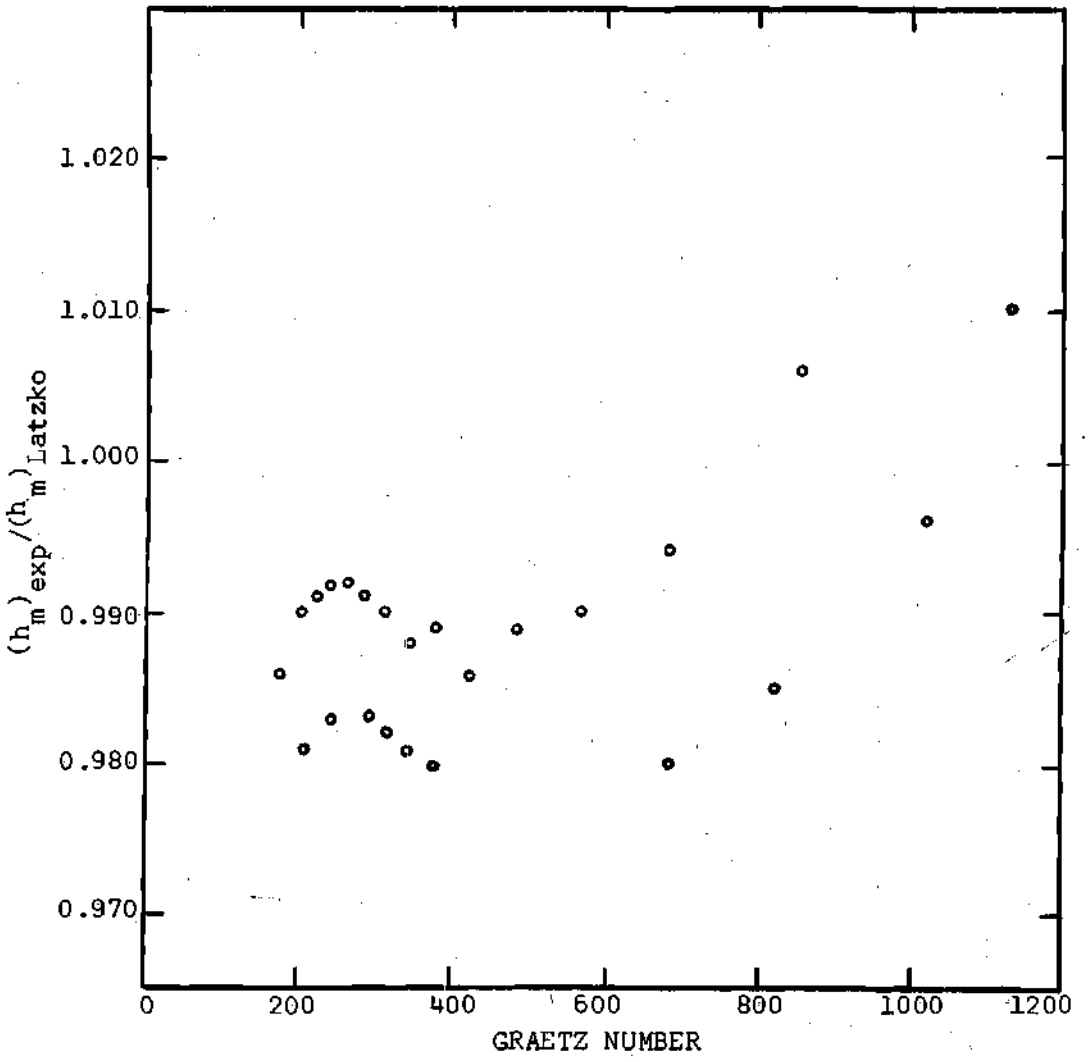

Figure 38. Correlation of No-Sound Data for Average Heat Transfer Coefficient.

transfer coefficient and the one computed from equation 5.7 for Reynolds numbers of 10384 and 12436. The conclusion to be drawn from these data is that the apparatus used in this investigation is quite reliable and that the correlation with Latzko's work is excellent.

Heat Transfer with Sound

Experiments were conducted at a resonant frequency of 91 cps and at two Reynolds numbers, approximately 10200 and 12400, to study the effect of resonant acoustic vibrations on the local heat transfer coefficients. In order to determine the effect of the amplitude of vibration, the Reynolds number, the inlet temperature, and the frequency were held constant while the sound pressure level was varied from 160.0 to 166.0 decibels. The results of the variation of this parameter are graphically illustrated in Figures 39 and 40. It was found from the experimental data that the local Nusselt number varied as a slightly damped periodic function. The period of the function, as determined by measurement from Figures 39 and 40, appeared to be one-half the wavelength of the vibration and the amplitude was a function of the intensity or amplitude of the vibration. The heat transfer coefficient with sound approached the no-sound coefficient slightly downstream of the position of the velocity node of vibration; i.e., there seemed to be a "heat transfer node" at a position near the velocity node. At that point the acoustic vibration had no effect on the heat transfer.

As discussed in the previous chapter, we can obtain an interesting correlation of the data by considering the quantity ΔNu_{max}. In the case of the experimental data shown in Figures 39 and 40 the following empirical equation can be derived:

$$(\Delta Nu_{max}/Nu_{no\text{-}sound})Re^{1.526} = 2.58 \times 10^{6}\ Mo^{2}/M.$$

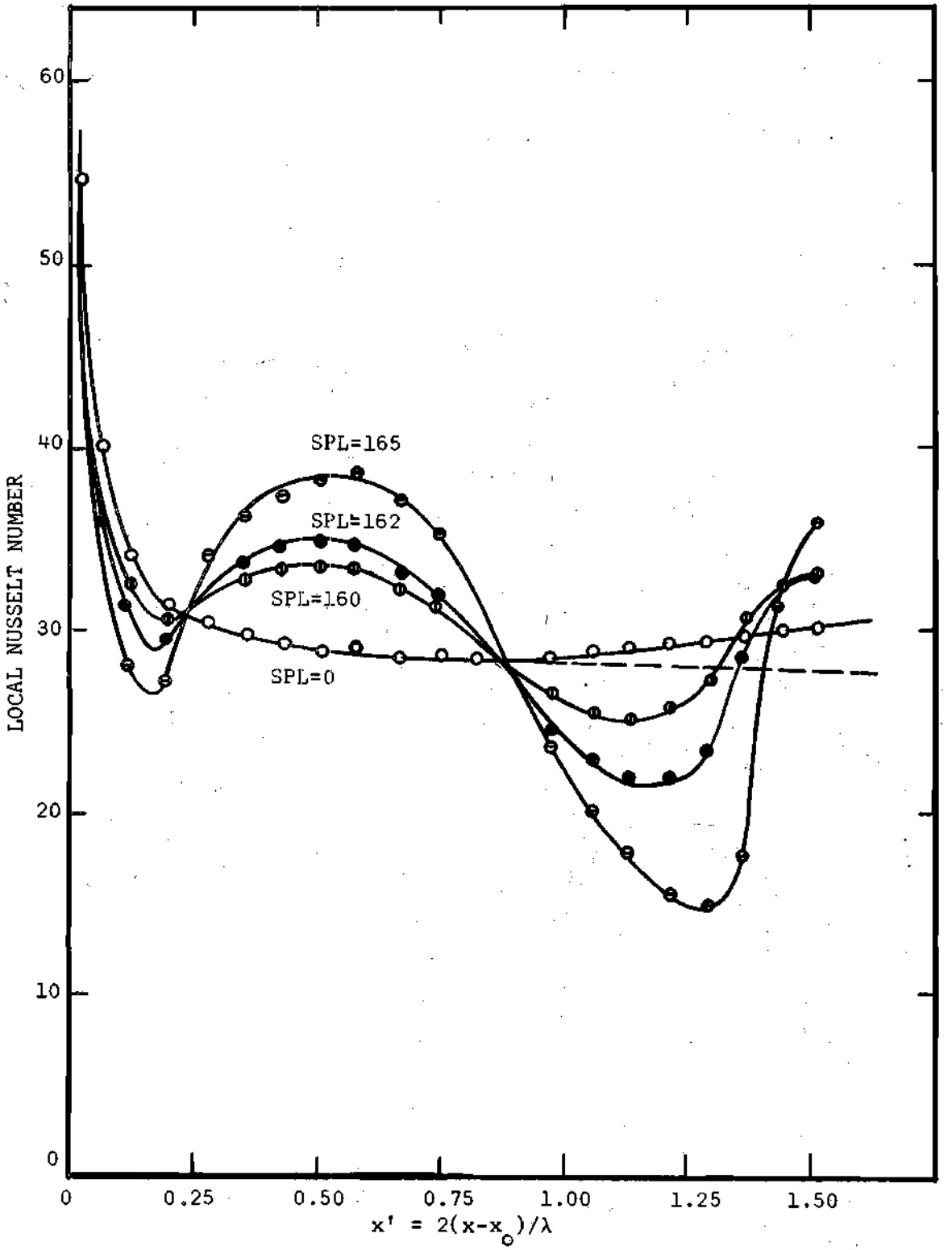

Figure 39. Local Nusselt Number vs. x'. Tube Reynolds Number = 10200, x_o = 2.64 ft.

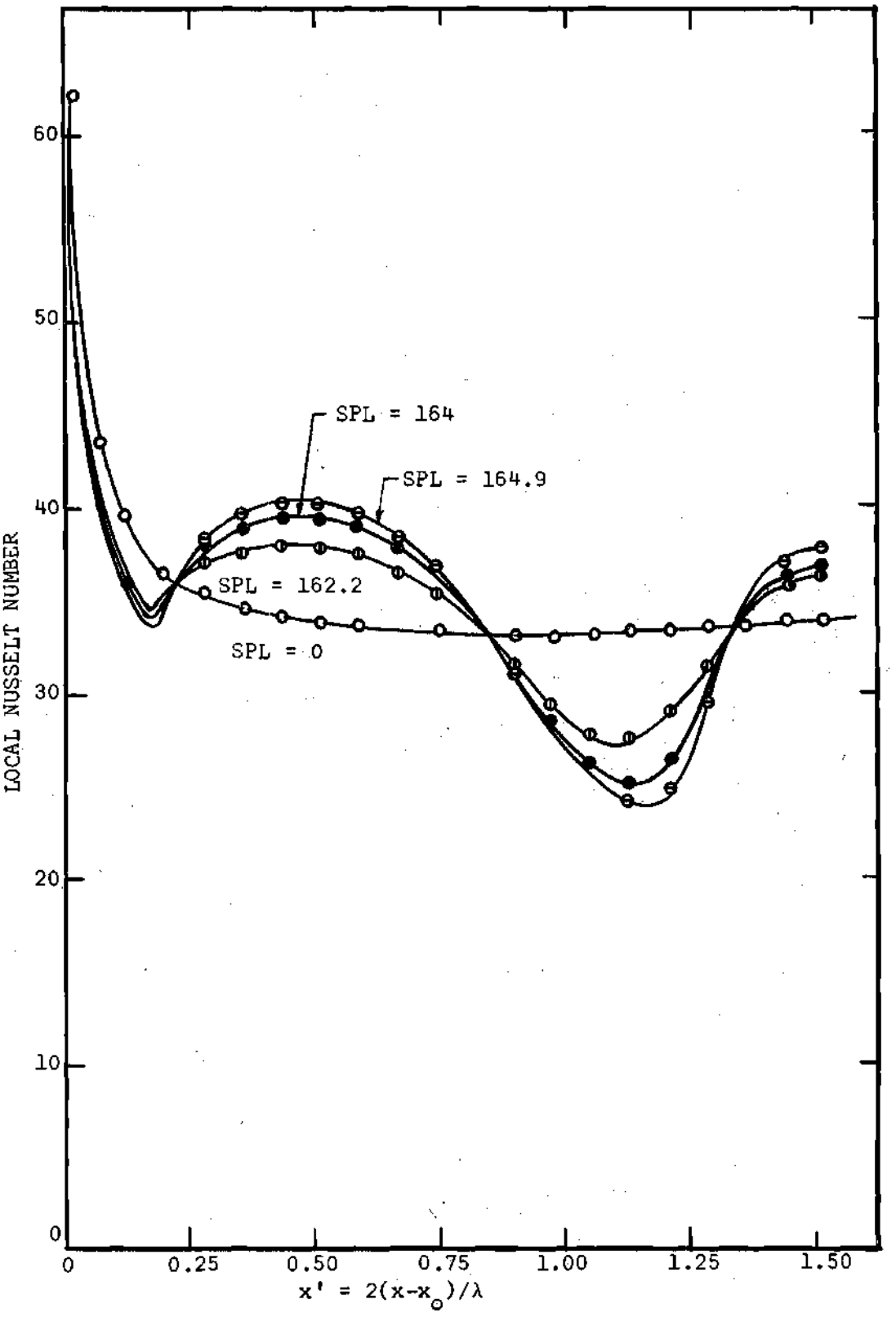

Figure 40. Local Nusselt Number vs. x'. Tube Reynolds Number = 12400, x_o = 2.64 ft.

CHAPTER VI

DISCUSSION OF RESULTS

A numerical solution of the energy equation for laminar flow between parallel plates under the influence of a resonant acoustic field and associated heat transfer results have been presented in Chapters III and IV. The results of an experimental investigation for the similar problem with a circular tube geometry have been presented in Chapter V. The results which directly pertained to each investigation have already been discussed in Chapters IV and V. The discussion which follows will be concerned with a qualitative comparison of the similarities of the results of the analytical solution for the parallel plate channel and the experimental results using the circular tube.

In each case the acoustical vibrations produced a local Nusselt number which was a slightly-damped periodic function which oscillated above and below the corresponding values of the no-sound Nusselt number. The amplitude of this periodic function is dependent upon the intensity, or amplitude, of the acoustical vibration.

Both the analytical and experimental investigations show that the maxima of the heat transfer coefficient (Nusselt number) occur at, or near, the velocity antinodes and the minima occur at, or near, the velocity nodes. Actually, there is a phase lag and the maxima and minima occur slightly downstream of the positions at which they would be expected to occur. This phase lag, in some instances, was as high as 20

per cent of the half-wavelength of the acoustic field. The phase lag seems to be dependent upon the flow rate and the intensity of the acoustic vibration.

The analytical investigation indicated that the heat transfer coefficient is dependent upon the parameters M/M_o^2, $(M_o\ a')^2\ Pr_o$ with the first parameter as the dominant one. Unfortunately, the experimental system made it impractical to study the effect of an individual variation of each of these parameters. The only parameter which could be varied independently is M/M_o^2; the variation is achieved by varying the through-flow Mach number, M. The experimental results show that an increase in the parameter M produces an increase in the amplitude of the local Nusselt number. This same result is obtained from the numerical solution of the energy equation. Both the analytical and experimental studies show that an increase in the parameter M_o produces an increase in the maximum deviation of the local Nusselt number from the corresponding no-sound value.

CHAPTER VII

CONCLUSIONS AND RECOMMENDATIONS

An analytical and experimental investigation of the effect of a resonant acoustic field on the rate of forced convective heat transfer has been made. The analytical study treated flow in an infinite parallel plate channel whereas the experimental study considered flow in a circular tube. The conclusions from these investigations are:

1. A resonant acoustic field will produce variations in the local heat transfer coefficient from the corresponding values obtained without the acoustic field.

2. The amplitude of the variations which are produced by the resonant acoustic field is, as far as can be ascertained from the governing differential equation, a function of the parameters M/M_o^2, and $(M_o a')^2 Pr_o$. It was found, however, that the maximum deviation from the no-sound Nusselt number could be correlated as a function of the parameter M_o^2/M by the equation

$$(\Delta Nu_{max}/Nu_{no\text{-}sound})Re^{-1/3} = 0.0335(M_o^2/M).$$

3. The frequency of the acoustic disturbance affects the local heat transfer rate negligibly except in the regions near the maximum deviation from the corresponding no-sound values.

4. The solution to the analytical model for the parallel plate

system predicts a phase-lag in the local heat transfer rate. According to Purdy's explanation of the effect of sound on heat transfer, the relative minima of the heat transfer rate would occur at the velocity nodes and the maxima would occur at the velocity antinodes. However, the numerical solution predicts a phase lag as high as 20 per cent of the half-wavelength of the impressed acoustic field.

It is recommended that further investigations involving experimental as well as additional analytical studies be conducted. The following studies are suggested:

1. Additional analytical development should be undertaken to determine if the results obtained here can be presented in a more universal form than has been established thus far.

2. Additional experimental as well as analytical studies should be conducted to study the effects of: (i) high intensity sound, (ii) off-resonance, and (iii) free convection on the flow field and on the rates of heat transfer. To include the effects of these additional factors would require a completely new order of magnitude analysis and would require that the continuity, momentum, and energy equations be solved simultaneously.

3. The solution for the circular tube geometry should also be obtained. The order of magnitude analysis and the reduction of the energy equation have already been performed as a supplement to the present investigation and are presented in Appendix D. Possibly the experimental work could then be correlated with the analytical results.

APPENDIX A

ORDER OF MAGNITUDE ANALYSIS

The following is a summary of the order of magnitude analysis which was used to reduce the energy equation to a form which was more amenable to a mathematical analysis. This analysis embodies the assumptions that the density, pressure, velocity, and fluid temperature may each be represented as the sum of a time-dependent component and a time-independent component and that the fluid properties--viscosity, specific heat, and thermal conductivity--are constant.

The first step in the analysis is to choose a characteristic value for each of the properties x, y, t, u, v, p, ρ, μ, c_p, k, and T, to be used in defining corresponding dimensionless properties. The characteristic values are selected such that the order of magnitude of a dimensionless property, which is formed by dividing the property by its characteristic value, is one. In addition, the characteristic values of length and time are selected such that derivatives with respect to these quantities are of the order of magnitude of one. The values which were chosen for this analysis are $\lambda/2$, δ_{ac} and a, $\lambda/2c_o$, $\bar{U}$ and U_o, $\bar{V}$ and V_o, p_o and $\rho_o c_o U_o$, ρ_o and $\rho_o M_o$, μ_o, c_{po}, k_o, and $(T_w - T_o)$ and $T_o M_o$, respectively. The dimensionless properties (denoted by a prime superscript) formed from these characteristic values are defined by

$$x = (\lambda/2)x' \tag{A.1}$$

$$y = \delta_{ac}y' \text{ or } a\bar{y}' \tag{A.2}$$

$$t = (\lambda/2c_o)t' \tag{A.3}$$

$$\bar{u} = \bar{U}\bar{u}'; \ \bar{U} = U_oM_o \tag{A.4}$$

$$u_1 = U_ou_1 \tag{A.5}$$

$$\bar{v} = \bar{V}\bar{v}'; \ \bar{V} = M_oU_o \ a/\lambda \tag{A.6}$$

$$v_1 = V_ov_1'; \ V_o = \pi(\delta_{ac}/\lambda)U_o \tag{A.7}$$

$$\bar{p} = p_o\bar{p}' \tag{A.8}$$

$$p_1 = \rho_oc_oU_op_1' = p_oM_op_{11}' \tag{A.9}$$

$$\bar{\rho} = \rho_o\bar{\rho}' \tag{A.10}$$

$$\rho_1 = \rho_oM_o\rho_1' \tag{A.11}$$

$$\mu = \mu_o\mu' \tag{A.12}$$

$$c_p = c_{p_o}c_p' \tag{A.13}$$

$$k = k_o k' \tag{A.14}$$

$$\bar{T} = T_w - (T_w - T_o)\bar{T}' \tag{A.15}$$

$$T_{1n} = T'_{1n}\theta_n;\ n = 1,2,---, \tag{A.16}$$

A justification of the characteristic values will now be given.

$\lambda/2$. The work of Purdy (27), Rayleigh (29), and Westervelt (30) indicates that the flow field for the problem under consideration will be duplicated in half wavelength sections. Due to the presence of a resonant acoustic field, the x-component of the periodic velocity will also be periodic in position x with a period of λ as shown by Purdy (27). In view of this it is anticipated that the temperature field will also have a component which is periodic in position x with a period of λ. Thus the derivatives of periodic velocity and temperature with respect to x' will be of order one. It is then assumed that the derivatives of the time-mean velocity and temperature with respect to x' will also be of no more than the order one.

δ_{ac}. The characteristic length, δ_{ac}, is referred to in the literature as the A.C. boundary layer thickness and is given by the expression $\delta_{ac} = \sqrt{2\nu_o/\omega}$, where ν_o is the kinematic viscosity and ω is the circular frequency of the resonant acoustic field. Periodic flow fields all have large changes in velocity in the direction normal to the wall. These changes, for the most part are restricted to a thin layer of fluid near the wall which is referred to as the A.C. boundary layer. Thus, by using δ_{ac} as the y-characteristic length the derivatives of the dimensionless

velocity with respect to y' should be of order one.

a. The characteristic length, a, is the half-width of the channel. The choice of a second characteristic value for the y-direction is necessary because δ_{ac} seems to be unsuitable when studying the derivative, $\frac{\partial T}{\partial y}$. In contrast to the velocity field, it is felt that (for the rates of flow being considered in this analysis) the changes which take place in the temperature of the fluid occur gradually over the entire width of the channel, rather than in the thin layer of fluid near the wall. Therefore, a new dimensionless length, $\bar{y}'$, is used to define the temperature derivatives and their orders of magnitude.

$\lambda/2c_o$. The characteristic time, $\lambda/2c_o$, or its equivalent, π/ω, is chosen since the circular frequency of the periodic components of density, pressure, velocity, and temperature is ω. Thus an order of magnitude change of one in time t' results in an order of magnitude change of one in the components ρ_1', p_1', u_1', v_1', and T_1'.

$\bar{U}$. The characteristic velocity, $\bar{U}$, is associated with the time-mean flow field. Its relation to the periodic flow field, as shown by Purdy (27), is given by $\bar{U} = U_o M_o$.

U_o. The characteristic velocity, U_o, is taken as the maximum amplitude of the x-component of the periodic velocity, u_1. It is assumed to be equal to the maximum amplitude of the periodic velocity for an inviscid fluid undergoing resonant acoustic vibrations.

$\bar{V}$. The characteristic velocity, $\bar{V}$, is associated with the y-component of the time-mean velocity. Its relation to $\bar{U}$, as shown by Purdy, is given by $\bar{V} = (a/\lambda)\,\bar{U}$.

V_o. The characteristic velocity, V_o, is associated with the y-component of the periodic velocity. Its relation to U_o is given by $V_o = U_o \delta_{ac}/\lambda$.

p_o. The characteristic pressure, p_o, is taken as the time-mean component of pressure at the position $x = 0$, $y = a$. For the through-flow rates to be considered, the pressure will not deviate appreciably from p_o.

$\rho_o c_o U_o$. The characteristic pressure, $\gamma p_o M_o$, is chosen since this represents the maximum amplitude of the periodic component of pressure for an inviscid fluid undergoing resonant acoustic vibrations and for which the maximum amplitude of velocity is U_o.

ρ_o. The characteristic density, ρ_o, is taken as the time-mean density at the position $x = 0$, $y = a$. It is assumed that the time-mean density of the fluid is constant and equal to ρ_o throughout the flow field.

$\rho_o M_o$. The characteristic density, $\rho_o M_o$, is chosen since the maximum amplitude of the periodic component of density for an inviscid fluid undergoing resonant acoustic vibrations and for a maximum amplitude of velocity, U_o, is $\rho_o M_o$.

μ_o. The characteristic viscosity, μ_o, is taken as the viscosity of the fluid. Since the viscosity has been assumed to be constant, μ' will be identically one.

c_{po}. The characteristic specific heat, c_{po}, is taken as the specific heat of the fluid. Since the specific heat has been assumed to be constant, c_p' will be identically one.

k_o. The characteristic thermal conductivity, k_o, is taken as the

thermal conductivity of the fluid. Since the thermal conductivity has been assumed to be constant, k' will be identically one.

$T_w - T_o$. The characteristic temperature, $T_w - T_o$, is taken as the maximum change in the time-mean temperature. Therefore, the dimensionless temperature, $\bar{T}'$, as defined by equation A.15, will have a minimum value of zero and a maximum value of one.

Energy Equation

The energy equation will now be analyzed in light of the foregoing changes of variable and the following assumptions concerning the orders of magnitude of the various quantities:

$$\theta[M_o,\ 2\delta_{ac}/\lambda,\ a/\lambda] = \delta \tag{A.17}$$

$$\theta\left[\frac{\partial \bar{p}'}{\partial x'}\right] = \delta^2 \tag{A.18}$$

$$\theta\left[\frac{\partial \bar{p}'}{\partial y'}\right] = \delta^4 \tag{A.19}$$

$$\theta\left[\frac{\partial}{\partial x'},\ \frac{\partial}{\partial y'},\ \frac{\partial}{\partial t'},\ \bar{u}',\ u_1',\ \bar{v}',\ v_1',\ \bar{\rho}',\ \rho_1',\ \mu',\ \frac{\partial p_1'}{\partial x'},\ \frac{\partial p_1'}{\partial t'}\right] = 1 \tag{A.20}$$

$$\theta[(T_w - T_o)/T_o] = 1 \tag{A.21}$$

$$\theta[\bar{T}',\ T_1',\ c_p',\ k'] = 1 \tag{A.22}$$

The assumptions listed in equations A.17, A.18, A.19 and A.20 are the same assumptions made by Purdy (27) in his analysis of the flow field

and since his solution for the velocity components is to be used in the present analysis it is imperative that we use the same assumptions. The assumptions listed in equation A.22 have already been justified in the previous discussion about the characteristic values. The remaining assumption, expressed by equation A.21, is based upon values of the temperatures, T_w and T_o, which are of practical interest. As an example, assume as representative values the following temperatures:

$$T_o = 120^\circ F$$

$$T_w = 212^\circ F.$$

The temperature ratio is thus seen to be

$$\frac{T_w - T_o}{T_o} = \frac{(212 + 459.69) - (120 + 459.69)}{(120 + 459.69)}$$

$$= 0.159.$$

Since this cannot be considered as a small number compared to unity, we must make the assumption given by equation A.21.

The energy equation, equation 3.5, in expanded form is

$$\rho c_p \{\frac{\partial T}{\partial t} + u \frac{\partial T}{\partial x} + v \frac{\partial T}{\partial y}\} = \{\frac{\partial p}{\partial t} + u \frac{\partial p}{\partial x} + v \frac{\partial p}{\partial y}\} + \qquad (A.23)$$

$$k\{\frac{\partial^2 T}{\partial x^2} + \frac{\partial^2 T}{\partial y^2}\} + \mu\Phi.$$

From the solution of the momentum and continuity equations, as given by Purdy (27), we have

$$\rho = \bar{\rho} + \text{Real}\,[\rho_{11}\exp(-i\omega t)] = \bar{\rho}(x,y) + \rho_1(x,y,t) \qquad (A.24)$$

$$p = \bar{p} + \text{Real}\,[p_{11}\exp(-i\omega t)] = \bar{p}(x,y) + p_1(x,y,t) \qquad (A.25)$$

$$u = \bar{u} + \text{Real}\,[u_{11}\exp(-i\omega t)] = \bar{u}(x,y) + u_1(x,y,t) \qquad (A.26)$$

$$v = \bar{v} + \text{Real}\,[v_{11}\exp(-i\omega t)] = \bar{v}(x,y) + v_1(x,y,t) \qquad (A.27)$$

where ρ_{11}, p_{11}, u_{11}, and v_{11} are, in general, complex functions of x and y.

Assume now that the temperature may be expressed as a Fourier series, i.e.,

$$T = \text{Real}\,\left[\sum_{n=0}^{\infty} T_{1n}(x,y)\exp(-in\omega t)\right]$$

or

$$T = \bar{T}(x,y) + \text{Real}\,\left[\sum_{n=1}^{\infty} T_{1n}(x,y)\exp(-in\omega t)\right] \qquad (A.28)$$

$$\equiv \bar{T} + T_1 \qquad (A.29)$$

If the above expressions for density, pressure, velocity, and temperature are substituted into the energy equation, A.23, remembering that the viscous dissipation function, Φ, is defined by equation 3.6, the resulting equation may be put into the form

$$\text{Real } [A_n(x,y)\exp(-in\omega t)] = \text{Real } [B_n(x,y)\exp(-in\omega t)] \quad (A.30)$$

Using a superscript R and I to indicate the real and imaginary components respectively of the functions $A_n(x,y)$ and $B_n(x,y)$, equation A.30 may be expanded to give the following equation

$$A_n^R\cos(n\omega t) + A_n^I\sin(n\omega t) = B_n^R\cos(n\omega t) + B_n^I\sin(n\omega t),$$

which implies that

$$A_n^R(x,y) = B_n^R(x,y)$$

$$A_n^I(x,y) = B_n^I(x,y)$$

From these two relations it follows that

$$A_n(x,y) = B_n(x,y).$$

Therefore, after having substituted equations A.24 through A.28 into the energy equation and rearranged the result into the form expressed by equation A.30, the following governing equations are obtained by equating the coefficients of $\exp(-in\omega t)$:

For n = 0;

$$c_p\{(\bar{\rho}\bar{u} + \frac{1}{2}\rho_{11}u_{11}^*)\frac{\partial\bar{T}}{\partial x} + (\bar{\rho}\bar{v} + \frac{1}{2}\rho_{11}v_{11}^*)\frac{\partial\bar{T}}{\partial y} + \quad (A.31)$$

$$\frac{1}{2}(\bar{\rho}u_{11}^{*} + \rho_{11}^{*}\bar{u})\frac{\partial T_{11}}{\partial x} + \frac{1}{2}(\bar{\rho}v_{11}^{*} + \rho_{11}^{*}\bar{v})\frac{\partial T_{11}}{\partial y} +$$

$$\frac{1}{2}(\rho_{11}^{*}u_{11}^{*}\frac{\partial T_{12}}{\partial x} + \rho_{11}^{*}v_{11}^{*}\frac{\partial T_{12}}{\partial y}) - \frac{i\omega}{2}\rho_{11}^{*}T_{11}] =$$

$$\bar{u}\frac{\partial \bar{p}}{\partial x} + \bar{v}\frac{\partial \bar{p}}{\partial y} + \frac{1}{2}u_{11}\frac{\partial p_{11}^{*}}{\partial x} + k(\frac{\partial^2 \bar{T}}{\partial x^2} + \frac{\partial^2 \bar{T}}{\partial y^2}) +$$

$$\mu\{2[(\frac{\partial \bar{u}}{\partial x})^2 + (\frac{\partial \bar{v}}{\partial y})^2 + \frac{1}{2}(\frac{\partial u_{11}}{\partial x})(\frac{\partial u_{11}^{*}}{\partial x}) + \frac{1}{2}(\frac{\partial v_{11}}{\partial y})(\frac{\partial v_{11}^{*}}{\partial y})] +$$

$$(\frac{\partial \bar{v}}{\partial x} + \frac{\partial \bar{u}}{\partial y})^2 + \frac{1}{2}(\frac{\partial v_{11}}{\partial x})(\frac{\partial v_{11}^{*}}{\partial x}) + \frac{1}{2}(\frac{\partial u_{11}}{\partial y})(\frac{\partial u_{11}^{*}}{\partial y}) + (\frac{\partial v_{11}}{\partial x})(\frac{\partial u_{11}^{*}}{\partial y}) -$$

$$\frac{2}{3}[(\frac{\partial \bar{u}}{\partial x} + \frac{\partial \bar{v}}{\partial y})^2 + \frac{1}{2}\{(\frac{\partial u_{11}}{\partial x})(\frac{\partial u_{11}^{*}}{\partial x}) + 2(\frac{\partial u_{11}}{\partial x})(\frac{\partial v_{11}^{*}}{\partial y}) + (\frac{\partial v_{11}}{\partial y})(\frac{\partial v_{11}^{*}}{\partial y})\}]\}.$$

For n = 1;

$$c_p\{-i\omega\bar{\rho}T_{11} + [\bar{\rho}\bar{u} + \frac{1}{4}(\rho_{11}u_{11}^{*} + \rho_{11}^{*}u_{11})]\frac{\partial T_{11}}{\partial x} + \qquad (A.32)$$

$$[\bar{\rho}\bar{v} + \frac{1}{4}(\rho_{11}v_{11}^{*} + \rho_{11}^{*}v_{11})]\frac{\partial T_{11}}{\partial y} + \frac{1}{2}(\bar{\rho}u_{11}^{*} + \rho_{11}^{*}\bar{u})\frac{\partial T_{12}}{\partial x} +$$

$$\frac{1}{2}(\bar{\rho}v_{11}^{*} + \rho_{11}^{*}\bar{v})\frac{\partial T_{12}}{\partial y} - i\omega\rho_{11}^{*}T_{12} +$$

$$\frac{1}{4}(\rho_{11}^{*}u_{11}^{*}\frac{\partial T_{13}}{\partial x} + \rho_{11}^{*}v_{11}^{*}\frac{\partial T_{13}}{\partial y}) + (\bar{\rho}u_{11} + \rho_{11}\bar{u})\frac{\partial \bar{T}}{\partial x} +$$

$$(\bar{\rho}v_{11} + \rho_{11}\bar{v})\frac{\partial\bar{T}}{\partial y}\} = -i\omega p_{11} + \bar{u}\frac{\partial p_{11}}{\partial x} + u_{11}\frac{\partial\bar{p}}{\partial x} +$$

$$v_{11}\frac{\partial\bar{p}}{\partial y} + k\left(\frac{\partial^2 T_{11}}{\partial x^2} + \frac{\partial^2 T_{11}}{\partial y^2}\right) +$$

$$\mu\{4[(\frac{\partial\bar{u}}{\partial x})(\frac{\partial u_{11}}{\partial x}) + (\frac{\partial\bar{v}}{\partial y})(\frac{\partial v_{11}}{\partial y})] +$$

$$2(\frac{\partial\bar{v}}{\partial x} + \frac{\partial\bar{u}}{\partial y})(\frac{\partial v_{11}}{\partial x} + \frac{\partial u_{11}}{\partial y}) -$$

$$\frac{4}{3}(\frac{\partial\bar{u}}{\partial x} + \frac{\partial\bar{v}}{\partial y})(\frac{\partial u_{11}}{\partial x} + \frac{\partial v_{11}}{\partial y})\}$$

For n = 2;

$$c_p\{-2i\omega\bar{\rho}T_{12} + [\bar{\rho}\bar{u} + \tfrac{1}{4}(\rho_{11}u_{11}^{*} + \rho_{11}^{*}u_{11})]\frac{\partial T_{12}}{\partial x} + \qquad (A.33)$$

$$[\bar{\rho}\bar{v} + \tfrac{1}{4}(\rho_{11}v_{11}^{*} + \rho_{11}^{*}v_{11})]\frac{\partial T_{12}}{\partial y} + \tfrac{1}{2}(\bar{\rho}u_{11}^{*} + \rho_{11}^{*}\bar{u})\frac{\partial T_{13}}{\partial x} +$$

$$\tfrac{1}{2}(\bar{\rho}v_{11}^{*} + \rho_{11}^{*}\bar{v})\frac{\partial T_{13}}{\partial y} - \frac{3}{2}i\omega\rho_{11}T_{13} - i\omega T_{11}\rho_{11} +$$

$$\tfrac{1}{2}(\bar{\rho}u_{11} + \rho_{11}\bar{u})\frac{\partial T_{11}}{\partial x} + \tfrac{1}{2}(\bar{\rho}v_{11} + \rho_{11}\bar{v})\frac{\partial T_{11}}{\partial y} +$$

$$\tfrac{1}{4}(\rho_{11}^{*}u_{11}^{*}\frac{\partial T_{14}}{\partial x} + \rho_{11}^{*}v_{11}^{*}\frac{\partial T_{14}}{\partial y}) + \tfrac{1}{2}(\rho_{11}u_{11}\frac{\partial\bar{T}}{\partial x} + \rho_{11}v_{11}\frac{\partial\bar{T}}{\partial y})\} =$$

$$\frac{1}{2}u_{11}\frac{\partial p_{11}}{\partial x} + k\left(\frac{\partial^2 T_{12}}{\partial x^2} + \frac{\partial^2 T_{12}}{\partial y^2}\right) + \mu\left\{\left(\frac{\partial u_{11}}{\partial x}\right)^2 + \left(\frac{\partial v_{11}}{\partial y}\right)^2 +$$

$$\frac{1}{2}\left(\frac{\partial v_{11}}{\partial x} + \frac{\partial u_{11}}{\partial y}\right)^2 - \frac{1}{3}\left(\frac{\partial u_{11}}{\partial x} + \frac{\partial v_{11}}{\partial y}\right)^2\right\} .$$

For $n > 2$;

$$c_p\left[\left(-i\omega n\bar{\rho}T_{1n} + \left[\bar{\rho}\bar{u} + \frac{1}{4}(\rho_{11}u_{11}^* + \rho_{11}^* u_{11})\right]\frac{\partial T_{1n}}{\partial x} + \right.\right. \qquad (A.34)$$

$$\left.\left[\bar{\rho}\bar{v} + \frac{1}{4}(\rho_{11}v_{11}^* + \rho_{11}^* v_{11})\right]\frac{\partial T_{1n}}{\partial y}\right\} + \left\{-\left(\frac{n-1}{2}\right)i\omega\rho_{11}T_{1,n-1} +$$

$$\frac{1}{2}(\bar{\rho}u_{11} + \rho_{11}\bar{u})\frac{\partial T_{1,n-1}}{\partial x} + \frac{1}{2}(\bar{\rho}v_{11} + \rho_{11}\bar{v})\frac{\partial T_{1,n-1}}{\partial y}\right\} +$$

$$\left\{-\left(\frac{n+1}{2}\right)i\omega\rho_{11}^* T_{1,n+1} + \frac{1}{2}(\bar{\rho}u_{11}^* + \rho_{11}^*\bar{u})\frac{\partial T_{1,n+1}}{\partial x} + \right.$$

$$\left.\frac{1}{2}(\bar{\rho}v_{11}^* + \rho_{11}^*\bar{v})\frac{\partial T_{1,n+1}}{\partial y}\right\} + \left\{\frac{1}{4}(\rho_{11}u_{11}\frac{\partial T_{1,n-2}}{\partial x} + \right.$$

$$\left.\rho_{11}v_{11}\frac{\partial T_{1,n-2}}{\partial y})\right\} + \left\{\frac{1}{4}(\rho_{11}^* u_{11}^*\frac{\partial T_{1,n+2}}{\partial x} + \rho_{11}^* v_{11}^*\frac{\partial T_{1,n+2}}{\partial y})\right\} =$$

$$k\left(\frac{\partial^2 T_{1n}}{\partial x^2} + \frac{\partial^2 T_{1n}}{\partial y^2}\right) .$$

In the above equations the asterisk superscript denotes the complex conjugate.

In the order of magnitude analysis of equations A.31 through A.34, the assumed order of magnitude of a function will be interpreted in the same manner as that in which the magnitude of a complex function is defined; therefore, the complex conjugate of a function will have the same order of magnitude as the function itself.

As a matter of convenience, equations A.31 through A.34 will be analyzed in reverse order, and in the case of equation A.34 we will consider each group of terms enclosed by { } separately to determine the most dominant term(s) in each group and then the results of the analyses of the individual groups will be combined to determine the most dominant term(s) in the equation. Therefore, we define z_1 by

$$z_1 = [\bar{\rho}\bar{u} + \frac{1}{4}(\rho_{11}u_{11}^{*} + \rho_{11}^{*}u_{11})] \frac{\partial T_{1n}}{\partial x} + \qquad (A.35)$$

$$[\bar{\rho}\bar{v} + \frac{1}{4}(\rho_{11}v_{11}^{*} + \rho_{11}^{*}v_{11})] \frac{\partial T_{1n}}{\partial y} - in\omega\bar{\rho}T_{1n}.$$

Introducing the dimensionless variables defined by equations A.1 through A.16, equation A.35 may be put into the form

$$z_1 = \frac{2\theta_n}{\lambda}\rho_o U_o M_o\{[\bar{u}' + \frac{1}{4}(\rho_{11}'u_{11}^{*'} + \rho_{11}^{*'}u_{11}')] \frac{\partial T_{1n}'}{\partial x'} +$$

$$1 \qquad 1\cdot 1 \qquad 1\cdot 1 \qquad 1$$

$$\frac{1}{2}[\bar{v}' + \frac{\pi}{2}(\frac{\delta_{ac}}{2a})(\rho_{11}{}'v_{11}^{*'} + \rho_{11}^{*'}v_{11}{}')] \frac{\partial T_{1n}'}{\partial \bar{y}'} - \frac{n\pi i}{M_o^2} T_{1n}'\}$$

$$1 \qquad \delta \qquad 1\cdot 1 \qquad 1\cdot 1 \qquad 1 \qquad (\frac{1}{\delta})^2 \cdot 1$$

The assumed orders of magnitude have been written directly under each term in the above equation. Retaining only the highest order of magnitude term we have

$$z_1 = - \frac{2n\pi i\theta_n}{\lambda M_o} \rho_o U_o T_{1n}' \qquad (A.36)$$

Following this procedure define z_2 by

$$z_2 = \frac{1}{2}(\bar{\rho}u_{11} + \rho_{11}\bar{u}) \frac{\partial T_{1,n-1}}{\partial x} - (\frac{n-1}{2})i\omega\rho_{11}T_{1,n-1} +$$

$$\frac{1}{2}(\bar{\rho}v_{11} + \rho_{11}\bar{v}) \frac{\partial T_{1,n-1}}{\partial y} .$$

By introducing dimensionless variables this may be rewritten as

$$z_2 = \frac{\rho_o U_o \theta_{n-1}}{\lambda} \{[u_{11}' + M_o^2\rho_{11}{}'\bar{u}'] \frac{\partial T_{1,n-1}'}{\partial x} +$$

$$1 \qquad \delta^2\cdot 1\cdot 1 \qquad 1$$

$$[\frac{\pi}{2}(\frac{\delta_{ac}}{a}) v_{11}' + \frac{1}{2} M_o^2\rho_{11}{}'v_{11}'] \frac{\partial T_{i,n-1}'}{\partial \bar{y}'} - (n-1)\pi i\rho_{11}{}'T_{1,n-1}'\}$$

$$\delta\cdot 1 \qquad \delta^2\cdot 1\cdot 1 \qquad 1 \qquad 1\cdot 1$$

Again, retaining only the dominant terms we have

$$z_2 = \frac{\rho_o U_o \theta_{n-1}}{\lambda} \left[u_{11}' \frac{\partial T_{1,n-1}'}{\partial x} - (n-1)\pi i \rho_{11}' T_{1,n-1}'\right] \qquad (A.37)$$

Defining z_3 as

$$z_3 = \frac{1}{4}\left(\rho_{11} u_{11} \frac{\partial T_{1,n-2}}{\partial x} + \rho_{11} v_{11} \frac{\partial T_{1,n-2}}{\partial y}\right)$$

and using a similar analysis we obtain

$$z_3 = \frac{2\rho_o U_o M_o \theta_{n-2}}{\lambda} \rho_{11}' u_{11}' \frac{\partial T_{1,n-2}'}{\partial x'} \qquad (A.38)$$

Similarly, the remaining groups of terms in equation A.34 become

$$z_4 = \frac{2\rho_o U_o M_o \theta_{n+2}}{\lambda} \rho_{11}^{*\prime} u_{11}^{*\prime} \frac{\partial T_{1,n+2}'}{\partial x'} \qquad (A.39)$$

$$z_5 = \frac{\rho_o U_o \theta_{n+1}}{\lambda} \left[u_{11}^{*\prime} \frac{\partial T_{1,n+1}'}{\partial x'} - (n+1)\pi i \rho_{11}' T_{1,n+1}'\right] \qquad (A.40)$$

$$z_6 = \frac{k\theta_n}{a^2} \frac{\partial^2 T_{1n}'}{\partial \bar{y}'^2} \qquad (A.41)$$

Now, combining the results expressed by equations A.36 through A.41, we have (after dividing by the factor, $-2c_p n\pi i \theta_n \rho_o U_o / \lambda M_o$)

$$T_{1n}' - \frac{M_o}{2n\pi i}\left(\frac{\theta_{n-1}}{\theta_n}\right)\left[u_{11}'\frac{\partial T_{1,n-1}'}{\partial x'} - (n-1)\pi i \rho_{11}' T_{1,n-1}'\right] +$$

$$1 \qquad \delta \quad (?) \qquad 1 \cdot 1 \qquad\qquad 1 \cdot 1$$

$$\left(-\frac{M_o^2}{2n\pi i}\right)\left(\frac{\theta_{n-2}}{\theta_n}\right)\rho_{11}' u_{11}'\frac{\partial T_{1,n-2}'}{\partial x'} - \left(\frac{M_o^2}{2n\pi i}\right)\left(\frac{\theta_{n+2}}{\theta_n}\right)\rho_{11}^{*\prime} u_{11}^{*\prime}\frac{\partial T_{1,n+2}'}{\partial x'} -$$

$$\delta^2 \cdot (?)\cdot 1 \cdot 1 \cdot 1 \qquad\qquad \delta^2 \cdot (?)\cdot 1 \cdot 1 \cdot 1$$

$$\left(\frac{M_o}{2n\pi i}\right)\left(\frac{\theta_{n+1}}{\theta_n}\right)\left[u_{11}^{*\prime}\frac{\partial T_{1,n+1}'}{\partial x'} - (n+1)\pi i \rho_{11} T_{1,n+1}'\right] =$$

$$\delta \quad (?) \quad 1 \cdot 1 \qquad\qquad 1 \cdot 1$$

$$\frac{iPr_o}{n}\left(\frac{1}{a'}\right)^2 \frac{\partial^2 T_{1n}'}{\partial \bar{y}'^2} \cdot$$

$$\delta^2 \cdot 1$$

As yet, no assumption has been made concerning the order of magnitude of the θ_n; however, the above equation indicates that if we assume all the θ_n to be equal; i.e., if

$$\theta_1 = \theta_2 = \theta_3 = \ldots = \theta_n \tag{A.42}$$

then we are led to the interesting and useful result

$$T_{1n}' = 0 \tag{A.43}$$

for all integral values of n greater than two.

Analyzing equation A.33 in a manner exactly analogous to that used

for equation A.34, and at the same time making use of equations A.42 and A.43 leads to the following equation

$$T_{12}' - \left(\frac{\theta_o}{\theta_1}\right)\left(\frac{M_o^2}{4\pi i}\right)\rho_{11}' u_{11}' \frac{\partial \bar{T}'}{\partial x'} = -\frac{(\gamma-1)M_o^2}{4\pi i}\left(\frac{T_o}{\theta_1}\right)\left[u_{11}' \frac{\partial p_{11}'}{\partial x'} + \frac{\pi}{4}\left(\frac{\partial u_{11}'}{\partial y'}\right)^2\right] \tag{A.44}$$

$$1 \quad (?)\cdot\delta^2\cdot 1\cdot 1\cdot 1 \qquad\qquad \delta^2\cdot(?) \quad 1\cdot 1 \qquad\qquad 1$$

No further analysis of the above equation will be made until some additional information can be obtained about the characteristic temperatures, θ_o and θ_1. Therefore, we shall proceed next with the analysis of equation A.32.

Using the same procedures on equation A.32 as were used on A.33 and A.34, equation A.32 may be reduced to

$$\left(\frac{\theta_o}{\theta_1}\right)\left(\frac{M_o}{\pi}\right)\left(u_{11}' \frac{\partial \bar{T}'}{\partial x'}\right) + iT_{11}' = i(\gamma-1)M_o\left(\frac{T_o}{\theta_1}\right)p_{11}'$$

or, since by definition

$$\theta_o = \bar{\theta} = T_w - T_o$$

$$\left(\frac{T_w - T_o}{T_o}\right)\left(\frac{T_o}{\theta_1}\right)\left(\frac{M_o}{\pi}\right)\left(u_{11}' \frac{\partial \bar{T}'}{\partial x'}\right) + iT_{11}' = i(\gamma-1)M_o\left(\frac{T_o}{\theta_1}\right)p_{11}'$$

$$1 \cdot (?)\cdot\delta\cdot 1\cdot 1 \qquad 1 \qquad\qquad \delta\cdot(?)\cdot 1$$

From this equation it may be seen that the only assumption which will give a nontrivial solution for T_{11}' is to assume the following order of

magnitude

$$\theta[T_o/\theta_1] = \frac{1}{\delta}$$

or, an equivalent assumption would be

$$\theta[(\gamma-1)M_o(T_o/\theta_1)] = 1$$

which may certainly be satisfied by choosing θ_1 to satisfy the relation

$$(\gamma-1)M_o(\frac{T_o}{\theta_1}) = 1$$

or

$$\theta_1 = (\gamma-1)M_oT_o \qquad (A.45)$$

Now if θ_o is as large as 100°R then

$$\theta[(\frac{\theta_o}{T_o})(\frac{T_o}{\theta_1})\ \frac{M_o}{\pi}] \simeq 1.$$

However, we have probably overestimated the change of $\bar{T}$ with respect to x'; i.e., for a Δx of $\lambda/2$, $\Delta\bar{T} < \theta_o$. Thus for smaller θ_o, the term

$$(\frac{T_w - T_o}{T_o})(\frac{T_o}{\theta_1})(\frac{M_o}{\pi})\ u_{11}'\ \frac{\partial\bar{T}'}{\partial x'}$$

can probably be neglected and the time-dependent temperature can be attributed to the isentropic compression-rarefaction process. Thus, the governing equation for T_{11}' is

$$T_{11}' = p_{11}' \tag{A.46}$$

or, in dimensional form, using Purdy's (27) solution for p_{11}',

$$T_{11} = - i(\gamma-1)M_o T_o \sin(\omega x/c_o) \tag{A.47}$$

Since θ_1 has been assumed to be given by equation A.45, then

$$\theta[\frac{\theta_o}{\theta_1}] = \theta[(\frac{T_w - T_o}{T_o})(\frac{T_o}{\theta_1})] = \frac{1}{\delta} \tag{A.48}$$

Using this order of magnitude in equation A.44 leads to the conclusion that

$$T_{12}' = 0. \tag{A.49}$$

Therefore, the governing equations for the time-dependent temperature components have now been solved and we have as a result

$$T_1(x,y,t) = \text{Real } [\sum_{n=1}^{\infty} T_{1n}(x,y)\exp(- in\omega t)]$$

$$= \text{Real } [T_{11}(x)\exp(- i\omega t)]. \tag{A.50}$$

We will now revert to equation A.31 which is the governing equation for the time-mean temperature $\tilde{T}(x,y)$. After introducing dimensionless variables equation A.31 can be reduced to (by retaining only the most dominant terms, and by considering only the real parts)

$$- 2\bar{u}' \frac{\partial \bar{T}'}{\partial x'} - \bar{v}' \frac{\partial \bar{T}'}{\partial \bar{y}'} = - \frac{\pi}{Pr_o (M_o a')^2} \frac{\partial^2 \bar{T}'}{\partial \bar{y}'^2}$$

or

$$\frac{\partial^2 \bar{T}'}{\partial \bar{y}'^2} - \frac{2}{\pi} Pr_o (M_o a')^2 \bar{u}' \frac{\partial \bar{T}'}{\partial x'} - \frac{1}{\pi} Pr_o (M_o a')^2 \bar{v}' \frac{\partial \bar{T}'}{\partial \bar{y}'} = 0 \qquad (A.51)$$

APPENDIX B

NUMERICAL METHODS

Analytical Investigations

The details of the numerical procedures referred to in Chapter IV are to be explained.

Numerical Solution of Equation 4.2

The equation to be solved is

$$\frac{\partial^2 \bar{T}'}{\partial \bar{y}'^2} + \phi_1(x',\bar{y}') \frac{\partial \bar{T}'}{\partial x'} + \phi_2(x',\bar{y}') \frac{\partial \bar{T}'}{\partial \bar{y}'} = 0 \qquad (B.1)$$

where

$$\phi_1(x',\bar{y}') = - \frac{2}{\pi} M_o^2 (a')^2 Pr_o \bar{u}'(x',\bar{y}') \qquad (B.2)$$

$$\phi_2(x',\bar{y}') = - \frac{1}{\pi} M_o^2 (a')^2 Pr_o \bar{v}'(x',\bar{y}') \qquad (B.3)$$

$$\bar{u}'(x',\bar{y}') = \frac{3M}{M_o^2} [\bar{y}' - \frac{1}{2} (\bar{y}')^2] - \qquad (B.4)$$

$$\frac{1}{8} \sin(2\pi x') \{[9 - \frac{27}{2a'}][\bar{y}' - \frac{1}{2} (\bar{y}')^2] -$$

$$3 + \exp(- a'\bar{y}')[2\cos(a'\bar{y}') + 6\sin(a'\bar{y}') + \exp(- a'\bar{y}')]\}$$

$$\bar{v}'(x',\bar{y}') = -\frac{\pi}{4}[\cos(2\pi x')\{[9 - \frac{27}{2a'}][\frac{1}{3}(\bar{y}')^3 - (\bar{y}')^2] + \quad (B.5)$$

$$6\bar{y}' - \frac{1}{a'}[10 - \exp(-a'\bar{y}')\{9\cos(a'\bar{y}') +$$

$$5\sin(a'\bar{y}') + \exp(-a'\bar{y}')\}]\} + \frac{1}{a'}[\exp(-a'\bar{y}')\{\cos(a'\bar{y}') +$$

$$\sin(a'\bar{y}')\} - 1]\ ].$$

The boundary conditions for equation B.1 are

$$\bar{T}'(x', 0) = 0 \quad (B.6)$$

$$\bar{T}'(0, y') = 1 \quad (B.7)$$

$$\frac{\partial\bar{T}'}{\partial\bar{y}'}\Big)_{\bar{y}'=1} = 0 \quad \text{for all } x' > 0. \quad (B.8)$$

In order to obtain a numerical solution for equation B.1 the following approximations will be used for the derivatives:

$$\frac{\partial\bar{T}'}{\partial\bar{y}'} = \frac{\bar{T}'_{i+1,j} - \bar{T}'_{i-1,j}}{2\Delta\bar{y}'}$$

$$\frac{\partial^2\bar{T}'}{\partial\bar{y}'^2} = \frac{1}{2(\Delta\bar{y}')^2}[(\bar{T}'_{i+1,j+1} - 2\bar{T}'_{i,j+1} + \bar{T}'_{i-1,j+1})$$

$$+ (\bar{T}'_{i+1,j} - 2\bar{T}'_{i,j} + \bar{T}'_{i-1,j})]$$

$$\frac{\partial \bar{T}'}{\partial x'} = \frac{1}{12\Delta x'} [(\bar{T}'_{i-1,j+1} - \bar{T}'_{i-1,j}) + 10(\bar{T}'_{i,j+1} - \bar{T}'_{i,j})$$

$$+ (\bar{T}'_{i+1,j+1} - \bar{T}'_{i+1,j})] .$$

These approximations are based upon a method suggested by Crank and Nicolson (35) and the grid-point pattern illustrated in Figure 10.

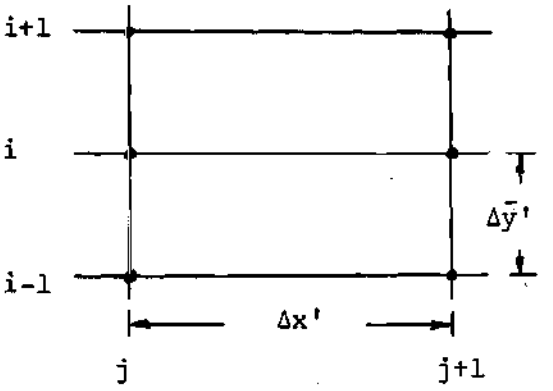

Figure 10. Grid-Point Pattern for Finite Difference Approximations.

Upon substitution of the above finite-difference approximations into equation B.1 we have

$$\frac{1}{2(\Delta \bar{y}')^2} [(\bar{T}'_{i+1,j+1} - 2\bar{T}'_{i,j+1} + \bar{T}'_{i-1,j+1}) \qquad (B.9)$$

$$+ (\bar{T}'_{i+1,j} - 2\bar{T}'_{i,j} + \bar{T}'_{i-1,j})]$$

$$+ \alpha_{i,j}\left(\frac{1}{12\Delta x'}\right)\left[\left(\bar{T}'_{i-1,j+1} - \bar{T}'_{i-1,j}\right) + 10\left(\bar{T}'_{i,j+1} - \bar{T}'_{i,j}\right)\right.$$

$$\left. + \left(\bar{T}'_{i+1,j+1} - \bar{T}'_{i+1,j}\right)\right] + \beta_{i,j}\left(\frac{1}{2\Delta\bar{y}'}\right)\left[\bar{T}'_{i+1,j} - \bar{T}'_{i-1,j}\right] = 0$$

where

$$\alpha_{i,j} = \phi_1(x'_j, \bar{y}'_{i,j}) \tag{B.10}$$

$$\beta_{i,j} = \phi_2(x'_j, \bar{y}'_{i,j}) \tag{B.11}$$

Since equation B.9 involves $\bar{T}'_{i+1,j+1}$ and $\bar{T}'_{i-1,j+1}$ as well as $\bar{T}'_{i,j+1}$, it is said to be an implicit difference equation. Given $\bar{T}'_{i,j}$ for $i = 1,2,\ldots, N$ as well as $\bar{T}'_{o,j}$, $\bar{T}'_{N+1,j}$, $\bar{T}'_{o,j+1}$, and $\bar{T}'_{N+1,j+1}$, in order to find $\bar{T}'_{i,j+1}$ for $i = 1,2,\ldots, N$ we must solve a system of N linear algebraic equations with N unknowns. After some rearranging equation B.9 may be written as

$$A_i\bar{T}'_{i+1,j+1} + B_i\bar{T}'_{i,j+1} + C_i\bar{T}'_{i-1,j+1} = D_i \tag{B.12}$$

where

$$A_i = \frac{6\Delta x'}{(\Delta\bar{y}')^2} + \alpha_{i,j}$$

$$B_i = 10\alpha_{i,j} - \frac{12\Delta x'}{(\Delta\bar{y}')^2}$$

$$C_i = A_i$$

$$D_i = \alpha_{i,j}[\bar{T}'_{i-1,j} + 10\bar{T}'_{i,j} + \bar{T}'_{i+1,j}]$$

$$- \frac{6\Delta x'}{(\Delta \bar{y}')^2}[\bar{T}'_{i+1,j} - 2\bar{T}'_{i,j} + \bar{T}'_{i-1,j}]$$

$$- \frac{6\Delta x'}{\Delta \bar{y}'} \beta_{i,j}[\bar{T}'_{i+1,j} - \bar{T}'_{i-1,j}]$$

Now boundary condition B.6 implies that

$$\bar{T}'_{o,j} = 0 \quad \text{for all } j,$$

and boundary condition B.8 implies that

$$\bar{T}'_{N+1,j} = \bar{T}'_{N-1,j} \quad \text{for all } j.$$

It is to be understood here that $\bar{T}'_{o,j}$ represents the wall temperature and $\bar{T}'_{N,j}$ represents the temperature at the centerline of the channel.

Taking cognizance of the latter two relations, equation B.12 becomes

$$A_1\bar{T}'_{2,j+1} + B_1\bar{T}'_{1,j+1} = D_1$$

$$A_i\bar{T}'_{i+1,j+1} + B_i\bar{T}'_{i,j+1} + C_i\bar{T}'_{i-1,j+1} = D_i \quad (i=2,3,\ldots,N-1)$$

$$A_N \bar{T}'_{N-1,j+1} + B_N \bar{T}'_{N,j+1} + C_N \bar{T}'_{N-1,j+1} = D_N$$

or, since $A_i = C_i$

$$B_1 \bar{T}'_{1,j+1} + A_1 \bar{T}'_{2,j+1} = D_1 \qquad \text{(B.13a)}$$

$$A_i \bar{T}'_{i-1,j+1} + B_i \bar{T}'_{i,j+1} + A_i \bar{T}'_{i+1,j+1} = D_i \quad (i=2,3,\ldots,N-1) \qquad \text{(B.13b)}$$

$$2\, A_N \bar{T}'_{N-1,j+1} + B_N \bar{T}'_{N,j+1} = D_N \qquad \text{(B.13c)}$$

Because the matrix of the linear system, equations B.13, is tri-diagonal; i.e., has no non-zero elements except on the main diagonal and on the diagonals adjacent to the main diagonal, there is a very simple algorithm for solving the equations which is easily derived by using the Gaussian elimination method. According to Young (36) the algorithm was first presented by Thomas (37) and was first used in connection with parabolic partial differential equations by Bruce, Peaceman, Rachford and Rice (38).

The solution of the equations B.13 can be determined by the following formulas:

$$b_1 = A_1/B_1 \qquad \text{(B.14a)}$$

$$b_i = A_i/(B_i - A_i b_{i-1}),\ i=2,3,\ldots,N-1 \qquad \text{(B.14b)}$$

$$q_1 = D_1/B_1 \tag{B.14c}$$

$$q_i = (D_i - A_i q_{i-1})/(B_i - A_i b_{i-1}), \quad i=2,3,\ldots,N-1 \tag{B.14d}$$

$$\bar{T}'_N = q_N \tag{B.14e}$$

$$\bar{T}'_i = q_i - b_i \bar{T}'_{i+1}, \quad i=N-1,N-2,\ldots,1. \tag{B.14f}$$

It should be pointed out that the above formulas are applicable only if the matrix of coefficients of the linear system satisfy certain requirements. In this particular application the formulas are valid if, and only if,

$$|B_i| \geq 2|A_i| \tag{B.15}$$

Heat Transfer Calculations

The local heat transfer coefficient is defined by the equation

$$hA\Delta T_{am} = \dot{m} c_p \Delta T_B \tag{B.16}$$

where A = Heat transfer area.

ΔT_{am} = Arithmetic mean temperature difference.

$\dot{m}$ = Mass rate of flow.

c_p = Constant pressure specific heat.

ΔT_B = Bulk-temperature difference.

h = Local heat transfer coefficient.

The local Nusselt number is defined by

$$Nu(x) = \frac{h(x)D}{k} \tag{B.17}$$

where h(x) = Local heat transfer coefficient.

D = Equivalent diameter = 4LS/A.

k = Thermal conductivity.

L = Length of duct from entrance of heated portion of duct.

S = Cross-sectional area for fluid flow.

A = Surface area of that part of duct which transfers heat.

Combining equations B.16 and B.17, the Nusselt number is

$$Nu(x) = \frac{\dot{m}c_p \Delta T_B D}{A \Delta T_{am} k} \tag{B.18}$$

For the parallel plate channel which is being analyzed (see Figure 41)

$$A = 2b\Delta x = b\lambda\Delta x' \tag{B.19}$$

where b represents a distance in the z-direction,

$$L = \Delta x$$

$$S = 2\ a\ b \tag{B.20}$$

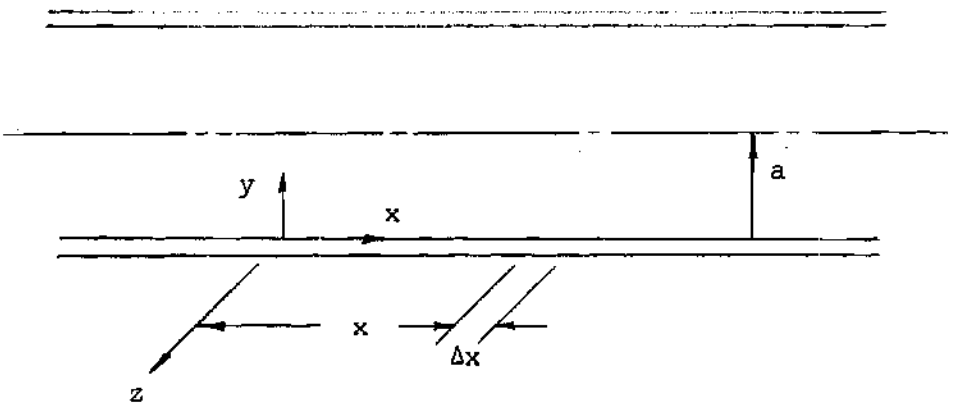

Figure 41. Coordinate System for Parallel Plate Channel.

Therefore, the equivalent diameter is

$$D = 4LS/A = 4a. \tag{B.21}$$

The product, $\dot{m}\, c_p$, is calculated by

$$\dot{m}c_p = c_p \int_o^{2a} b\rho_o \bar{u}(x,y)dy$$

$$= 2c_p \int_o^{a} b\rho_o \bar{u}(x,y)dy \ .$$

Introducing dimensionless parameters into the integrand we have

$$\dot{m}c_p = 2bc_p\rho_o U_o M_o a \int_o^{1} \bar{u}'(x',\bar{y}')d\bar{y}'$$

$$= 2 \frac{\rho_o U_o \lambda/2}{\mu_o} \frac{\mu_o c_p}{k} \frac{abkM_o}{\lambda/2} \int_0^1 \bar{u}'(x',\bar{y}')d\bar{y}'$$

$$= \frac{4abkM_o}{\lambda} Re_o Pr_o \int_o^1 \bar{u}'(x',\bar{y}')d\bar{y}'$$

Since the mass rate of flow must be constant (for steady flow) the integral in the above equation may be evaluated at any convenient value of x', say x' = 0. Therefore,

$$\int_o^1 \bar{u}'(x',\bar{y}')d\bar{y}' = \int_o^1 \bar{u}'(o,\bar{y}')d\bar{y}' \qquad \text{(B.22a)}$$

$$= \int_o^1 \frac{3M}{M_o^2} [\bar{y}' - \frac{1}{2}(\bar{y}')^2]d\bar{y}'$$

$$= M/M_o^2 \qquad \text{(B.22b)}$$

Hence

$$\dot{m}c_p = \frac{4abkM_o}{\lambda} Pe_o M/M_o^2$$

The Peclet number can be shown to be given by the equation

$$Pe_o = \frac{4}{\pi} M_o Pr_o (\lambda/2\delta_{ac})^2 \qquad \text{(B.23)}$$

Making use of this relation

$$\dot{m}c_p = \left(\frac{4abkM_o}{\lambda}\right)\left[\frac{2}{\pi}M_o Pr_o\left(\frac{\lambda}{2\delta_{ac}}\right)^2\right]\frac{M}{M_o^2}$$

$$\dot{m}c_p = \frac{8}{\pi}\,\frac{abk}{\lambda}\,Pr_o M(\lambda/2\delta_{ac})^2 \qquad (B.24)$$

The temperature differences are to be written in terms of dimensionless temperatures as follows:

$$\Delta T_{am} = \frac{1}{2}\left[(T_W - T_B)_{j+1} + (T_W - T_B)_j\right] \qquad (B.25)$$

where T_B is the fluid bulk-temperature which is defined by

$$T_B = \frac{\int_o^a \rho_o \bar{u}(x,y)T(x,y)dy}{\int_o^a \rho_o \bar{u}(x,y)dy}. \qquad (B.26)$$

Equation B.21 may be rewritten as

$$\Delta T_{am} = \frac{1}{2}\left[T_W - \{T_W - (T_W - T_o)T'_{B_{j+1}}\}\right.$$

$$\left. + T_W - \{T_W - (T_W - T_o)T'_{Bj}\}\right]$$

$$\Delta T_{am} = \frac{1}{2}(T_W - T_o)(T'_{B_{j+1}} + T'_{B_j}) \qquad (B.27)$$

Similarly,

$$\Delta T_B = T_{B_{j+1}} - T_{B_j}$$

$$= [T_W - (T_W - T_o)T'_{B_{j+1}}] - [T_W - (T_W - T_o)T'_{B_j}]$$

$$\Delta T_B = (T_W - T_o)(T'_{B_j} - T'_{B_{j+1}}) \tag{B.28}$$

Substituting B.19, B.21, B.24, B.27, and B.28 into equation B.18 the following result is obtained.

$$Nu(x'_{j+1}) = \frac{16(a')^2}{\pi \Delta x'} Pr_o M\left(\frac{T'_{B_j} - T'_{B_{j+1}}}{T'_{B_j} + T'_{B_{j+1}}}\right) \tag{B.29}$$

The average heat transfer coefficient may be defined by the equation

$$\bar{h}(x)\Delta T_{lm}\bar{A} = \int_o^x h(\xi)\Delta T_{am}(b\,d\xi) \tag{B.30}$$

where $\bar{A}$ represents the total area and is given by (for one plate only)

$$\bar{A} = b\ x \tag{B.31}$$

and where ΔT_{lm} is the logarithmic temperature difference which may be

written in terms of the dimensionless bulk temperature as

$$\Delta T_{lm} = (T_W - T_o) \frac{T_B' - 1.0}{\log T_B'} \tag{B.32}$$

Solving for $\bar{h}$ (x) the result is

$$\bar{h}(x) = \frac{1}{x\Delta T_{lm}} \int_o^x \frac{k}{D} Nu(\xi) \Delta T_{am} d\xi$$

When equations B.27, B.29, and B.32 are substituted into the above equation, the indicated integration carried out, and the average Nusselt number is formed the result is

$$\overline{Nu}(x'_{j+1}) = - \frac{8(a')^2}{\pi x'_{j+1}} Pr_o M \log_e T'_{B_{j+1}} . \tag{B.33}$$

Evaluation of the Parameter Φ

The paper by Norris and Streid (41) makes use of a parameter Φ which is defined by

$$\Phi = \frac{c_p GD^2}{kL} \tag{B.34}$$

where G = w/s = weight velocity, lb. per sq. ft. per hr., and the other symbols are as previously defined. For the parallel plate channel

$$w = \int_0^{2a} b\rho_o \bar{u}(x,y)dy$$

$$= 2\int_0^{a} b\rho_o \bar{u}(x,y)dy$$

But, from the development of equation B.24, it may be seen that the above equation can be expressed as

$$w = \frac{8}{\pi}\frac{abk}{\lambda c_p} Pr_o M(\lambda/2\delta_{ac})^2$$

and

$$G = w/S = \frac{4k}{\pi\lambda c_p} Pr_o M(\lambda/2\delta_{ac})^2 \qquad (B.35)$$

Since

$$D = 4a = 4\delta_{ac}a'$$

$$L = x = (\lambda/2)\, x'$$

equation B.34 becomes

$$\Phi = \frac{c_p(\frac{4k}{\pi\lambda c_p})Pr_o M(\lambda/2\delta_{ac})^2(4\delta_{ac}a')^2}{k(\lambda/2)x'}$$

$$\Phi = \frac{32}{\pi} (a')^2 Pr_o M/x' \qquad (B.36)$$

Channel Reynolds Number

The channel Reynolds number based on the average through-flow velocity and equivalent diameter is

$$Re = \frac{\rho_o U_{avg} D}{\mu_o}$$

$$= \frac{wD}{S\mu_o} = \frac{GD}{\mu_o}$$

$$Re = \frac{8a'}{\pi} \left(\frac{\lambda}{2\delta_{ac}}\right) M \qquad (B.37)$$

Development of Equation 4.18

For the case of laminar flow in a duct with opposite walls at the same temperature, Sellars, Tribus, and Klein (4) give the following equation for the heat flux at the wall:

$$q(x^+) = - \frac{k}{a} (T_W - T_o) \Sigma K_n Y_n'(1) \exp(- \frac{8}{3} \lambda_n^2 x^+)$$

where

$$x^+ = \frac{x}{a} (RePr)^{-1}$$

$$- K_n Y_n'(1) = 2.025 \lambda_n^{-1/3}$$

$$\lambda_n = 4n + 5/3 \ .$$

In terms of the dimensionless length, x'

$$x^+ = \frac{\lambda x'}{2a} (RePr)^{-1}$$

where λ is not to be confused with the eigenvalues λ_n, but instead it is the wavelength of the impressed acoustic vibrations. Hence,

$$q(x') = 2.025 \frac{k(T_W - T_o)}{a} \Sigma\lambda_n^{-1/3} \exp[- \frac{8}{3} \lambda_n^2 (\frac{\lambda}{2a}) \frac{x'}{RePr}] \quad (B.38)$$

The heat transferred over the interval $[0,x']$ is found by

$$Q = 2 \int_o^{x'} b(\lambda/2)q(x')dx' \quad (B.39)$$

where the coefficient 2 is introduced to account for the heat transferred at both walls. Substituting B.38 into B.39 and integrating, the result is

$$Q = 3.0375(\frac{bk}{2})(T_W - T_o)RePr_o\Sigma\lambda_n^{-7/3} [1 - \quad (B.40)$$

$$\exp\{- \frac{8}{3} \lambda_n^2 (\lambda/2a)(x'/RePr_o)\}]$$

This quantity may also be defined by means of

$$Q = \dot{m} c_p \Delta T_B \tag{B.41}$$

If equation B.28 is applied to the interval [0,x'], then

$$\Delta T_B = (T_W - T_o)[1 - T_B'(x')]$$

Substituting this and equation B.24 into B.41 we have

$$Q = \frac{4}{\pi} \left(\frac{\lambda}{2\delta_{ac}}\right) Pr_o Ma' kb (T_W - T_o)[1 - T_B'(x')] \tag{B.42}$$

Equating the expressions in (B.41) and (B.42) and solving for $T_B'(x')$ the result is

$$T_B'(x') = 1 - 3.0375 \Sigma \lambda_n^{-7/3} [1 - \exp\{-\frac{\pi}{3} \left(\frac{\lambda_n}{a'}\right)^2 \frac{x'}{MPr_o}\}] . \tag{B.43}$$

The average heat transfer coefficient can be defined as

$$\bar{h}(x') = \frac{Q(x')}{A \Delta T_{lm}(x')}$$

and the average Nusselt number is

$$\overline{Nu}(x') = \frac{\bar{h}(x') D}{k}$$

where D = 4a is the hydraulic, or equivalent, diameter. Hence,

$$\overline{Nu}(x') = \frac{Q}{bx'\Delta T_{lm}(x')} \frac{4a}{k}$$

Utilizing B.42 and the definition of the logarithmic mean temperature difference

$$\Delta T_{lm}(x') = (T_W - T_o) \frac{T_B'(x') - 1.0}{\log_e T_B'(x')}$$

the Nusselt number becomes

$$\overline{Nu}(x') = - \frac{8(a')^2}{\pi x'} Pr_o M \log_e T_B'(x') \qquad (B.44)$$

Using the parameter Φ defined by

$$\Phi = \frac{32}{\pi} (a')^2 Pr_o M/x'$$

equations B.43 and B.44 become

$$T_B'(\Phi) = 1. - 3.0375 \Sigma \lambda_n^{-7/3} [1 - \exp\{- \frac{32}{3} \lambda_n^2/\Phi\}] \qquad (B.45)$$

$$\overline{Nu}(\Phi) = - \frac{1}{4} \Phi \log_e T_B'(\Phi) \qquad (B.46)$$

Development of Equations 4.21—4.23

The total heat transferred over the interval $[x', x'+\Delta x']$ is found by

$$Q = 2b(\lambda/2)\int_{x'}^{x'+\Delta x'} q(x')dx'$$

Substituting equation B.38 into the integrand and carrying out the integration we obtain

$$Q = \frac{6.075}{\pi}\frac{bk\lambda}{a}(a')^2 Pr_o M(T_W - T_o)\sum_{n=0}^{\infty}\xi_n \qquad (B.47)$$

where

$$\xi_n = \lambda_n^{-7/3}\exp[-\frac{\pi}{3}(\frac{\lambda_n}{a'})^2\frac{x'}{Pr_o M}]\{1 - \exp[-\frac{\pi}{3}(\frac{\lambda_n}{a'})^2\frac{\Delta x'}{Pr_o M}]\}$$

The arithmetic mean temperature difference, as shown in equation B.27, is

$$\Delta T_{am} = \frac{1}{2}(T_W - T_o)[T_B'(x') + T_B'(x' + \Delta x')] \qquad (B.48)$$

The local heat transfer coefficient is calculated by

$$h(x') = \frac{Q}{A\Delta T_{am}}$$

and the local Nusselt number is defined by

$$Nu(x') = \frac{h(x')D}{k} = \frac{QD}{Ak\Delta T_{am}} \qquad (B.49)$$

Substituting from equations B.19, B.21, B.36, B.47 and B.48 into equation B.49, the result is

$$Nu(\Phi) = \frac{48.6}{32} \frac{\Phi^2[1 - \frac{\Delta\Phi}{\Phi}]}{\Delta\Phi} \frac{f(\Phi)}{g(\Phi)} \tag{B.50}$$

where

$$f(\Phi) = \sum_{n=0}^{\infty} \xi_n(\Phi) \tag{B.51}$$

$$g(\Phi) = T_B'(\Phi) + T_B'(\Phi + \Delta\Phi) \tag{B.52}$$

$$T_B'(\Phi + \Delta\Phi) = 1 - 3.0375 \sum_{n=0}^{\infty} \zeta_n(\Phi) \tag{B.53}$$

$$\zeta_n(\Phi) = \lambda_n^{-7/3} \{1 - \exp[-\frac{32}{3} \lambda_n^2 (\frac{1}{\Phi} + \frac{\Delta\Phi}{\Phi^2(1 - \frac{\Delta\Phi}{\Phi})})] \}$$

Experimental Investigations

Laminar Flow Meter Equations

A Meriam Laminar Flow Meter, Model 50MC2-4PF, with a flow rate of 200 SCFM at a differential pressure of four inches of water was used to measure the mass flow rate of air through the system. In order to incorporate the operating characteristics of this device in the data reduction computer program the analysis presented here has been performed.

The operation of the laminar flow meter is predicated on fully-developed laminar flow and therefore the salient characteristics of this

device can be determined from the analysis of fully-developed channel flow; i.e.,

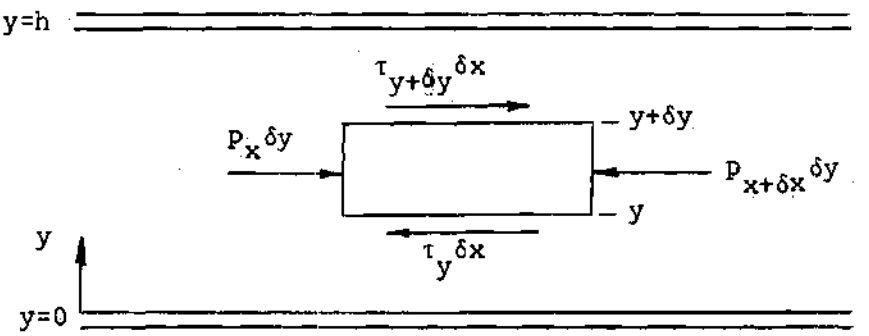

where x is greater than the development length; thus, from the momentum equation

$$\Sigma F_x = 0 = p_x\delta y + \tau_{y+\delta y}\delta x - \tau_y\delta x - p_{x+\delta x}\delta y$$

or, after dividing by $\delta x\delta y$ and taking the limit as δx and δy approach zero, we have

$$\frac{d\tau}{dy} = \frac{dp}{dx}$$

From Newton's "law" for shear stress

$$\tau = \mu \frac{du}{dy}$$

we obtain

$$\frac{d^2u}{dy^2} = \frac{1}{\mu}\frac{dp}{dx} \tag{B.54}$$

with the "no-slip" boundary conditions

$$\begin{aligned} u(0) &= 0 \\ u(h) &= 0 \end{aligned} \tag{B.55}$$

Solving B.54 subject to the boundary conditions B.55 gives the result

$$u = -\frac{h^2}{2\mu}\frac{dp}{dx}\left[\frac{y}{h} - \left(\frac{y}{h}\right)^2\right]$$

The volumetric flow rate per unit width is

$$Q = \int_{y=0}^{y=h} u\,dy$$

or,

$$Q = -\frac{h^3}{12}\ \frac{1}{\mu}\ \frac{dp}{dx}$$

The pressure gradient, $\frac{dp}{dx}$, for fully-developed laminar flow is constant and therefore equal to

$$\frac{dp}{dx} = \frac{p_2 - p_1}{x_2 - x_1} = - \frac{\Delta p}{L}$$

where

$$\Delta p = p_1 - p_2$$

$$L = x_2 - x_1$$

and, finally,

$$Q = \frac{h^3}{12L} \frac{1}{\mu} \Delta p = C_{geom} \frac{1}{\mu} \Delta p.$$

The coefficient, C_{geom}, is a function of geometry only. For the laminar flow meter this was obtained experimentally by calibration at the factory. The volumetric flow rate is seen to be directly proportional to the pressure drop and, therefore, from the calibration curve

$$\frac{C_{geom}}{\mu_o} = \frac{Q}{\Delta p} = \frac{215.0 \text{ cu.ft./min.}}{4.000 \text{ in.water}}$$

$$= 53.75 \text{ cu.ft./min. per inch of water}$$

where $\mu_o = \mu_{air}$ at 70°F. and 29.92 inches of Hg. For any other flow meter temperature

$$Q = 53.75\ C_\mu \Delta p (ft^3/min)$$

where $C_\mu = \mu_o/\mu$.

For air at "normal" temperatures the viscosity ratio may be approximated by

$$C_\mu = \mu_o/\mu = (T_o/T)^{0.76}$$

(The viscosity data for air was taken from reference 39.) For use in the data reduction program, the viscosity data for air in the temperature range from 8°F. to 242°F. were fitted with first, second, third, and fourth degree polynomials by the method of least squares. The following second degree polynomial gave the "best" fit:

$$\mu = 3.9383352 \times 10^{-2} + 6.8045312 \times 10^{-5}\ T$$

$$- 2.6794193 \times 10^{-8}\ T^2$$

where T is the static temperature in degrees Fahrenheit.

To estimate the tube Reynolds number, the following equations are used:

$$Re = \frac{\rho V D}{\mu}$$

$$\dot{m} = \rho V D \left(\frac{\pi D}{4}\right)$$

or

$$\rho VD = \frac{4\dot{m}}{\pi D}$$

and

$$Re = \frac{4\dot{m}}{\pi D}\left(\frac{1}{\mu}\right)$$

But

$$\dot{m} = \rho Q = \rho\left(\frac{C_{geom}}{\mu_o}\right)\left(\frac{\mu_o}{\mu}\right)\Delta p$$

and since

$$\rho = p/RT$$

$$Re = \frac{4C_{geom}}{\pi\mu_o}\left(\frac{\Delta p}{D}\right)\left(\frac{\mu_o}{\mu}\right)\left(\frac{1}{\mu}\right)\left(\frac{p}{RT}\right)$$

or

$$Re = \left(\frac{C_{geom}}{\mu_o}\right)\left(\frac{4}{\pi D}\right)\left(\frac{1}{\mu_o}\right)\left(\frac{\mu_o}{\mu}\right)_{T_3}\left(\frac{\mu_o}{\mu}\right)_{T_4}\left(\frac{P_o}{RT_o}\right)\left(\frac{P_3}{P_o}\right)\left(\frac{T_o}{T_3}\right)\Delta p$$

$$= \left(\frac{C_{geom}}{\mu_o}\right)\left(\frac{4}{\pi D}\right)\left(\frac{1}{\mu_o}\right)\left(\frac{P_o}{RT_o}\right)\left(\frac{T_o}{T_3}\right)^{1.76}\left(\frac{T_o}{T_4}\right)^{0.76}\left(\frac{P_3}{P_o}\right)\Delta p$$

where T_o = 529.6°R.

p_o = 29.92 inches of Hg.

R = 53.35 ft-lbm/lbf-sec^2.

D = 3.86 inches.

T_3 = Laminar flow meter temperature -°R.

T_4 = Plenum chamber temperature -°R.

P_3 = Laminar flow meter static pressure (upstream) - inches of Hg.

Δp = Differential pressure drop across laminar flow meter - inches of water.

Now

$$\left(\frac{4}{\pi}\right)\left(\frac{1}{D}\right)\left(\frac{1}{\mu_o}\right)\left(\frac{P_o}{RT_o}\right) = 403.82 \text{ min./cu.ft.}$$

and finally

$$Re = 2.1705 \times 10^4 \left(\frac{T_o}{T_3}\right)^{1.76} \left(\frac{T_o}{T_4}\right)^{0.76} \left(\frac{P_3}{P_o}\right)^{0.76} \Delta p \qquad (B.56)$$

Data Reduction and Correlation

The object of the experimental program on convective heat transfer was to determine the effect of pulsating flow on the convective heat transfer rate. The heat transfer test section is shown schematically in Figure 42. The symbols in the sketch are defined as follows:

$\dot{m}$ = Mass flow rate of primary air - cu.ft./hr.

$\dot{m}_i$ $(i = 1,2,\ldots,21)$ = Condensate flow rate of saturated liquid water - lbm/hr.

q_i ($i = 1,2,\ldots,21$) = Heat transfer rate from the condensing steam to the primary air steam-BTU/hr.

T_i ($i = 1,2,\ldots,21$) = Mixed mean air temperature at the end of each section - degrees F.

A_{x_i} ($i = 1,2,\ldots,21$) = Surface area of each section - sq.ft.

A_i ($i = 1,2,\ldots,21$) = Total surface area from the thermal entrance ($x = 0$) to the end of section i (chamber i) - sq.ft.

x_i ($i = 1,2,\ldots,21$) = Distance from the thermal entrance to the end of section i - ft.

x_{x_i} ($i = 1,2,\ldots,21$) = Distance from the thermal entrance to the midpoint in section i; i.e., $x_{x_i} = (x_i + x_{i-1})/2$ - ft.

T_o = Mixed mean air temperature at the thermal entrance ($x = 0$) - degrees F.

T_{o_a} = Mixed mean air temperature at the beginning of chamber 1 ($x_{o_a} = 0.38$ inches) - degrees F.

q_{o_a} = Heat transfer rate from the condensing steam to the primary air stream (this must be estimated since the condensate was not collected) - BTU/hr.

T_s = Saturation temperature of the condensing steam - degrees F.

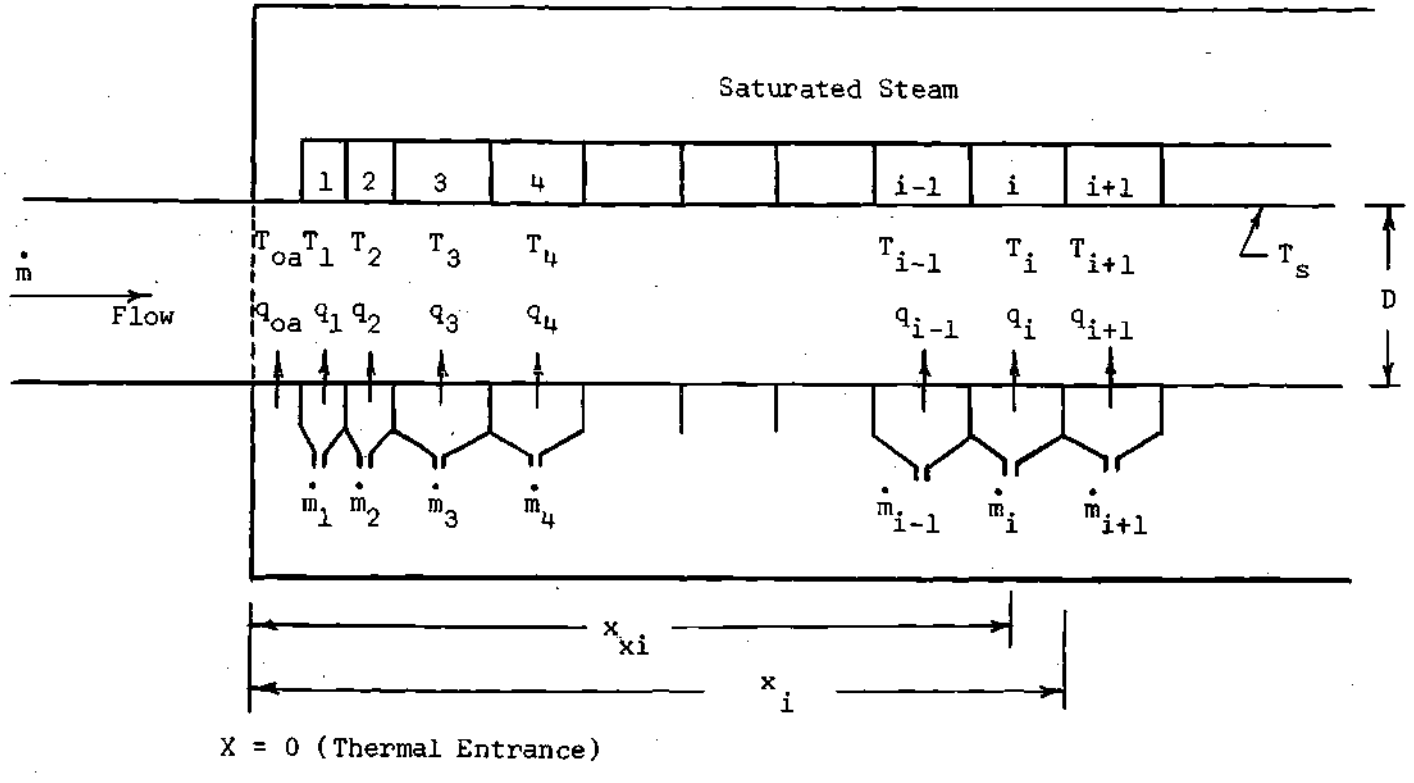

Figure 42. Schematic Diagram of Heat Transfer Section.

The governing equations for this flow system are:

Continuity:

$$\dot{m} = \rho A V \tag{B.57}$$

$$G = \dot{m}/A = \rho V = \text{Constant}$$

where

$$A = \pi D^2/4 \tag{B.58}$$

Energy: For the system (control volume consists of the 3.86 inch I.D. tube from $x = 0$ to $x = x_i$) under consideration changes in kinetic energy and potential energy are very small in comparison to changes in enthalpy and may be neglected. The energy equation under this assumption becomes

$$\frac{dQ_i}{dt} = \dot{m}(h_i - h_o) \tag{B.59}$$

where

$$\frac{dQ_i}{dt} = q_{oa} + \sum_{j=1}^{i} q_j \tag{B.60}$$

But

$$q_j = \dot{m}_j h_{fg} \tag{B.61}$$

where h_{fg} is the enthalpy of vaporization for water at the conditions of the saturated steam. Thus,

$$\frac{dQ_i}{dt} = q_{oa} + h_{fg} \sum_{j=1}^{i} \dot{m}_j \tag{B.62}$$

Equation of State: The primary air is a mixture of dry air and water vapor with a specific humidity of γ lbm water/lbm dry air. For this mixture the following "perfect gas" relations are used:

$$p\ v = R\ (T + 459.69) \tag{B.63}$$

$$c_p = \text{Constant} \tag{B.64}$$

where

$$R = \frac{53.35 + 85.58\gamma}{1 + \gamma} \text{ - ft-lbf/lbm-deg.R} \tag{B.65}$$

$$c_p = \frac{0.240 + 0.446\gamma}{1 + \gamma} \text{ - ft-lbf/lbm-deg.R} \tag{B.66}$$

p = static pressure - lbf/sq.ft.

v = specific volume - cu.ft./lbm

T = temperature - degrees F.

γ = specific humidity - lb.water/lb.dry air.

As a consequence of the foregoing relations, the following expression for $(h_i - h_o)$ may be used:

$$h_i - h_o = c_p (T_i - T_o) \tag{B.67}$$

Temperature Distribution: The mixed-mean temperature distribution may now be found from equations B.59, B.62, and B.67; i.e.,

$$T_i - T_o = \frac{1}{\dot{m}c_p} \frac{dQ_i}{dt}$$

$$= \frac{1}{\dot{m}c_p} [q_{oa} + h_{fg} \sum_{j=1}^{i} \dot{m}_j]$$

or

$$T_i = T_o + \frac{1}{\dot{m}c_p} [q_{oa} + h_{fg} \sum_{j=1}^{i} \dot{m}_j] \tag{B.68}$$

Equation B.68 is not as straightforward as it may seem because the quantities T_o and q_{oa} are unknown; however, they may be estimated from known data. For this purpose the following analyses are given.

Inlet Temperature Correction: The sketch shown below defines the present system:

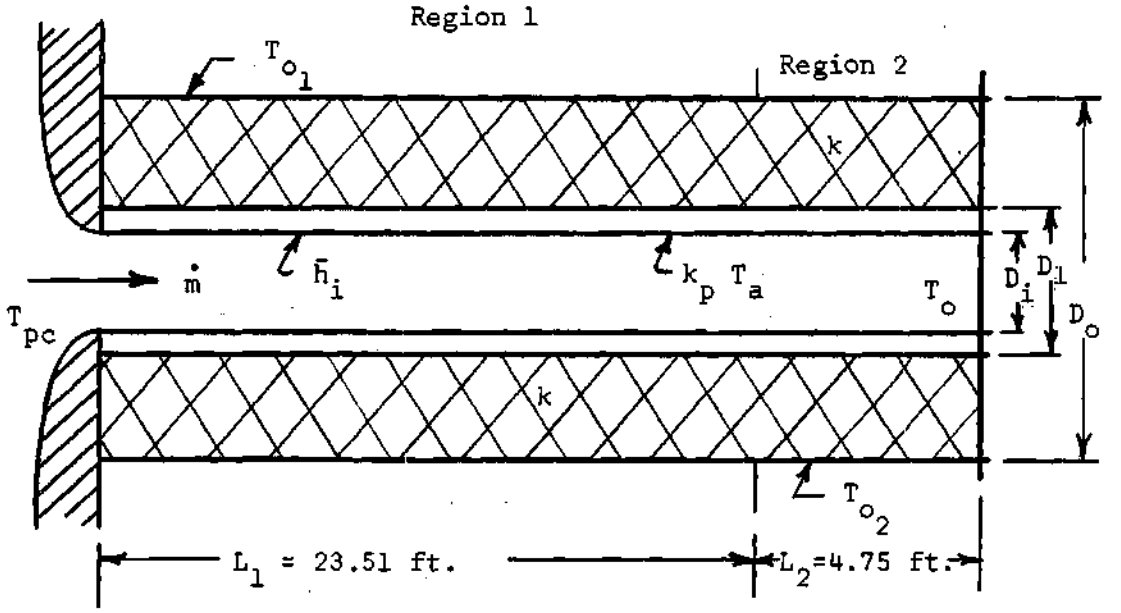

Region 1 is the uncontrolled laboratory. Region 2 is the controlled atmosphere within the acoustic shield. The known data consist of

$\dot{m}$ = Mass flow rate of primary air.

D_o = Outside diameter of the insulating material.

D_1 = Outside diameter of copper tube.

D_i = Inside diameter of copper tube.

k = Thermal conductivity of insulating material.

k_p = Thermal conductivity of copper.

T_{pc} = Temperature of air inside plenum chamber.

T_{o_1} = Temperature of outer fibers of the insulating material in Region 1.

T_{o_2} = Temperature of outer fibers of the insulating material in Region 2.

The overall heat transfer coefficient for this system is

$$U = \frac{1}{D_o/D_i\bar{h}_i + D_o\log(D_1/D_i)/2k_p + D_o\log(D_o/D_1)/2k}$$

where

D_i = 3.86 inches.

D_1 = 4.125 inches.

D_o = 8.125 inches.

k_p = 220 BTU/hr-ft-deg.F.

k = 0.22 BTU-in/hr-sq.ft.-deg.F.

$\bar{h}_i = 0.023\ Re^{0.8}\ Pr^{1/3}\ k_f/D_i$.

Thus

$$\frac{D_o}{D_i\bar{h}_i} = 29.4\ Re^{-0.8}\ Pr^{-1/3}/k_f$$

$$\frac{D_o\log(D_1/D_i)}{2k_p} \approx 0$$

$$\frac{D_o\log(D_o/D_1)}{2k} = 12.52$$

$$U = \frac{1}{12.52 + 29.4\ Re^{-0.8}Pr^{-1/3}/k_f}$$

For a given Reynolds number U is constant, and therefore, from the steady-flow energy equation we have

$$dq = U(T - T_{o_i})\pi D_o dx = - \dot{m}c_p dT$$

$$= - \dot{m}c_p d(T - T_{o_i})$$

or

$$\frac{d(T - T_{o_i})}{T - T_{o_i}} = - \frac{\pi D_o U}{\dot{m}c_p} dx$$

Integrating we have

$$\log \left(\frac{T_a - T_{o_1}}{T_{pc} - T_{o_1}}\right) = - \frac{\pi D_o U}{\dot{m}c_p} L_1$$

or

$$T_a - T_{o_1} = (T_{pc} - T_{o_1})\exp[- \pi D_o U L_1/\dot{m}c_p]$$

Similarly

$$\log\left(\frac{T_o - T_{o_2}}{T_a - T_{o_2}}\right) = - \frac{\pi D_o U L_2}{\dot{m}c_p}$$

or

$$T_o - T_{o_2} = (T_a - T_{o_2})\exp[-\pi D_o U L_2/\dot{m}c_p]$$

Finally

$$T_o = T_{o_2} + (T_{o_1} - T_{o_2})\exp(-\pi D_o U L_2/\dot{m}c_p)$$

$$+ (T_{pc} - T_{o_1})\exp(-\pi D_o U[L_1 + L_2]/\dot{m}c_p)$$

Now

$$\pi D_o L_2 = 10.11$$

$$\pi D_o (L_1 + L_2) = 60.2$$

Therefore

$$T_o = T_{o_2} + (T_{o_1} - T_{o_2})\exp(-10.11U/\dot{m}c_p) \qquad (B.69)$$

$$+ (T_{pc} - T_{o_1})\exp(-60.2U/\dot{m}c_p)$$

Estimation of q_{oa}. The sketch shown below defines the present system:

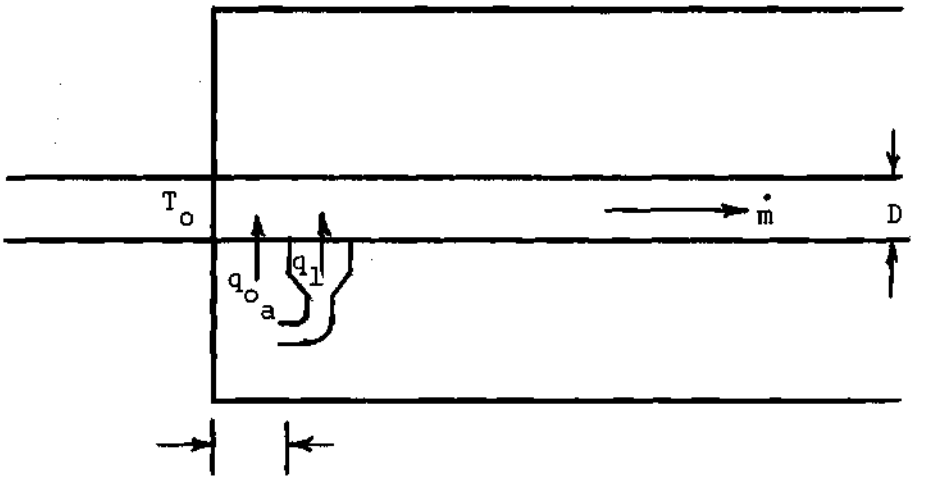

The known data consist of

$\dot{m}$ = Mass flow rate of primary air.

c_p = Constant pressure specific heat.

D = Inside diameter of copper tube.

T_o = Temperature of the air at x = 0.

Writing the steady-flow energy equation for the control volume, which consists of the 3.86 inch I.D. tube from x = 0 to x = L, we have

$$q_{oa} = \dot{m}c_p(T_{o_a} - T_o)$$

where

$$\dot{m} = \rho AV = \frac{\pi}{4} \mu DRe$$

The heat transfer may also be computed by

$$q_{oa} = h\pi DL(T_s - T_o)$$

or, equating the two expressions,

$$\frac{T_{o_a} - T_o}{T_s - T_o} = \frac{\pi hDL}{\dot{m}c_p}$$

If the flow is laminar then Léveque's solution (40) for "h" yields

$$\frac{T_{o_a} - T_o}{T_s - T_o} = 5.55\left(\frac{\dot{m}c_p}{kL}\right)^{-2/3} = 5.55\left(\frac{\pi}{4} RePr\frac{D}{L}\right)^{-2/3}$$

Since D = 3.86 inches and L = 0.38 inches

$$T_{o_a} = T_o + 1.39\ (T_s - T_o)(RePr)^{-2/3}$$

The heat transfer correction then becomes

$$q_{oa} = \dot{m}c_p(T_{o_a} - T_o)$$

$$= \dot{m}c_p[5.55(T_s - T_o)(\frac{kL}{\dot{m}c_p})^{2/3}]$$

$$q_{oa} = 5.55(T_s - T_o)(kL)^{2/3}(\dot{m}c_p)^{1/3} \qquad (B.70)$$

This equation should be used for Re < 2500.

For turbulent flow the problem is more difficult. However, an approximate value for "h" can be determined from Latzko's (40) prediction for the starting region in a tube with a bellmouth entry; i.e.,

$$Nu = \frac{hD}{k} = \{0.023\ Re^{0.8}Pr^{1/3}\}\{1.11Re^{0.055}(\frac{D}{L})^{0.22}\}$$

Thus

$$q_{oa} = hA\Delta T$$

$$= 0.0255Re^{0.855}Pr^{1/3}(\frac{D}{L})^{0.22}(\frac{k_f}{D})(\pi DL)(T_s - T_o)$$

$$q_{oa} = 4.229Re^{0.855}Pr^{1/3}(k_f \times 10^{-3})(T_s - T_o)$$

Since the Prandtl number is approximately 0.708

$$q_{oa} = 3.769 \times 10^{-3}Re^{0.855}k_f(T_s - T_o). \qquad (B.71)$$

With equations B.69 and B.70 or B.71, the temperature distribution may be determined with the aid of equation B.68. The temperature

distribution for this system may be represented graphically as shown in Figure 43.

The following quantities can now be determined:

h_i = Average heat transfer coefficient based on the logarithmic-mean temperature difference.

Nu_i = Average Nusselt number.

Gz_i = Average Graetz number.

Gr_i = Average Grashof number.

h_{x_i} = Local heat transfer coefficient based on the arithmetic-mean temperature difference.

Nu_{x_i} = Local Nusselt number.

Gz_{x_i} = Local Graetz number.

Gr_{x_i} = Local Grashof number.

These quantities will be calculated in the following manner:

$\underline{h_i}$. From the definition of the heat transfer coefficient we have

$$h = \frac{dQ}{dt}/A\Delta T$$

where $\frac{dQ}{dt}$ = Rate of heat transfer in BTU/hr.

A = Surface area of tube in sq.ft.

ΔT = Temperature difference.

The average, or mean, heat transfer coefficient h_i will be based on the logarithmic-mean temperature difference; i.e.,

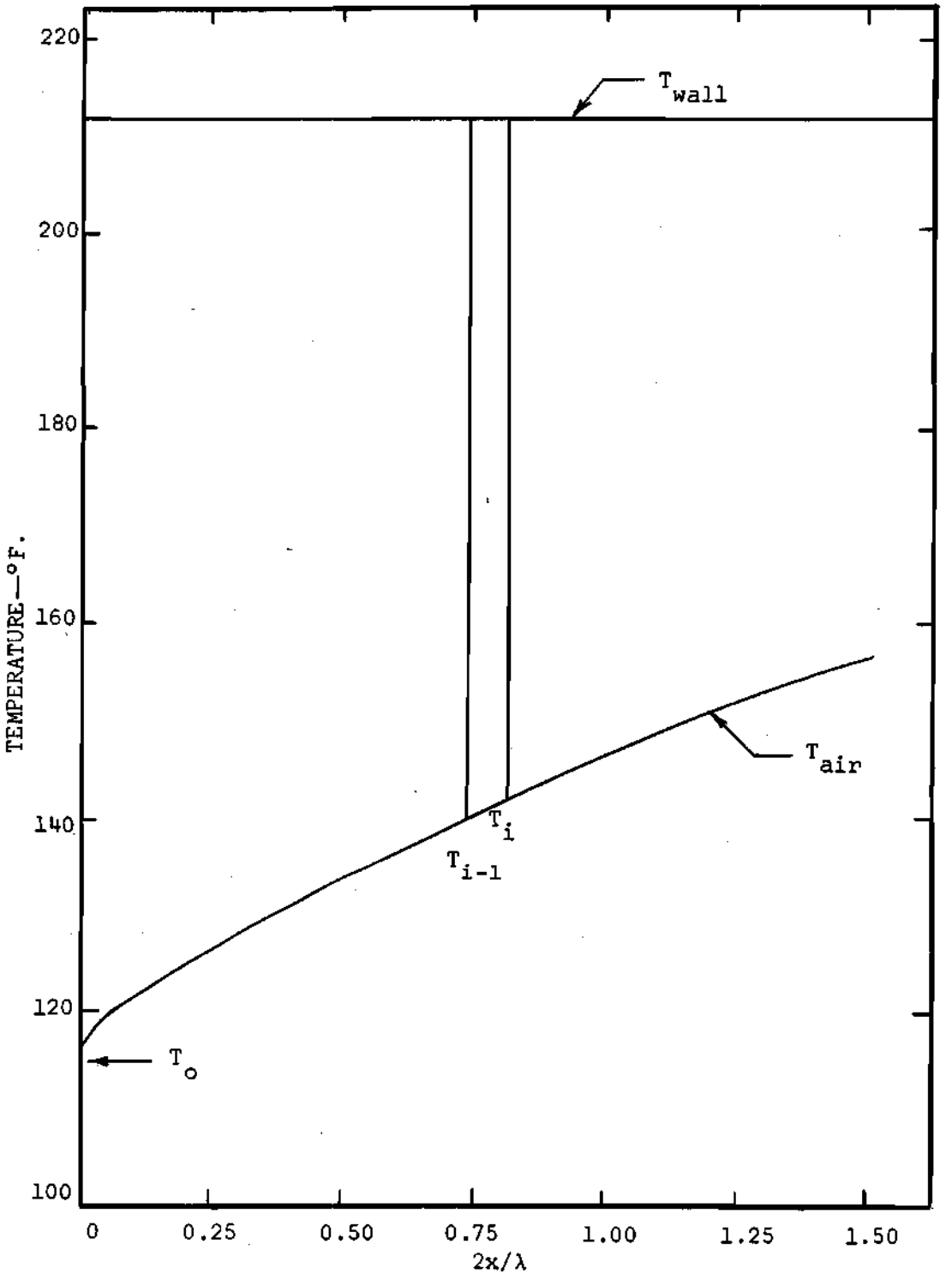

Figure 43. Typical Temperature Distribution of Air in Heated Tube.

$$\Delta T_i = \Delta T_{lm_i} \equiv \frac{\Delta T_{x_i} - \Delta T_{x=0}}{\log \left(\frac{\Delta T_{x_i}}{\Delta T_{x=0}}\right)}$$

$$= \frac{T_i - T_o}{\log \left(\frac{T_s - T_o}{T_s - T_i}\right)}$$

Thus

$$h_i = \frac{dQ_i}{dt} \Big/ A_i \Delta T_{lm_i}$$

Now

$$T_i - T_o = \frac{1}{\dot{m} c_p} \frac{dQ_i}{dt}$$

and, therefore,

$$h_i = \frac{\dot{m} c_p}{A_i} \log \left(\frac{T_s - T_o}{T_s - T_i}\right)$$

$\underline{Nu_i}$. From the definition of the Nusselt number we have

$$Nu_i = h_i \, D/k_{f_i}$$

where k_f = thermal conductivity of air based on the film temperature; i.e,

$$T_{f_i} = \frac{2T_s + T_o + T_i}{4}$$

$$D = A_i/\pi x_i$$

or

$$Nu_i = \frac{\dot{m}c_p}{\pi x_i k_{f_i}} \log \left(\frac{T_s - T_o}{T_s - T_i}\right)$$

$\underline{Gz_i}$. By definition

$$Gz_i = \dot{m}c_p/k_{f_i} x_i$$

$\underline{Gr_i}$. By definition

$$Gr_i = Z_f D^3 \left(\frac{p}{29.92}\right)^2 \Delta T_{lm_i}$$

where Z_f is the Grashof number based on the film temperature T_{f_i} and a characteristic length and temperature difference of one foot and one degree F, respectively. The system pressure, p, expressed in inches of Hg is assumed to be constant.

h_{x_i}. Again from the definition of the heat transfer coefficient we have

$$h_{x_i} = q_i / A_{x_i} \Delta T_{am_i}$$

where ΔT_{am_i} is the average arithmetic mean temperature difference for section i; i.e.,

$$\Delta T_{am_i} = \frac{1}{2} [(T_s - T_{i-1}) + (T_s - T_i)]$$

$$= \frac{1}{2} (2T_s - T_{i-1} - T_i)$$

Nu_{x_i}. By definition

$$Nu_{x_i} \equiv h_{x_i} D / k_{f_x}$$

where k_{f_x} is based on the local film temperature; i.e.,

$$T_{f_{x_i}} = \frac{1}{4} (2T_s + T_{i-1} + T_i)$$

Gz_{x_i}. By definition

$$Gz_{x_i} \equiv \dot{m} c_p / k_{f_x} x_{x_i}.$$

$\underline{Gr_{x_i}}$. By definition

$$Gr_{x_i} \equiv Z_{f_x} D^3 \left(\frac{p}{29.92}\right)^2 \Delta T_{am_i}.$$

APPENDIX C

Table 1. Summary Tabulation of Local Data (Experimental Results)

T_o = 116.34°F. Max. SPL = 160.0 db.

T_{sat} = 212.02°F. Frequency = 91.2 cps.

Re = 10100

Chamber	T	H	Nu	Gz	Gr
1	119.0	2.880	53.72	18134.5	3.216
2	120.5	1.976	36.80	4158.9	3.122
3	123.5	1.746	32.46	2159.7	3.027
4	125.7	1.644	30.53	1312.9	2.913
5	128.2	1.727	32.00	942.3	2.804
6	130.7	1.777	32.87	735.3	2.697
7	133.2	1.795	33.15	602.2	2.593
8	135.6	1.811	33.39	508.9	2.491
9	137.9	1.822	33.55	441.3	2.395
10	140.1	1.731	31.82	389.0	2.304
11	142.2	1.697	31.14	344.4	2.219
12	144.1	1.605	29.41	314.3	2.142
13	145.9	1.551	28.39	286.7	2.071
14	147.5	1.447	26.47	263.5	2.006
15	149.0	1.390	25.38	243.7	1.947
16	150.5	1.372	25.04	226.8	1.891
17	152.0	1.416	25.80	212.0	1.837
18	153.5	1.491	27.15	199.0	1.782
19	155.1	1.653	30.06	187.4	1.724
20	156.8	1.766	32.09	177.1	1.664
21	158.5	1.799	32.66	167.8	1.604

Table 2. Summary Tabulation of Average Data (Experimental Results)

T_o = 116.34°F. Max. SPL = 160.0 db.

T_{sat} = 212.02°F. Frequency = 91.2 cps.

Re = 10100

Chamber	T	H	Nu	Gz	Gr
1	119.0	2.880	53.72	6088.5	3.2160
2	120.5	2.431	45.32	3195.1	3.1803
3	123.2	2.090	38.92	1644.1	3.1186
4	125.7	1.937	36.05	1101.6	3.0614
5	128.2	1.881	34.97	830.6	3.0039
6	130.7	1.857	34.49	666.3	2.9464
7	133.2	1.843	34.21	555.7	2.8899
8	135.6	1.836	34.05	475.9	2.8340
9	137.9	1.832	33.94	417.4	2.7809
10	140.1	1.818	33.67	369.9	2.7298
11	142.2	1.805	33.39	333.2	2.6827
12	144.1	1.785	33.01	302.9	2.6391
13	145.9	1.764	32.60	277.5	2.5977
14	147.5	1.739	32.11	256.0	2.5601
15	149.0	1.713	31.61	237.6	2.5247
16	150.5	1.689	31.16	221.8	2.4908
17	152.0	1.671	30.82	207.9	2.4565
18	153.5	1.660	30.59	195.5	2.4209
19	155.1	1.658	30.54	184.5	2.3824
20	156.8	1.663	30.61	174.7	2.3424
21	158.5	1.669	30.70	165.9	2.3028

Table 3. Results of Analytical Investigations
Channel Reynolds Number = 1000,

$M_0^2/M = 0.8196$

x'	T_B'	Φ	Nu	Nu	r
0.10	0.938	1480.3	17.49	23.58	1.011
0.20	0.898	740.2	14.58	19.75	1.014
0.30	0.866	493.5	12.09	17.61	1.014
0.40	0.842	370.1	9.58	15.91	1.012
0.50	0.823	296.1	7.45	14.42	1.010
0.60	0.808	246.7	6.26	13.14	1.008
0.70	0.795	211.5	6.21	12.14	1.008
0.80	0.781	185.0	7.11	11.45	1.009
0.90	0.764	164.5	8.52	11.04	1.012
1.00	0.746	148.0	9.78	10.86	1.016
1.10	0.725	134.6	10.46	10.80	1.019
1.20	0.705	123.4	10.31	10.77	1.021
1.30	0.687	113.9	9.32	10.70	1.021
1.40	0.671	105.7	7.80	10.55	1.021
1.50	0.658	98.7	6.32	10.31	1.020
1.60	0.648	92.5	5.49	10.03	1.019
1.70	0.639	87.1	5.61	9.76	1.019
1.80	0.628	82.2	6.56	9.56	1.020
1.90	0.616	77.9	7.99	9.44	1.022
2.00	0.602	74.0	9.28	9.40	1.024
2.10	0.586	70.5	10.03	9.41	1.026
2.20	0.570	67.3	9.95	9.44	1.027

Table 4. Chambers Dimensions

Chamber	A_i	x_i	A_{x_i}	x_{x_i}
1	0.2794	0.2767	0.2794	0.0929
2	0.5321	0.5270	0.2474	0.4045
3	1.0331	1.0232	0.4956	0.7778
4	1.5405	1.5257	0.5019	1.2772
5	2.0415	2.0219	0.4956	1.7765
6	2.5425	2.5181	0.4956	2.2727
7	3.0461	3.0168	0.4981	2.7702
8	3.5538	3.5197	0.5023	3.2726
9	4.0490	4.0101	0.4897	3.7676
10	4.5652	4.5213	0.5107	4.2684
11	5.0649	5.0162	0.4943	4.8131
12	5.5680	5.5145	0.4977	5.2681
13	6.0736	6.0153	0.5002	5.7676
14	6.5793	6.5161	0.5002	6.2684
15	7.0854	7.0173	0.5006	6.7694
16	7.5872	7.5143	0.4964	7.2685
17	8.0907	8.0130	0.4981	7.7664
18	8.5974	8.5148	0.5012	8.2666
19	9.1041	9.0166	0.5012	8.7684
20	9.6103	9.5180	0.5008	9.2700
21	10.1149	10.0177	0.4991	9.7705

APPENDIX D

ANALYTICAL SOLUTION FOR CIRCULAR TUBE

Introduction

At the beginning of the present investigation, the solution for the velocity profile for the problem of laminar flow in a circular duct under the influence of a resonant acoustic field was not available. The solution for the similar problem of a parallel plate channel geometry was available, however. Because of the availability of the velocity solution, a parallel plate channel geometry was chosen to study the effects of acoustical vibrations on heat transfer. Since the solution for the velocity field for the circular tube is now available, an outline of the solution of the energy equation will be presented. The approach to the problem and method of solution will be the same as that presented in Chapters III and IV.

Statement of the Problem

The mathematical model of the problem as shown in Figure 44 consists of "fully-developed," laminar, compressible flow in a circular tube. The fluid is assumed to be a viscous, ideal gas. Superimposed upon this flow is a resonant acoustic field having a pressure node (velocity antinode) at $z = 0$.

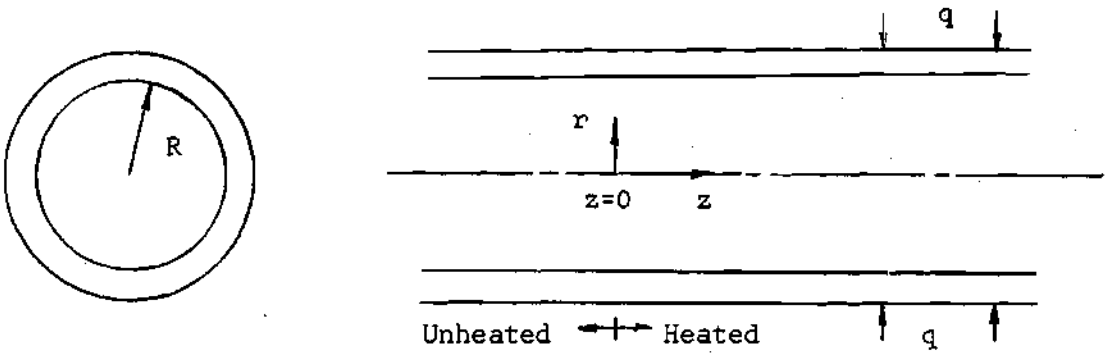

Figure 44. Model of the Flow System.

Assumptions

In order to develop the mathematics to describe the selected model, the following assumptions will be made:

(A1) The fluid and the duct wall are assumed to be at a constant temperature throughout the hydrodynamic entrance length; i.e., for $z < 0$. The wall of the tube in the entrance length is assumed to be maintained at a fixed temperature, say T_o. The tube wall in the heated section is also assumed to be at a constant temperature, T_w, where T_w is greater than T_o.

(A2) The fluid is assumed to be flowing laminarly in the positive z-direction. The flow is assumed to be axially symmetric, but due to the impressed acoustic field there will be an r-component of velocity; hence, the flow is two-dimensional.

(A3) The fluid properties--viscosity, specific heat, and thermal conductivity--will be taken as constant.

(A4) The temperature variations in the gas are assumed to be small enough so that free convection effects may be neglected. This as-

sumption simplifies the mathematics considerably by allowing the continuity and momentum equations to be solved independently of the energy equation.

Governing Equations and Boundary Conditions

The problem is described mathematically by the following basic equations together with their associated boundary conditions:

Continuity

$$\frac{\partial \rho}{\partial t} + \frac{1}{r} \frac{\partial}{\partial r}(r\rho v) + \frac{\partial}{\partial z}(\rho w) = 0 \qquad (D.1)$$

$$\int_0^R \bar{\rho}\bar{w}(2\pi r)dr = \text{Constant} \qquad (D.2)$$

Momentum

$$\rho \left[\frac{\partial v}{\partial t} + v \frac{\partial v}{\partial r} + w \frac{\partial v}{\partial t}\right] = \gamma_r - \frac{\partial p}{\partial r} + \qquad (D.3)$$

$$\mu \left[\frac{4}{3} \frac{\partial^2 v}{\partial r^2} + \frac{4}{3} \frac{1}{r} \frac{\partial v}{\partial r} + \frac{\partial^2 v}{\partial z^2} - \frac{4}{3} \frac{v}{r^2} + \frac{1}{3} \frac{\partial^2 w}{\partial r \partial z}\right]$$

$$\rho \left[\frac{\partial w}{\partial t} + v \frac{\partial w}{\partial r} + \omega \frac{\partial w}{\partial z}\right] = \gamma_z - \frac{\partial p}{\partial z} + \qquad (D.4)$$

$$\mu \left[\frac{1}{3} \frac{\partial^2 v}{\partial r \partial z} + \frac{1}{3} \frac{1}{r} \frac{\partial v}{\partial z} + \frac{4}{3} \frac{\partial^2 w}{\partial z^2} + \frac{\partial^2 w}{\partial r^2} + \frac{1}{r} \frac{\partial w}{\partial r}\right]$$

The boundary conditions for the momentum equations are

$$v\,(R,z,t) = w\,(R,z,t) \equiv 0 \tag{D.5}$$

$$v\,(0,z,t) = 0 \tag{D.6}$$

$$\frac{\partial w}{\partial r} = 0;\ r = 0,\ \text{all } z \text{ and } t. \tag{D.7}$$

Energy

$$\rho c_p \frac{DT}{Dt} = \frac{Dp}{Dt} + k\nabla^2 T \tag{D.8}$$

where

$$\frac{DT}{Dt} = \frac{\partial T}{\partial t} + v\frac{\partial T}{\partial r} + w\frac{\partial T}{\partial z} \tag{D.9}$$

$$\frac{Dp}{Dt} = \frac{\partial p}{\partial t} + v\frac{\partial p}{\partial r} + w\frac{\partial p}{\partial z} \tag{D.10}$$

$$\nabla^2 T = \frac{\partial^2 T}{\partial r^2} + \frac{1}{r}\frac{\partial T}{\partial r} + \frac{\partial^2 T}{\partial z^2} \tag{D.11}$$

The boundary conditions are

$$T\,(R,z,t) = T_w = \text{Constant} \tag{D.12}$$

$$\frac{\partial T}{\partial r} = 0;\ r = 0,\ \text{all } z \text{ and } t \tag{D.13}$$

$$T(r,0,t) = T_o, \quad 0 \leq r < R \tag{D.14}$$

It should be pointed out here that the term involving viscous dissipation has been neglected in the energy equation. It can be surmised from experience with the solution of the parallel plate problem that this term is negligible.

Reduction of the Governing Equations

Assumptions

In addition to the assumptions previously made the following assumptions will be made:

(A5) Since Purdy, et al. (32), have solved the continuity and momentum equations corresponding to this problem, their solution for the velocity and pressure fields will be used to determine the coefficients in the energy equation. The validity of this approach is based upon one of the previous assumptions; i.e., that free convection effects are negligible.

(A6) The velocity components, $v(r,z,t)$ and $w(r,z,t)$, and the pressure, $p(r,z,t)$ are known functions of position and time. Purdy, et al. (32), in their analysis of the velocity field formed by resonant acoustic vibrations in a circular tube, assumed that the density, pressure, and velocity components could be represented as the sum of a time-dependent component (denoted by a subscript, "1") and a time-mean component (denoted by a barred term). It is plausible, therefore, to assume that the temperature of the fluid may be represented in a similar fashion. Thus, we have

$$\rho(r,z,t) = \bar{\rho}(r,z) + \rho_1(r,z,t) \tag{D.15}$$

$$p(r,z,t) = \bar{p}(r,z) + p_1(r,z,t) \tag{D.16}$$

$$v(r,z,t) = \bar{v}(r,z) + v_1(r,z,t) \tag{D.17}$$

$$w(r,z,t) = \bar{w}(r,z) + w_1(r,z,t) \tag{D.18}$$

$$T(r,z,t) = \bar{T}(r,z) + T_1(r,z,t) \tag{D.19}$$

(A7) The energy equation in its present form will not yield readily to a mathematical analysis and, therefore an order of magnitude analysis will be performed to reduce the energy equation to a more tractable form. In order to perform an order of magnitude analysis it is necessary first to introduce dimensionless forms of each of the properties in the governing equations. In addition, it is necessary to assume an order of magnitude for various quantities.

Dimensionless Variables

Before defining the dimensionless forms of the properties the following characteristic values are assumed:

Property	Characteristic Value
r	δ_{ac} and R
z	$\lambda/2$
t	$\lambda/2c_o$
$\bar{v}$	$\bar{V}$
v_1	V_o

Property	Characteristic Value
$\bar{w}$	$\bar{W}$
w_1	W_o
$\bar{p}$	p_o
p_1	$\gamma p_o M_o = \rho_o c_o W_o$
$\bar{\rho}$	ρ_o
ρ_1	$\rho_o M_o$
μ	μ_o
c_p	c_{p_o}
k	k_o
$\bar{T}$	$T_w - T_o$
T_{1n}	θ_n

Utilizing these characteristic values, the following dimensionless variables are formed:

$$r = \delta_{ac} r' \text{ or } R\bar{r}'$$

$$z = (\lambda/2)z'$$

$$t = (\lambda/2c_o)t'$$

$$\bar{v} = \bar{V}\bar{v}'$$

$$v_1 = V_o v_1'$$

$$\bar{w} = \bar{W}\bar{w}'$$

$$w_1 = W_o w_1'$$

$$\bar{p} = p_o \bar{p}'$$

$$p_1 = \rho_o c_o \bar{W}_o p_1'$$

$$\bar{\rho} = \rho_o \bar{\rho}'$$

$$\rho_1 = \rho_o M_o \rho_1'$$

$$\mu = \mu_o \mu'$$

$$c_p = c_{p_o} c_p'$$

$$k = k_o k'$$

$$\bar{T} = T_w - (T_w - T_o)\,\bar{T}'$$

$$T_{1n} = \theta_n T_{1n}'$$

where the prime superscript denotes dimensionless variables. Purdy (32) has shown that the characteristic velocities $\bar{W}$, $\bar{V}$, and V_o should be related to the other characteristic properties as follows:

$$\bar{W} = M_o W_o$$

$$\bar{V} = (\pi R/\lambda)\, M_o W_o$$

$$V_o = W_o \delta$$

Orders of Magnitude

Following the same reasoning as used in Chapter III, the following orders of magnitude are assumed:

$$\theta\left[\frac{\partial}{\partial r'}, \frac{\partial}{\partial z'}, \frac{\partial}{\partial t'}, \bar{w}', w_1', \bar{v}', v_1', \bar{p}', p_1', \bar{\rho}', \rho_1', \mu', c_p', k', \bar{T}', T_1'\right] = 1$$

$$\theta\left[2\delta_{ac}/\lambda,\ W_o/c_o,\ \bar{W}/W_o,\ R/\lambda\right] = \delta$$

$$\theta\left[\frac{\partial \bar{p}'}{\partial z'},\ \frac{\partial p_1'}{\partial r'}\right] = \delta^2$$

$$\theta \left[\frac{\partial \bar{p}'}{\partial r'}\right] = \delta^4$$

$$\theta \left[\frac{\partial p_1'}{\partial z'}, (T_w - T_o) / T_o\right] = 1 .$$

The Reduced Equations

In a manner exactly analogous to that shown in Appendix A the dimensionless energy equation for the circular tube may be reduced to the following two equations:

$$T_1(r,z,t) = \text{Real}\left[- i(\gamma-1)M_o T_o \sin(\omega z/c_o)\exp(- i\omega t)\right] \quad (D.20)$$

$$\frac{\partial^2 \bar{T}'}{\partial \bar{r}'^2} + \frac{1}{\bar{r}'}\frac{\partial \bar{T}'}{\partial \bar{r}'} - \frac{2}{\pi}(M_o R')^2 Pr_o \bar{w}' \frac{\partial \bar{T}'}{\partial z'} - (M_o R')^2 Pr_o \bar{v}' \frac{\partial \bar{T}'}{\partial \bar{r}'} = 0. \quad (D.21)$$

As may be noted these equations are very similar to equations 4.1 and 4.2. The boundary conditions which must be satisfied by equation D.21 are

$$\bar{T}'(1,z') = 0 \quad (D.22)$$

$$\frac{\partial \bar{T}'}{\partial \bar{r}'} = 0;\ r = 0,\ \text{all } z' \quad (D.23)$$

$$\bar{T}'(\bar{r}', 0) = 1,\ 0 \le r < R. \quad (D.24)$$

The condition at $\bar{r}' = 1$ is based on the assumption that the fluid immediately adjacent to the tube wall will have the same temperature as the wall. The condition expressed by equation D.23 corresponds to the assumed symmetry condition at the centerline of the tube. The remaining boundary condition, D.24, is due to the assumption that the fluid is isothermal until it reaches the thermal entrance at $z' = 0$.

By utilizing the solution for the velocity components, $\bar{w}(\bar{r}',z')$ and $\bar{v}'(\bar{r}',z')$, as given by Purdy (32), and by employing the same method which is outlined in Chapter IV and Appendix B, a solution for equation D.21 subject to the boundary conditions D.22, D.23, and D.24 may be obtained numerically.

LITERATURE CITED

1. P. N. Kubanskii, "Flow Near a Heated Solid Body in a Standing Acoustic Wave," *Zhurnal Technicheskoi Fiziki, 22,* (1952), pp. 585-592.

2. P. N. Kubanskii, "Effects of Acoustic Vibrations of Finite Amplitude on the Boundary Layer," *Zh. tekh. Fiz., 22,* (1952), pp. 593-601; *Fuel Abstracts, 14,* (1953), pp. 171-172.

3. H. A. Haveman and N. N. Narayan Rao, "Heat Transfer in Pulsating Flow," *Nature, 174,* (1954), p. 41.

4. J. R. Sellars, M. Tribus, and J. S. Klein, "Heat Transfer to Laminar Flow in a Round Tube or Flat Conduit--The Graetz Problem Extended," *Transactions of the American Society of Mechanical Engineers, 78,* (1956), pp. 441-448.

5. G. B. Darling, "Heat Transfer to Liquids in Intermittent Flow," *Petroleum, 22,* (1959), pp. 177-178.

6. F. B. West and A. T. Taylor, "The Effect of Pulsations on Heat Transfer; Turbulent Flow of Water Inside Tubes," *Chemical Engineering Progress, 48,* (1952), pp. 39-43.

7. J. P. Holman, Harold E. Gartrell, and Erich E. Soehngen, "A Study of Free Convection Boundary Layer Oscillations and Their Effects on Heat Transfer," *WADD Technical Report 59-3,* Wright Air Development Division, (1959).

8. R. Anantanarayanan and A. Ramachandran, "Effects of Vibration on Heat Transfer from a Wire to Air in Parallel Flow," *Trans. of ASME, 80,* (1958), pp. 1426-1432.

9. R. Lemlich, "Effect of Vibration on Natural Convective Heat Transfer," Symposium on Pulsatary and Vibrational Phenomena, *Industrial and Engineering Chemistry, 47,* (1955), pp. 1175-1180.

10. A. L. Sprott, J. P. Holman and F. L. Durand, "An Experimental Study of the Interaction of Strong Sound Fields with Free Convection Boundary Layers," *WADC Technical Report 59-717,* Wright Air Development Center, (1959).

11. J. P. Holman and T. P. Mott-Smith, "The Effects of Constant-Pressure Sound Fields on Free Convection Heat Transfer from a Horizontal Cylinder," *Journal of the Aero/Space Sciences, 26,* (1959), p. 188.

12. R. M. Fand and J. Kaye, "The Influence of Sound on Free Convection from a Horizontal Cylinder," *Trans. of ASME, Series C, 83,* (1961), pp. 133-148.

13. R. M. Fand, J. Raos, P. Cheng, and J. Kaye, "The Local Heat Transfer Coefficient Around a Heated Horizontal Cylinder in an Intense Sound Field," *Trans. of ASME, Series C, 84,* (1962), pp. 245-250.

14. R. C. Martinelli and L. M. K. Boelter, "The Effect of Vibration on Heat Transfer by Free Convection from a Horizontal Cylinder," *Proceedings, Fifth International Congress of Applied Mechanics,* (1938), pp. 578-584.

15. T. W. Jackson, W. B. Harrison, and W. C. Boteler, "Free Convection, Forced Convection and Acoustic Vibrations in a Constant Temperature Vertical Tube," *Trans. of ASME, Series C,* (1959), pp. 68-74.

16. W. B. Harrison, W. C. Boteler, T. W. Jackson, A. Lowi, and F. A. Thomas, "Heat Transfer to Vibrating Air Columns," Final Report, Project No. A-183, Engineering Experiment Station, Georgia Institute of Technology, (1955).

17. J. M. Spurlock, T. W. Jackson, K. R. Purdy, C. C. Oliver, and H. L. Johnson, "The Effects of Resonant Acoustic Vibrations on Heat Transfer to Air in Horizontal Tubes," *WADC Technical Note 59-330,* Wright Air Development Center, (1959).

18. T. W. Jackson, K. R. Purdy, and C. C. Oliver, "The Effects of Resonant Acoustic Vibrations on the Nusselt Numbers for a Constant Temperature Horizontal Tube," *International Developments in Heat Transfer, Part II,* (1961), pp. 483-489.

19. T. W. Jackson and H. L. Johnson, "Convective Flow Due to Acoustic Vibrations in Horizontal Resonant Tubes," Final Report, Contract No. AF 49(638)-459, Engineering Experiment Station, Georgia Institute of Technology, (1960).

20. D. E. Alford, *Turbulent Convective Heat Transfer in an Acoustically Resonant Tube,* M. S. Thesis, Georgia Institute of Technology, (1963).

21. Ian Eastwood, *Threshold Values for Resonant Acoustic Vibrations on Convection Heat Transfer in a Horizontal, Isothermal Tube,* M. S. Thesis, Georgia Institute of Technology, (1961).

22. M. Perlmutter and R. Siegel, "Unsteady Laminar Flow in a Duct with Unsteady Heat Addition," *Transactions of ASME, Series C, 83,* (1961), pp. 432-440.

23. S. L. Zeiberg and W. K. Mueller, "Transient, Laminar, Combined Free and Forced Convection in a Duct," *Trans. of ASME, Series C, 84,* (1962), pp. 141-148.

24. R. Siegel and M. Perlmutter, "Heat Transfer for Pulsating Laminar Duct Flow," *Trans. of ASME, Series C, 84,* (1962), pp. 111-123.

25. R. Siegel and M. Perlmutter, "Two-Dimensional Pulsating Laminar Flow in a Duct with a Constant Wall Temperature," *International Developments in Heat Transfer, Part II,* (1961), pp. 517-525.

26. R. L. Ewen, *Laminar Heat Transfer with Oscillating Flow in a Parallel Plate Channel,* Ph.D. Dissertation, University of Pittsburgh, (1962).

27. K. R. Purdy, *Viscous Fluid Flow Under the Influence of a Resonant Acoustic Field,* Ph.D. Dissertation, Georgia Institute of Technology, (1963).

28. H. Schlichting, *Boundary Layer Theory,* third edition, New York: Pergamon Press, (1955).

29. Lord Rayleigh, "On the Circulation of Air Observed in Kundt's Tubes and on Some Allied Acoustical Problems," *Philosophical Transactions of the Royal Society of London, 175,* Part I, (1883), p. 1.

30. P. J. Westervelt, "The Theory of Steady Rotational Flow Generated by a Sound Field," *Journal of the Acoustical Society of America, 25,* (1953), p. 60.

31. J. V. Sanders, "A Photomultiplier-Schlieren for Acoustic Measurement and Some Investigations of the Kundt's Tube," *Dissertation Abstracts,* (February, 1962).

32. Kenneth R. Purdy, Thomas W. Jackson, Donald A. Willoughby, H. Grady Keith, and Charles E. Willbanks, *The Effect of a Resonant Acoustic Field on Laminar Flow in a Circular Tube,* Report, Project 7063, Engineering Experiment Station, Georgia Institute of Technology, (1963).

33. H. Latzko, "Der Wärmeübergang an einen turbulenten Flüssigkeits— oder Gasstrom," *Zeitschrift fur angewandte Mathematik und Mechanik, 1,* (1921), pp. 268-290.

34. W. H. McAdams, *Heat Transmission,* McGraw-Hill Book Company, Inc., New York, 3rd ed., (1954), pp. 219-225.

35. J. Crank and P. Nicolson, "A Practical Method for Numerical Evaluation of Solutions of Partial Differential Equations of the Heat-Conduction Type," *Proceedings of the Cambridge Philosophical Society, 43,* (1947), pp. 50-67.

36. David Young, *The Numerical Solution of Elliptic and Parabolic Partial Differential Equations,* Space Technology Laboratories NN-106, (1958).

37. L. H. Thomas, *Elliptic Problems in Linear Difference Equations Over a Network*, unpublished manuscript, Watson Scientific Computing Laboratory.

38. G. H. Bruce, D. W. Peaceman, H. H. Rachford, Jr., and J. D. Rice, "Calculation of Unsteady-State Gas Flow Through Porous Media," *Petroleum Transactions, A.I.M.E., 98*, (1958), pp. 79-92.

39. J. Hilsenrath, *Tables of Thermal Properties of Gases*, National Bureau of Standards Circular 564, Washington, D. C., (1955).

40. Max Jakob, *Heat Transfer*, I, Wiley, 1958.

41. R. H. Norris and D. D. Streid, "Laminar-Flow Heat-Transfer Coefficients for Ducts," *Trans. of ASME, 62*, (1940), pp. 525-533.

VITA

Henry Grady Keith was born in Atlanta, Georgia on March 5, 1934. He attended elementary and high school in Atlanta and was graduated from Fulton High School in 1952. He entered the Georgia Institute of Technology in the same year and was graduated in 1956, receiving the degree of Bachelor of Mechanical Engineering. After graduation, he was employed by the Lockheed-Georgia Company as an Associate Aircraft Engineer in the Mathematical Analysis Department. In September of 1958, he entered the Graduate Division of the Georgia Institute of Technology on a part-time basis and received the degree of Master of Science in Engineering Mechanics in 1960. Shortly after graduation he was promoted to the position of Mathematician, Senior. In September, 1961, he was granted a leave of absence from the Lockheed-Georgia Company to devote full-time to graduate studies toward the Doctorate. He returned to Lockheed-Georgia Company in September, 1963 as an Associate Scientist in the Computer Programming Division and in January, 1964 he was transferred to his present supervisory position in the Scientific Programming Department.